

AFML-TR-76-124

ADA033078

OFFICIAL FILE COPY

INFLUENCE OF CROSSLINKING ON THE MECHANICAL PROPERTIES OF HIGH T_G POLYMERS

MATERIALS RESEARCH CENTER
LEHIGH UNIVERSITY
BETHLEHEM, PENNSYLVANIA 18015

JULY 1976

TECHNICAL REPORT AFML-TR-76-124
FINAL REPORT FOR PERIOD MAY 1975 - APRIL 1976

Approved for public release; distribution unlimited

AIR FORCE MATERIALS LABORATORY
AIR FORCE WRIGHT AERONAUTICAL LABORATORIES
AIR FORCE SYSTEMS COMMAND
WRIGHT-PATTERSON AIR FORCE BASE, OHIO 45433

Best Available Copy

20040301126

NOTICE

When Government drawings, specifications, or other data are used for any purpose other than in connection with a definitely related Government procurement operation, the United States Government thereby incurs no responsibility nor any obligation whatsoever; and the fact that the Government may have formulated, furnished, or in any way supplied the said drawings, specifications, or other data, is not to be regarded by implication or otherwise as in any manner licensing the holder or any other person or corporation, or conveying any rights or permission to manufacture, use, or sell any patented invention that may in any way be related hereto.

Copies of this report should not be returned to the Air Force Materials Laboratory unless return is required by security considerations, contractual obligations, or notice on a specific document.



CAPT. ANTHONY WERETA, JR.
Project Scientist

FOR THE COMMANDER



DR. R. L. VAN DEUSEN
Chief, Polymer Branch
Nonmetallic Materials Division

UNCLASSIFIED

SECURITY CLASSIFICATION OF THIS PAGE (When Data Entered)

REPORT DOCUMENTATION PAGE		READ INSTRUCTIONS BEFORE COMPLETING FORM
1. REPORT NUMBER AFML-TR-76-124	2. GOVT ACCESSION NO.	3. RECIPIENT'S CATALOG NUMBER
4. TITLE (and Subtitle) INFLUENCE OF CROSSLINKING ON THE MECHANICAL PROPERTIES OF HIGH T _G POLYMERS		5. TYPE OF REPORT & PERIOD COVERED Final Report for Period May 1975 - April 1976
		6. PERFORMING ORG. REPORT NUMBER
7. AUTHOR(s) John A. Manson Soojaa L. Kim Leslie H. Sperling		8. CONTRACT OR GRANT NUMBER(s) F33615-75-C-5167
9. PERFORMING ORGANIZATION NAME AND ADDRESS Materials Research Center Lehigh University Bethlehem, Pa. 18015		10. PROGRAM ELEMENT, PROJECT, TASK AREA & WORK UNIT NUMBERS 73420307
11. CONTROLLING OFFICE NAME AND ADDRESS Air Force Materials Laboratory Wright-Patterson AFB, Ohio 45433		12. REPORT DATE July 1976
		13. NUMBER OF PAGES 102
14. MONITORING AGENCY NAME & ADDRESS (if different from Controlling Office)		15. SECURITY CLASS. (of this report) Unclassified
		15a. DECLASSIFICATION/DOWNGRADING SCHEDULE
16. DISTRIBUTION STATEMENT (of this Report) Approved for Public Release; Distribution Unlimited		
17. DISTRIBUTION STATEMENT (of the abstract entered in Block 20, if different from Report)		
18. SUPPLEMENTARY NOTES		
19. KEY WORDS (Continue on reverse side if necessary and identify by block number) Bamford networks, Crosslinked networks, Decrosslinking, Density and Distribution of crosslinks, Epoxy resins, Fatigue, Fracture mechanics, Glass transition temperature, High T _G resins, Labile crosslinks, Mechanical properties, Model networks, Swelling behavior, Viscoelastic behavior.		
20. ABSTRACT (Continue on reverse side if necessary and identify by block number) Research was begun on the effects of crosslinking on the mechanical properties of high-T _G polymers, with particular emphasis on the role of cross- link density, variations in the distribution of crosslink segment lengths, and the role of network imperfections. Two systems were selected: one based on the use of the Bamford synthesis to provide model, well defined networks, and the other based on the use of bisphenol-A-type epoxy/methylene dianiline resins synthesized to provide controlled variations in network properties.		

DD FORM 1 JAN 73 1473

EDITION OF 1 NOV 65 IS OBSOLETE

UNCLASSIFIED

SECURITY CLASSIFICATION OF THIS PAGE (When Data Entered)

UNCLASSIFIED

SECURITY CLASSIFICATION OF THIS PAGE(When Data Entered)

20. ABSTRACT - cont'd

To date, the feasibility of varying network characteristics in a model system by introducing hydrolyzable or permanent crosslinks has been demonstrated using copolymers of styrene or ethyl acrylate with acrylic acid anhydride. The creep and stress relaxation behavior was found to reflect the characteristics of the networks.

Several series of fully cured epoxy resins were prepared having (1) varying values of \bar{M}_c , (2) varying distributions of crosslink chain lengths at constant \bar{M}_c , and (3) varying stoichiometries at constant \bar{M}_c . Characterization of swelling, dynamic mechanical behavior, fracture toughness, and fatigue crack growth was performed. It was shown that the viscoelastic behavior was determined by \bar{M}_c , regardless of how the given value of \bar{M}_c was attained. Fracture toughness and fatigue crack growth rates both varied with the amine/epoxy ratio. Effects of the distribution at crosslink lengths on viscoelastic behavior were negligible, but broad distributions caused modest increases in the swell ratio and possibly in fracture toughness.

UNCLASSIFIED

SECURITY CLASSIFICATION OF THIS PAGE(When Data Entered)

FOREWORD

The Lehigh Project Co-Directors were Dr. John A. Manson, Professor of Chemistry and Director of the Polymer Laboratory, Materials Research Center, and Dr. Leslie H. Sperling, Associate Professor of Chemical Engineering, and Senior Staff member, the Polymer Laboratory. The Faculty Associates were: Dr. Richard W. Hertzberg, Professor of Metallurgy and Materials Science and Director of the Mechanical Behavior Laboratory, and Dr. John W. Vanderhoff, Professor of Chemistry and Associate Director - Coatings, Center for Surface and Coatings Research. Special advice on synthesis was provided by Professor N. D. Heindel, Professor of Chemistry. Also contributing to the project were Research Associate Dr. S. L. Kim, Visiting Scientist S. Yamoda, and Graduate Students Subodh C. Misra, Michael Skibo, Carol M. Vasold, and Dave Siegfried.

TABLE OF CONTENTS

SECTION		Page
I	SUMMARY	1
	A. General	1
	B. Model Networks	1
	C. Epoxy Networks	2
II	INTRODUCTION	4
	A. Statement of the Problem	4
	B. Objective and Scope of the Program	4
	C. General Discussion	5
III	TECHNICAL APPROACH	10
IV	SYNTHESIS OF MODEL NETWORKS	12
	A. Introduction	12
	B. Experimental Details, Results, and Discussion	15
V	PROPERTIES OF MODEL SYSTEMS	20
	A. Introduction	20
	B. Experimental Details, Results, and Discussion	20
VI	SYNTHESIS OF EPOXY NETWORKS	35
	A. Structure and Stoichiometry	36
	B. Experimental Details, Results, and Discussion	39
VII	CHARACTERIZATION OF EPOXY NETWORKS	45
	A. Introduction	45
	B. Experimental Details, Results, and Discussion	48
VIII	FRACTURE TOUGHNESS, STRENGTH, AND FATIGUE CRACK PROPAGATION (FCP) OF EPOXY NETWORKS	67
	A. Introduction	67
	B. Experimental Data, Results, and Discussion	71
IX	CONCLUSIONS AND RECOMMENDATIONS	82
	A. Model Networks	82
	B. Epoxy Networks	83

	Page
APPENDIX	87
LIST OF SPECIAL CHEMICAL STRUCTURES	87
REFERENCES	88

LIST OF TABLES

Table		Page
1	\bar{M}_c for PS-AAA Crosslinked Networks.	21
2	Characterization of Crosslinked PEA Networks.	22
3	Characterization of PEA Networks with 0.68% 1-Dodecanethiol.	23
4	Characterization of PEA Networks Capable of Complete Hydrolysis.	23
5	Characteristics of Epoxy Prepolymers.	37
6	Compositions of Series A Epoxy Resins.	41
7	Compositions of Series B (Blends) Epoxy Resins.	42
8	Compositions of Series C Resins.	43
9	Compositions of Series D (Versamid-cured) Epoxy Resins.	43
10	Swelling Behavior of Series B Epoxy Resins.	52
11	Dynamic Mechanical Data for Series A Epoxy Resins (Variable Stoichiometry).	56
12	β Transition of Series A Epoxy Resins (Variable Stoichiometry).	56
13	Molecular Weight Between Crosslinks, \bar{M}_c , for Series A Epoxy Resins.	60
14	Dynamic Mechanical Data of Series B.	61
15	Viscoelastic Parameters for Series E Epoxy Resins (Homopolymers).	62
16	Stress Relaxation of Series A Epoxy Resins at 150°C.	64
17	Fracture Toughness and Fatigue Characteristics of Epoxy Resins.	73

LIST OF ILLUSTRATIONS

Figure		Page
1	Schema showing typical variations in nature and composition of cross-linked polymer networks (after reference 2).	7
2	Values of $M_c(E)$ as a function of AAA and 1-Doth levels, before and after hydrolysis. -○-0.68% 1-Doth before hydrolysis -○-0.68% 1-Doth after hydrolysis -.-1.3% 1-Doth before hydrolysis -●-1.3% 1-Doth after hydrolysis.	25
3	Values of $\log 3G$ <u>vs.</u> time in the glass transition temperature range of PEA.	26
4	Values of $\log 3G$ <u>vs.</u> time for a series of temperatures for a material containing 0.68% 1-Doth.	27
5	$\log 3G$ vs temperature for PEA, after hydrolysis, for a PEA containing 1.2 ml of AAA and 0.68% 1-Doth.	28
6	Stress relaxation of PEA networks before and after hydrolysis.	29
7	Stress relaxation of PEA networks containing both permanent and temporary crosslink sites.	30
8	Stress relaxation of PEA networks as a function of hydrolysis time.	32
9	Tensile creep modulus of several PEA samples, after hydrolysis for 24 hours at 25°C.	33
10	Creep modulus of samples having little or no network properties after hydrolysis for 24 hours at 25°C in 28% NH_4OH .	34
11	Schemata showing (a) effects of crosslinking stoichiometry on molecular structure, and (b) effects of crosslinking on modulus-temperature behavior.	47
12	Comparison of M_c data from swelling tests: Series B (point includes all specimens).	50
13	Solvent-induced cracking during swelling of a Series A epoxy resin (A-16), as observed by optical microscopy (66.5X).	51

Figure		Page
14	Dynamic mechanical data for A-20 epoxy resin, $f = 110$ Hz.	54
15	Dynamic mechanical properties of Series A epoxy resins as functions of M_C : o, amine in excess; ●, epoxy in excess; ●, specimen A-10A.	57
16	Dynamic mechanical properties of Series A epoxy resins as functions of stoichiometry: O, A-10A; ■, Series B.	58
17	β transition of Series A epoxy resin: Δ A-10A.	59
18	Electron micrograph of polyamide-cured epoxy resin, sample D-2, etched in acetone 7 days, 130,000X (1000 A = 0.77 cm).	64
19	Fracture toughness, K_{IC} , and FCP parameters ΔK^{\ddagger} (ΔK at 3×10^{-4} mm/cyc), and slope of the da/dN curve as a function of the stress intensity factor range, ΔK , as function of stoichiometry: Circles and triangles for Series A, open corresponding to A-10A; shaded area for Series B.	74
20	Fracture toughness, K_{IC} , and FCP parameters ΔK^{\ddagger} (ΔK at 3×10^{-4} mm/cycl), and slope of the da/dN curve as a function of the stress intensity factor range, ΔK , as function of M_C : open circle amine excess in Series A, closed circle epoxy excess, shaded area for Series B.	75
21	Typical FCP behavior as a function of ΔK , Specimen, A-18; $f=10$ Hz.	76
22	FCP behavior of Series A epoxy resins; $f = 10$ Hz.	77
23	Fracture toughness and impact strength (in arbitrary units) of Epon 828/MDA epoxy resins as a function of amine/epoxy ratio: o, data of Selby and Miller (17) from 3 different measurements of toughness; Δ , data of Bell (36) for impact strength.	78
24	FCP behavior of Series B (broad distribution) epoxy resins: rate of crack growth per cycle as a function of ΔK ; $f = 10$ Hz.	79
25	FCP behavior of Series D (polyamide-cured) epoxy resins: Only the first and last points shown; $f = 10$ Hz.	80

SECTION I

SUMMARY

A. General

In order to gain more understanding of the effects of crosslinking on the mechanical properties of high T_g polymers a fundamental study of the role of crosslink density, distribution of segment lengths between crosslinks, and network imperfections was begun. A dual approach was selected: the preparation and study of novel networks based on the use of syntheses developed by Bamford et al. (initiation of polymerization at chlorine containing comonomer sites, using a molybdenum carbonyl initiator), and the preparation and study of epoxy/diamine networks. The former was selected because the system, while not of inherent interest as a material, offers the possibility of preparing well defined novel networks. The latter was selected because resins of this type are of practical interest, though the networks are susceptible to somewhat less control than in the former case.

B. Model Networks

To test the feasibility of cleaving crosslinks based on anhydride groups, crosslinked networks were synthesized by the copolymerization of styrene and acrylic acid anhydride. Techniques were developed for cleavage of the anhydride linkages using ethylene diamine. It was shown that complete hydrolysis could be effected; on hydrolysis the molecular behavior reverted to a value characteristic of uncrosslinked polymer. Thus, when the Bamford networks are synthesized using the mixed anhydride of acrylic acid and trichloroacetic acid, it will be possible to selectively cleave some of the crosslinks and examine the effects of the imperfect networks thus created.

In another variation, crosslinked networks were synthesized by first copolymerizing ethyl acrylate with tetraethylene glycol dimethacrylate and acrylic acid anhydride in various proportions. It was found that addition of a mercaptan made it possible to avoid parasitic crosslinking. Since these networks contain both stable and hydrolyzable crosslinks, the possibility of constructing and modifying networks in additional ways was established. Measurements of creep and stress relaxation as a function of the degree of hydrolysis reflected the state of the network (uncleaved, partially cleaved, or wholly cleaved).

While optimum conditions for the Bamford synthesis have not yet been worked out with a chlorine-containing comonomer, polymerization of styrene was demonstrated using carbon tetrachloride as co-initiator with molybdenum carbonyl.

The principal difficulty has been to obtain a comonomer containing chlorine (to serve as an initiating site) a vinyl group, and an anhydride group (to permit easy cleavage) to obtain a variety of network structures. Since suitable monomers containing all three reactive sites had never been synthesized, it was decided to attempt the synthesis of the mixed anhydride of trichloroacetic acid and acrylic acid in the laboratory. While what is believed to be a crude product has been obtained by the reaction of acryloyl chloride with trichloroacetic acid in pyridine (other approaches having been unsuccessful), optimum conditions need to be determined. The reaction liberates hydrochloric acid, and removal of all of the pyridine hydrochloride byproduct is difficult.

Work is continuing with the synthesis of the mixed anhydride, and, pending resolution of the synthetic problems, the preparation of networks using other methods such as those mentioned above, as well as methods not involving hydrolyzable linkages, are planned.

C. Epoxy Networks

Several series of bisphenol-A-based epoxy resins were prepared using methylene dianiline as curing agent. Essentially complete curing was attained, as shown by measurements of dynamic mechanical response. In series A, the average molecular weight between crosslinks, \bar{M}_C , was varied by altering the stoichiometry, with amine excess varying from -30 percent to +100 percent. In series B, \bar{M}_C was held constant, while the distribution of M_C was varied by blending epoxy prepolymers having different molecular weights. In series C, \bar{M}_C was again held constant, but the amine content was varied. In series D, several resins were prepared using polyamide curing agents. In series E, \bar{M}_C was varied at 1:1 stoichiometry by use of epoxy prepolymers having different molecular weights.

Characterization of the following properties was begun: \bar{M}_C , by swelling and measurements of rubbery modulus; the state of cure, by differential scanning calorimetry (DSC) and dynamic mechanical spectroscopy (DMS); viscoelastic response per se by DMS; stress-strain response; stress-relaxation; fracture toughness and fatigue crack propagation (FCP) behavior; and morphology, by electron microscopy.

The following characterizations were completed: preliminary study of \bar{M}_C by swelling and DMS for series A; \bar{M}_C by swelling and DMS for series B; the state of cure by DMS for series A; the viscoelastic response for series A, B, and E; preliminary study of stress relaxation for series A; fracture toughness and FCP behavior for series A, B, and D; and preliminary study of morphology for series A and D.

So far, a rather precise baseline of viscoelastic behavior, fracture toughness, and FCP response has been established for series A (varying stoichiometry) and a similar baseline of viscoelastic behavior

for series E (varying molecular weight of the epoxy). This baseline now serves as a standard against which the effects of other network variations may be compared with confidence.

As expected, an increase in the degree of crosslinking (or a decrease in \bar{M}_c) causes an increase in T_g (T_α), T_β (the temperature of a lower-lying transition), the breadth of the transitions, the rubbery modulus, and the swelling ratio. However, absolute values of T_g were higher than expected based on the experiences of others with the same system. Increased crosslinking also caused a decrease in the magnitude of $\tan \delta_{\max}$ near the T_g , the extent of stress relaxation, and the slope of the modulus-temperature curve at T_g . In most cases, the dependence of viscoelastic parameters on \bar{M}_c was similar for specimens having an excess or deficit of amine; the one exception was the transition slope, which varied differently depending on whether amine or epoxy was in excess.

One apparently new quantitative observation was made: that the dependence of a given viscoelastic parameter on \bar{M}_c is essentially the same whether a given value of \bar{M}_c was attained by varying the stoichiometry or by varying the molecular weight of the prepolymer. This fact should facilitate the comparison of effects of other network variations.

In contrast to results reported by others, the fracture toughness, K_{Ic} , was found to depend in an almost linear fashion on the amine/epoxy ratio. In comparison with even brittle linear polymers, all resins are quite brittle. FCP response was also studied using a special notching technique, which permits examination of brittle specimens. The stress intensity factor range, ΔK^F , required to drive a crack at constant velocity was found to behave in a manner generally similar to that of K_{Ic} , while the slope of the essentially linear curves of crack growth per cycle vs ΔK also appears to be independent of stoichiometry.

So far, effects of the distribution of segment lengths between crosslinks have been minimal. While no clear effect on dynamic mechanical parameters has been observed, there appears to be a tendency, at constant \bar{M}_c , for solubility, swelling, and possibly K_{Ic} , to be higher, the greater the proportion of longer chains between crosslinks.

Preliminary examination of specimens using electron microscopy (in transmission and scanning modes, as well as using replication) revealed considerable variation in features seen. While some results were consistent with the existence of a 2-phase microstructure, confirmation will require further study. Similarly, preliminary examination of fracture surfaces by optical microscopy revealed variations in surface features, depending on stoichiometry and ΔK level; these variations are yet to be interpreted.

Completion of the studies begun but not finished is in progress, and the synthesis and characterization of broader-distribution specimens and specimens containing imperfections such as network diluents, are planned.

SECTION II

INTRODUCTION

A. Statement of the Problem

Crosslinked polymer networks comprise some of the oldest and most useful polymers in modern technology. Because of their good dimensional stability, resistance to viscous flow at elevated temperatures, and resistance to water and solvents, resins based on such materials as epoxies, phenolics, polyesters, and aminoplasts find many applications, for example as components for mechanical and electrical uses, as composite matrices, and as protective coatings. Similarly, cured elastomers fill many common engineering needs.

Although such crosslinked or "thermoset" networks can often be made easily, with relatively little technical expertise, knowledge of structure-property relationships is in a much less satisfactory state than with thermoplastics (1-3).

Reasons include inherent complexity of the chemistry involved, sensitivity to processing conditions (often poorly controlled), intractability and difficulty of characterization, and a frequent lack of attention because many ordinary service demands can be met without sophisticated technical knowledge. However, as technology moves towards more and more demanding technical specifications, as in the case of aerospace materials, and towards more precise and demanding balances between costs, benefits, and materials conservation, much more must be learned about these materials. At present, the engineer would still like more information (in comparison to other materials) to use as a basis for materials selection or component design.

Thus, relatively little is known about such basic parameters as the degree and distribution of crosslinking as a function of composition, morphology and processing conditions, on the one hand, and as related to mechanical behavior such as creep, stress-strain behavior, and fracture, on the other.

B. Objective and Scope of the Program

a. Objective

The principal objective of this program is to determine the influence of crosslinking and network structure, in particular variations in the distribution of chain lengths between crosslinks, on the mechanical properties of polymers exhibiting high glass transition temperatures, T_g 's, above the temperature of use.

b. Scope

The scope of the program includes the study of both model and practical high- T_g resins, as follows:

1. Development of syntheses for, and characterization of, model crosslinked systems which permit control of the degree and distribution of crosslinks.
2. Synthesis and characterization of high- T_g epoxy resins having controlled degrees and distributions of crosslinks.
3. Characterization of viscoelastic behavior, including stress-strain response at high and low rates of loading, and creep or stress relaxation to reflect both short-term and long-term response.
4. Determination of static and cyclic (fatigue) fracture behavior.
5. Determination of typical morphologies by optical, electron and scanning electron microscopy.
6. Correlation of fundamental properties, especially composition and degree and distribution of crosslinking, with engineering behavior under static and cyclic loading.

B. General Discussion

As discussed in section A, the increasing use of crosslinked polymers for critical and demanding engineering applications requires much better fundamental knowledge about the molecular networks concerned, and the relationships between the network characteristics, synthesis or processing, and mechanical and other properties. A major reason for the deficiency in our knowledge is the complexity and variety of network structures which may be encountered (1,2). This complexity leads to several difficulties in experimental studies of the type concerned in this discussion.

First, it is difficult to characterize important characteristics of crosslink density (or M_c , the average molecular weight between crosslinks), the distribution in the length of chains between crosslinks, and the amount of material not incorporated in the network. Second, such characteristics are sensitive to process variables such as stoichiometry, temperature, and additives (2,5-22). A third problem is the tendency for the curing of many systems such as epoxy resins to be often complex with respect to both a multiplicity of simultaneous reactions and to morphology (2,7-9). From the simplest chemical point of view, an ideal polymeric network may be conceived of as a three dimensional system of connected chains forming a single macroscopic molecule (Figures 1a, 1b).

A "single molecule" is formed, because a Maxwell's demon may traverse the entire system, stepping only upon regular covalent bonds. Clearly, the behavior must depend on the tightness of the network with such a model; a network such as shown in Figure 1a would exhibit less swelling than the network in Figure 1b, which has a larger M_c . Even with such models for an "ideal" homogeneous unimolecular network, however, a problem arises, for in many real cases (Figures 1c, 1d) the lengths of chains between crosslinks may vary depending on the structure of the monomers or prepolymers, or on the vagaries of reaction kinetics. Of particular interest to this study is the effect of a distribution in M_c .

Furthermore, as shown in Figures 1e to 1h, a real polymer network is usually quite different from the ideal in structure. Not only do loops and dangling chain ends detract from the effectiveness of the structure, but shorter chains, either linear or branched, may exist without direct chemical connection to the network. Also in some cases reactive diluents such as styrene oxide may be added reacting at one end of the molecule and leaving the other dangling. Such entities largely serve to dilute the network, and tend to adversely affect physical and mechanical properties (1).

Finally, the topology and morphology of the networks may vary still more from the picture presented (2). Considerable evidence suggests that at least in some cases composition may be quite heterogeneous, even to the point that distinct phases may coexist, especially in the neighborhood of interfaces (1,8,9,13,22,23). Indeed, in such cases a better model might be an inverted version of, for example, Figure 1g, with highly branched or crosslinked domains embedded in a lower molecular weight matrix; Figure 1h illustrates such a domain model, as well as the general case of compositional heterogeneity (noting that phase boundaries need not be sharp). Variations may also exist if one of the multifunctional reactants has itself a distribution of molecular weight between its functional groups (Figure 2); such variations are characteristic of epoxy resins.

Typical methods for study of networks have been directed primarily at determining an average value for M_c , and have been mainly based on stoichiometric predictions, swelling, elastic moduli, creep, mechanical damping, and glass transition behavior (1,2; see also section B.b). Thus, classical theories developed by Flory (24, chapter IX) and others (1,2) have served to predict gelation and crosslinking in a statistical way, albeit to an approximation which may or may not be a good one (2). In the case of vulcanized rubbers, which exhibit high values of M_c (say, 5000), much understanding of elastomeric networks has already been achieved. While our knowledge remains incomplete, the theory of rubber elasticity (1, chapter XI), the Flory-Rehner swelling theory (1, chapter IX), and the theory of viscoelasticity (25) provide guideposts for determining not only chemical properties such as crosslink density, but

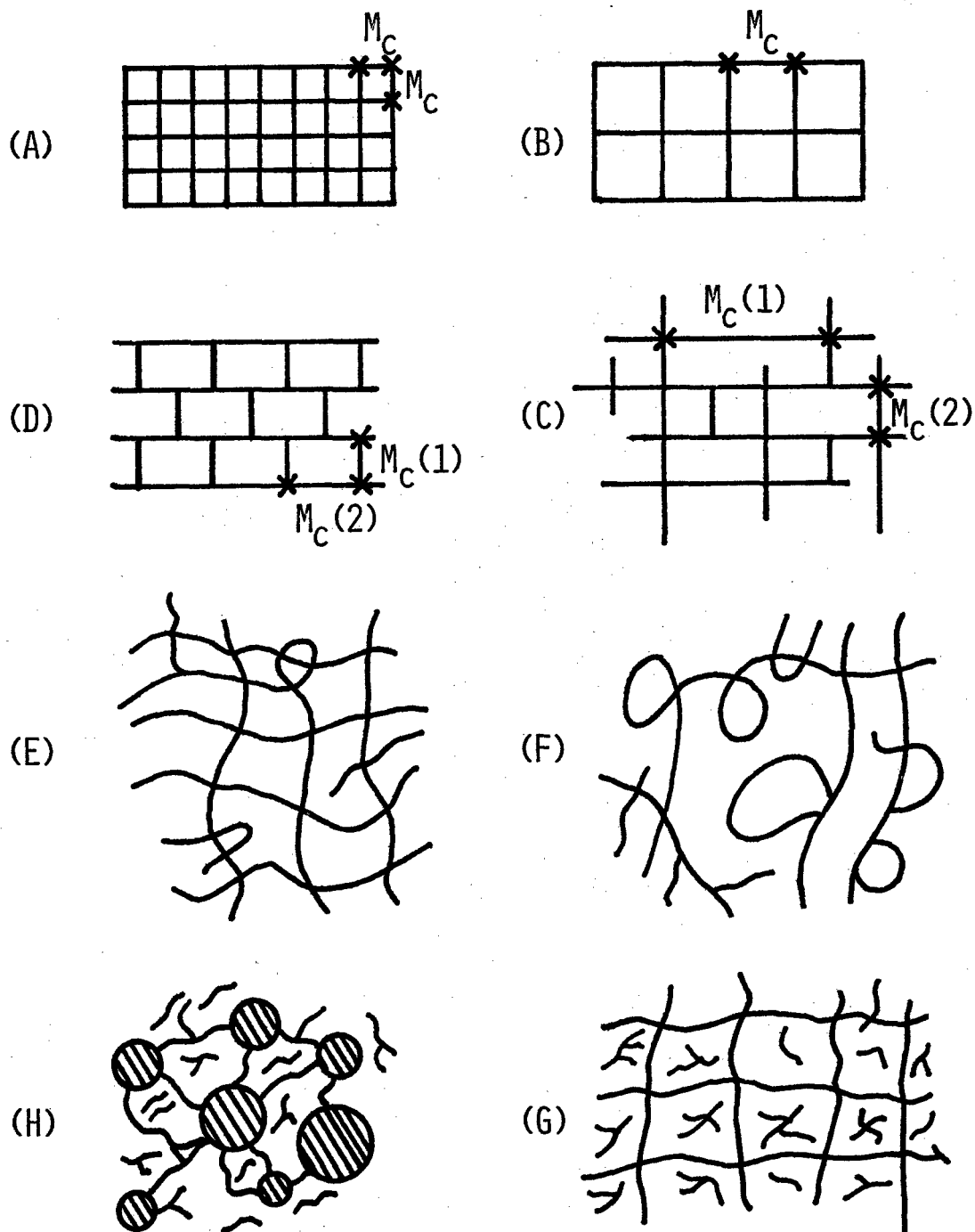


FIGURE 1: SCHEMA SHOWING TYPICAL VARIATIONS IN NATURE AND COMPOSITION OF CROSS-LINKED POLYMER NETWORKS (AFTER REFERENCE 2).

also a practical basis for estimating modulus, creep, stress-strain behavior, and fracture (26-33). However, treatment of the distribution of crosslinks has constituted one of the unsolved problems of polymer science. Nevertheless, it should be possible (see section III below) to measure the distribution of crosslinks by tagging them with heavy atoms and obtaining the low-angle X-ray scattering function, as has been done with linear polymers to find mean end-to-end lengths (34,25).

At room temperature, all such elastomers, of course, are above their glass transition temperature, T_g . If the crosslinked polymer is below its glass transition temperature, its molecular chains are incapable of long range coordinated motion, and the material becomes stiff and glassy. Such "thermoset" resins are typified by a variety of commercial materials, including phenolformaldehyde resins, melamine resins, crosslinked polyesters, and epoxy resins. Unfortunately, with materials of this type, which exhibit high degrees of crosslinking and great chemical complexity ($M_c \ll 5,000$, ~ 300 for some common epoxies), equations useful for elastomers tend to fail and require empirical modification (2), and in addition many characterization parameters in the glassy state are insensitive to the nature of the crosslinking. Moreover, as pointed out cogently by Nielsen (1,2), there is surprisingly little fundamental study of mechanical behavior using materials characterized to the limits of the state-of-the-art. To be sure, there are exceptions, for example, recent studies of epoxy behavior by a number of authors (6,7,14-19,36-38), but studies correlating fundamental and engineering behavior are not as common as might be supposed.

Another difficulty with gelling or thermosetting systems is that, as pointed out long ago by Nielsen (8) and others (2), and more recently by Gillham (5), the temperature of cure plays a role far beyond that of simply altering reaction rates in a chemical sense. As curing proceeds at a given nominal temperature, the network develops and its T_g increases. However, when the T_g of the network reaches ambient temperature (which may exceed the nominal temperature due to adiabatic self-heating), the rate of further crosslinking is drastically reduced due to slowing of reactant diffusion by the stiffening of the network. Thus, if the specimen is heated to above its curing temperature, as might well be the case in a modulus-temperature study, additional curing may occur during the test itself. Information about the network deduced from such tests is relevant only to the material subjected to the additional thermal history of the test, not to the original specimen as cured. Clearly, the curing temperature must be higher than the maximum test temperature if one is to achieve a network which will be stable during testing.

In summary, because of the importance of thermoset resins to present and future technology, we need much better experimental and theoretical understanding of the relationships between processing, the

network formed, and its behavior. At present, detailed empirical or semi-empirical studies are relatively few in number, especially with respect to fracture behavior.

SECTION III

TECHNICAL APPROACH

From the standpoint of relevance to the engineering applications, an epoxy resin system would be of considerable interest. Although the chemistry is complex, the systems are easily adaptable to specimen preparation, an increasing number of quantitative studies relating at least average or relative network properties such as M_c to stoichiometry and curing conditions have appeared (5-23,36-40). In several studies by others and this group (7,39,40), it has been possible to demonstrate that full curing can be effectively obtained using special cure histories. Also, at least some qualitative evidence is available relating viscoelastic parameters such as damping to the breadth of the presumed distribution of crosslinks (2), and some evidence is available on stress-strain behavior (7,36), fracture (28,29), and impact strength (36), the latter as a function of M_c . Disadvantages include difficulty in precisely controlling the distribution and nature of crosslinks (due to the fact that commercial resins usually exhibit a distribution of molecular weight) and in directly measuring the crosslink distribution. Nevertheless, it seemed reasonable to conclude that a thorough characterization of viscoelastic behavior in blends of epoxy resin should enable correlation of the distribution of M_c and other network variable with ultimate behavior under static and cyclic loading. Existing studies were of insufficient scope to permit such a correlation.

To complement this study, and in a sense to calibrate it, it seemed desirable to also study a still more definable model system. For this purpose a novel network system developed by Bamford and others was selected (for a review, see reference 4). This system, which is described in detail below (section IV) has several advantages. It is versatile chemically, well tested and studied in the laboratory, and, being free-radical in nature, readily interpretable in terms of statistical calculations and predictions of cross-link densities and distributions. While average densities are still obtained, due to the statistical nature of free radical polymerizations, it should be noted that fairly narrow distributions of M_c would be obtainable (and quite predictable) in the case of polystyrene. In fact (41), the ratio of weight to number-average molecular weight must be 1.5 in this case (termination by combinations) - a value much lower than is found for most other free-radical polymerizations (values usually > 2), and close to the range characteristic of the living polymer technique, 1.1 to 1.5. Another advantage is that the system selected inherently contains multiple heavy halogen atoms at the crosslinks, thus permitting direct calculation of the distribution from X-ray scattering (34,35); M_c can be

varied easily, and synthetic distributions can easily be prepared by mixing prepolymers with different M_c values. Finally, the system can be designed to contain a predictable proportion of linear chains or branches, and to be controllably degraded to give branched species. All these advantages can be gained without the sensitivity of network characteristics to whether or not curing temperature is above the test temperature. In fact, as the gel point is approached, the reaction may autoaccelerate (in contrast to the retardation with epoxies). However, if such an effect is observed, M_c values can be calculated from knowledge of polymerization parameters (4); in any case, autoacceleration can be avoided by keeping rates and conversions below critical values, which for polystyrene are reasonably high.

In short, two complementary candidate systems were selected: one a potentially good, though not perfect, approximation to an ideal network model of academic interest as a material, and the other a less good approximation to an ideal model, but a system with existing engineering application. Thus, the two approaches should be considered as a dual model system: a primary, well definable model coupled with a model which is less easily defined, but of greater technical per se. The primary model should serve to illuminate and calibrate the secondary model, the epoxy system; the two should be considered together.

Specific discussions of each system follow in sections IV and V.

SECTION IV

SYNTHESIS OF MODEL NETWORKS

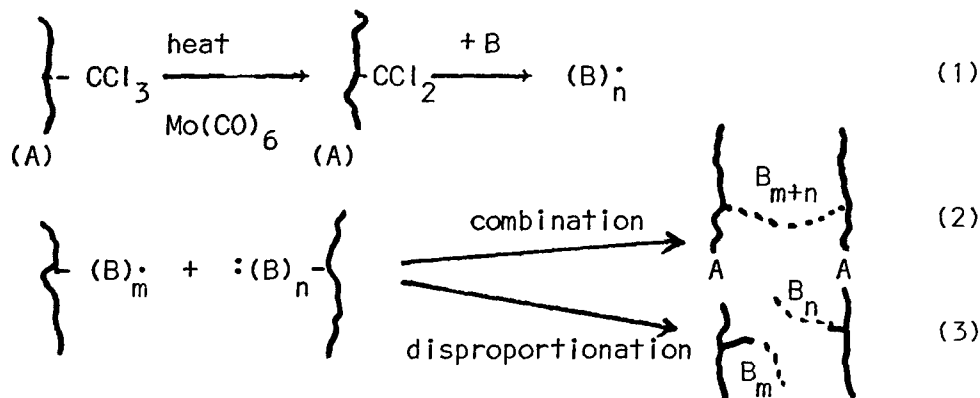
A. Introduction

The principal aim of this research is to show how the mechanical behavior of glassy networks depend upon the distribution of M_c values and how free or dangling chains alter behavior. Polystyrene, with a glass transition temperature, T_g , of $+100^\circ\text{C}$ was selected as the model network, because its glass temperature is above room temperature, its network structure is susceptible to control, and its general physical behavior is well known.

Two objectives were sought: (1) To prepare networks with two distributions of M_c through the use of the Bamford synthesis (4) and (2) to produce controlled network structures through the use of decrosslinking. The latter makes use of acid anhydride monomers, which can easily be hydrolyzed.

a. Bamford Networks

Model networks of polystyrene, with easily degradable crosslink sites, can be synthesized using a novel variation of the Bamford technique (4). Bamford et al. have made crosslinked polymers, designated as AB crosslinked copolymers, using vinyl trichloroacetate, or similar chlorinated monomers X in polymer A. Such sites serve as controlled initiation points for formation of polymer B. A variety of photochemical techniques provide convenient initiation. A single network is formed if the second polymerization terminates via a combination reaction, as shown below.



Since Bamford was primarily interested in a novel type of graft copolymer, monomer A and monomer B were different. However, as mentioned above, for our model network studies of thermoset plastics, polystyrene will serve

for both reactions, because of (a) its otherwise well-known behavior, (b) its high glass transition temperature, 100°C. In addition, polystyrene radicals undergo termination by combination, giving a narrower molecular weight distribution than otherwise (41). Branching can be introduced controllably by adding known amounts of a photosensitive solvent (4).

The networks can also be made controllably degradable if anhydride groups can be introduced at some or all of the crosslink sites. For example, it should be possible to incorporate p-carboxystyrene-trichloroacetic acid mixed anhydride, PCSTAMA, or trichloroacetic acid-acrylic acid mixed anhydride, TCAAAMA (monomers not hitherto synthesized) in polymer A, to serve as the initiating site for polymerization B. The anhydride junction could then be easily broken by soaking in hot water, ethylene diamine, or aqueous ammonium hydroxide.

The amount of PCSTAMA or TCAAAMA and the amount of monomer B added should control the average molecular weight of chain segments between crosslink sites, \bar{M}_C , in polymer A and B separately. Therefore, two \bar{M}_C values will be required to characterize each network. Incorporation of p-2,2,2, trichloroethylstyrene in greater or lesser amounts should generate a stable crosslink site. On hydrolysis of a polymerized B chain having one end joined via the anhydride, and the other end joined stably, a branch will be generated. If both ends contain the anhydride, a free chain of known average molecular weight will be generated.

Thus, several distinct model polymers can be synthesized in a controlled manner via the above reaction scheme:

- (1) Linear polystyrene of known molecular weight.
- (2) A network of known average crosslink density, containing two separate but controllable and known \bar{M}_C values (the distribution of \bar{M}_C being known precisely, as it is governed by the well understood kinetics of styrene polymerization).
- (3) A network containing known amounts of branches or free polymer, the molecular weights of the branches or free polymer being determined by known kinetic parameters.
- (4) Synthetic distributions made by mixing reactions having different spacings between potential crosslink sites. Again, the distributions will be calculable from available information.

b. Specific Syntheses Planned

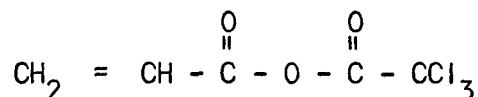
It was decided to begin network syntheses using the following comonomers with styrene:

(1) p-2,2,2-trichloroethyl styrene (PCES), for the introduction of permanent crosslinks in Bamford networks.

(2) the mixed anhydride of p-carboxy styrene (PCS) and trichloroacetic acid (PCSTAMA), for the introduction of degradable crosslinks.

(3) the mixed anhydride of vinyl phenylacetic acid (VPA) and trichloroacetic acid (VPATAMA), on a alternate for PCSTAMA.

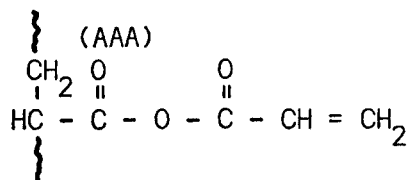
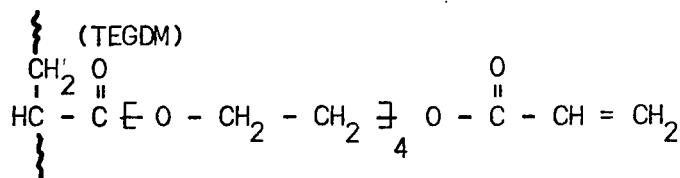
However, PCES and VPA proved to be unavailable commercially, and PCS was quoted at a prohibitive price (45), \$650/25g. While a synthesis for VPA is known (46), it was decided instead to attempt the



synthesis of the mixed anhydride of acrylic acid with trichloroacetic acid (TCAAAMA), which would involve only common reagents.

The latter new monomer should be capable of copolymerizing with styrene, to yield through the Bamford reaction, a suitable crosslinked network. The anhydride component could then be hydrolyzed to yield a product having the characteristics of either a linear polymer, or more interestingly, one with a lower level of crosslinking. The TCAAAMA can also be mixed with a conventional crosslinking agent in various proportions, to produce new model networks having both permanent and degradable crosslinks.

Since the synthesis of TCAAAMA involved considerable difficulty it was decided to confirm the feasibility of using degradable crosslinks by synthesizing polystyrene containing acrylic acid anhydride (AAA) as a hydrolyzable crosslink. For a similar reason, in order to examine viscoelastic behavior in the rubbery region in a system containing hydrolyzable crosslinks, poly(ethyl acrylate)s were prepared containing tetraethylene glycol dimethacrylate (TEGDM) and AAA - the former



yielding permanent, and the latter hydrolyzable, crosslinks.

So far, a crude product believed to be TCAAAMA has been obtained, copolymers of styrene and ethyl acrylate with AAA have been successfully

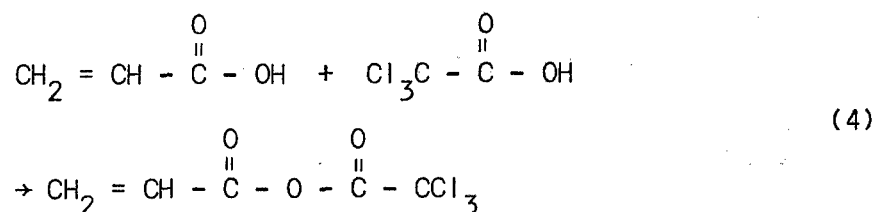
synthesized, and hydrolysis of the crosslinked latter copolymers demonstrated.

Also, the Bamford synthesis itself was tested successfully, using CCl_4 and trichloroacetic acid as initiators. Experiments using 2,2,2-trichloroethyl acrylate as a comonomer with styrene, and Mo(CO)_6 as catalyst at 80°C were unsuccessful, but are being repeated using an inert atmosphere.

B. Experimental Details, Results, and Discussion

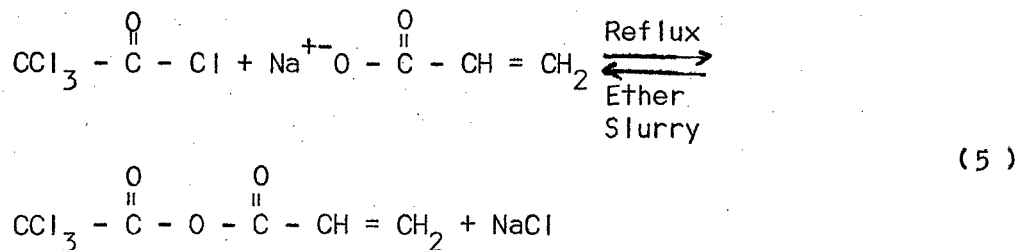
a. Mixed Anhydride Synthesis

As mentioned above, the synthesis of the mixed acid anhydride of acrylic acid and trichloroacetic acid was more complex than originally anticipated. The reaction desired is the following:



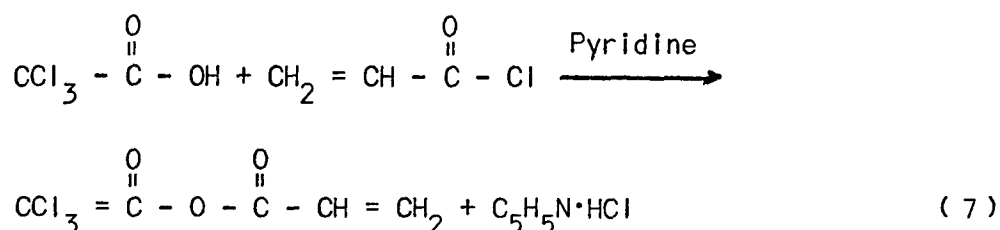
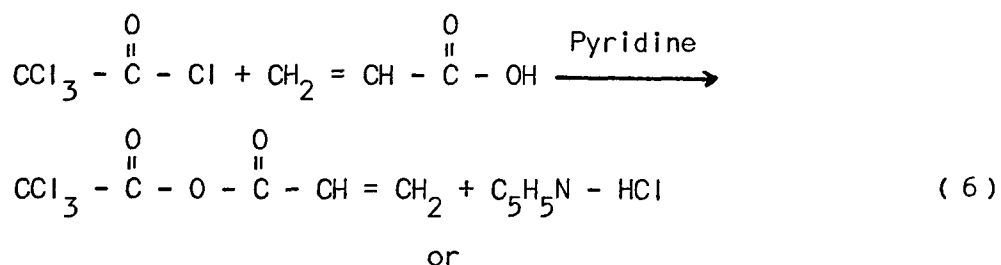
A review of standard literature sources revealed that the proposed compound had never been prepared before. After the first few unsuccessful attempts, informal consultation with a synthetic organic chemist, Dr. Ned Heindel, Department of Chemistry, was also arranged. The specific approaches are discussed below.

1. Reaction of the acyl chloride with a carboxylic salt (42,43).



Probably due to the heterogeneous nature of the system the kinetics of anhydride formation were slow, and no product was recovered. In order to effect some solution of the salt which would aid in speeding up the reaction, various polar solvents such as dimethyl formamide were tried, without success. Acetonitrile (dipole moment = 3.92 D) was unsuccessfully used in a Soxhlet extraction of the salt. This route has been set aside.

2. Reaction of the acyl chloride with a carboxylic acid (42,44).



Reaction (7) gave better results than reaction (6).

During these trials, the need for a rigorously dry atmosphere became apparent. Presently a leak-proof dry box with phosphorous pentoxide as drying agent and a continuous dry nitrogen flow (no water and no oxygen) is being employed.

An exact description of the best procedure to date, which did yield a crude product, is as follows:

A solution of 0.1 mole of dry pyridine is made in 50 ml of dry benzene and 0.1 mole of acryloyl chloride is added dropwise with stirring. The temperature rose (to about 60 °C) and a yellow pyridinium complex separate. While stirring is continued, 0.1 mole of trichloroacetic acid in benzene solution is added dropwise; 0.2 percent of antioxidant 330 (Ethyl Corporation) was also used. The temperature changes little, and soon stirring becomes difficult to continue due to the formation and coagulation of solids, after stirring is stopped (about 30 min), a distinct red liquid phase separates on the bottom of the reaction mixture. The identity of the red liquid, which becomes more viscous after volatiles are removed, is still uncertain. It is only slightly soluble in benzene, styrene, and carbon tetrachloride.

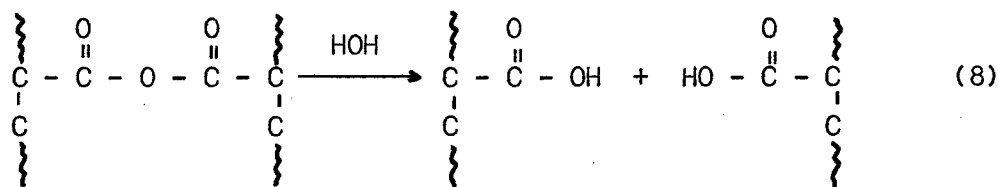
Distillation of the product caused polymerization. However, the benzene could be removed under vacuum conditions. An elemental analysis of the liquid showed significant contamination with pyridine and pyridine hydrochloride.

Efforts are now being made to find a selective solvent. An anti-oxidant is being added (0.2%) to reduce the tendency to polymerize for the red liquid may be actually an oligomer of some sort. A side reaction requiring attention involves the addition of HCl across the double bond.

Preliminary attempts to copolymerize the crude product with styrene are in progress.

b. Synthesis and Hydrolysis of Polystyrene-AAA Networks

Model experiments demonstrated the feasibility of synthesizing polystyrenes containing degradable crosslinks consisting of AAA units.



Control polystyrenes with stable crosslinks were also prepared using divinyl benzene (DVB) as crosslinking agent.

Samples of polystyrene were synthesized in bulk (temperature, 60°C; initiator: lauroyl peroxide, 0.4%; time, ~3 days). Three types were prepared: (1) linear polystyrene, (2) polystyrene containing 0.2 wt. percent AAA, and (3) polystyrene containing 0.2 wt. percent DVB. Crosslinking in the latter two cases was demonstrated by the fact that specimens swelled by a factor of about 10 in toluene, but did not dissolve. Thus the AAA, as well as the well known DVB, introduces true chemical crosslinking. Although initial experiments were unsuccessful, suitable conditions for the hydrolysis were found more easily than expected.

First, samples treated in dilute NaOH (0.1 N), boiling aqueous NaOH (0.1 N), or dilute HCl (0.1 N) showed no detectable increase in swelling. Hence, no hydrolysis had occurred - a fact to be expected in view of the limited hydrophilic character of the networks. Samples were also swelled in another potentially hydrolytic agent, pyridine, which swells PS networks as much as toluene. The samples were then placed in water where they turned white and brittle. However, when placed in toluene, the whiteness disappeared and swelling occurred to the same extent as with untreated samples. (Note: linear PS dissolves in pyridine.) Again, no hydrolysis had occurred. Since water is soluble in pyridine, various pyridine:water mixtures were used to effect hydrolysis of the anhydride bonds; no swelling occurred in such mixtures. Some samples were then left to soak in pyridine:water mixtures for about 3 weeks. Since these samples swelled much more in toluene than untreated samples, at least partial hydrolysis must have occurred. Moreover, it was also found that samples swelled in pyridine and left in pyridine dissolved completely in about 2 days. Thus complete hydrolysis was obtained.

However, best results were obtained using ethylene diamine, a very basic liquid. When samples were soaked in ethylene diamine, little swelling occurred. However, after treatment for less than one hour, hydrolysis had occurred, for the specimens could be dissolved in toluene. Solutions of a few drops of ethylene diamine in toluene also dissolved the networks. In contrast, PS crosslinked with DVB, which contains no hydrolyzable groups, was unaffected by ethylene diamine.

Proof of the reversibility of crosslinking was adduced by the following experiment, using a sample of linear PS and one containing AAA crosslinks.

After hydrolysis of the latter polymer in ethylene diamine, both polymers were dissolved in toluene, and the intrinsic viscosities, $[\eta]$, determined. Viscosity-average molecular weights, \bar{M}_v , were calculated for both polymers using the Mark-Houwink relationship ($[\eta]=KM^a$), with constants from the Polymer Handbook (47).

<u>Polymer</u>	<u>\bar{M}_v</u>
Linear Polystyrene	3.3×10^5
AAA containing PS, hydrolyzed	3.2×10^5

These results, identical within experimental error, indicate that the original polymerization kinetics were not significantly affected by the presence of the AAA, except to introduce crosslinking.

Network characteristics, including the crosslink density, are described in section V-B.

c. Synthesis and Hydrolysis of Poly(ethyl acrylate) - AAA Networks

The photochemical method of synthesizing poly(ethyl acrylate) (PEA) networks in bulk with UV light has been previously described (48). In brief, benzoin was used as the initiator (0.3 percent), acrylic acid anhydride (AAA) as the labile crosslinker and tetraethylene glycol dimethacrylate (TEGDM) as the permanent crosslinker. The chain transfer agent 1-dodecanethiol (1-Doth) was employed to control molecular weight. This last was necessary because side reactions during the polymerization of ethyl acrylate lead to gelation even without added crosslinker. The exact levels of TEGDM, AAA, and 1-Doth employed are shown in Tables 1, 2 and 3.

Decrosslinking studies were done using ethylene diamine and ammonium hydroxide. As mentioned in section IV-b, it was found that ethylene diamine was effective in decrosslinking polystyrene networks; however, soaking the PEA for 24 hours in 28% NH_4OH was very effective,

and this reagent was adopted for the present study.

d. Conclusion

In summary, the PEA-AAA system shows that AAA crosslinks can be easily and selectively hydrolyzed to yield a wide range of viscoelastic behavior patterns. In combination with permanent type crosslinks, AAA systems were made and hydrolyzed to give novel structures between those of a regular crosslinked network and a branched soluble system.

SECTION V

PROPERTIES OF MODEL NETWORKS

A. Introduction

The physical and mechanical behavior of polymer networks depends upon the crosslink density, the distribution of molecular weights of chain segments between crosslinks, M_c , the number of free or dangling chains, and the temperature. Three general temperature regions have been identified: (1) above the glass-rubber transition region, where the material behaves like an elastomer, (2) within the glass-rubber transition region, where the material is viscoelastic, and (3) below the glass-rubber transition region, where more or less glassy behavior predominates. The experiments performed under this contract are primarily directed towards region (3), with some effort placed in region (2) to show the changes in behavior that may be expected as the polymer chains gain mobility. Region (1) is of interest only in the analytical determination of crosslink density (see section a, below).

Properties of particular interest include creep or stress relaxation (to determine long-term behavior), stress-strain response, and fracture characteristics. Progress to date is discussed below.

Since the synthesis of the AATAMA has been more difficult than anticipated, experiments have been directed not only to PS systems crosslinked with AA, but also to poly(ethyl acrylate) systems crosslinked with diethylene glycol dimethacrylate (DEGM) and AAA. The latter systems are especially convenient for characterization of effects of reversible crosslinking on viscoelastic behavior.

B. Experimental Details, Results, and Discussion

a. Crosslink Density

While absolute values of crosslinking cannot generally be obtained with densely crosslinked systems such as epoxy resins (2), approximate values in more "open" systems can be estimated in several ways, the most common being by swelling and by measurement of the modulus in the rubbery state.

Thus values of \bar{M}_c , the average molecular weight between crosslink sites, were obtained by swelling samples before and after hydrolysis in methyl ethyl ketone (MEK) and using the Flory-Rehner equation (24,49):

$$\frac{1}{\bar{M}_C} = \frac{\ln(1-v_2) + v_2 + \chi_{12} v_2^2}{\rho V_O (v_2^{1/3} - v_2/2)} \quad (9)$$

where v_2 represents the volume fraction of polymer in the sample at equilibrium, V_O is the solvent molar volume, of density ρ , and χ_{12} the polymer-solvent interaction parameter was taken as 0.47. In each case volumes were assumed to be additive. Values reported in Tables 1-3 were based on actual weight gain, $\bar{M}_C(\text{wg})$, and on length change, $\bar{M}_C(\text{L})$.

In addition, values of \bar{M}_C were estimated from Young's modulus, E , by means of the theory (24) of rubber elasticity, to give $\bar{M}_C(E)$:

$$\bar{M}_C(E) = \frac{3\rho RT}{E} \quad (10)$$

where ρ is the density, R the gas constant, and T the absolute temperature.

Results for the various systems are discussed below:

1. PS-AAA Systems. In this case, the Flory-Rehner equation (equation 3) was employed to estimate \bar{M}_C . Based on the increase in weight of the swollen sample, v_2 was found to be 0.0802. Based on the increase in length, $v_2 = 0.102$. Using $\chi_1 = 0.47$, the \bar{M}_C values were then estimated, and compared with the values calculated from the known addition of AAA in Table 1.

Table 1. \bar{M}_C for PS-AAA Crosslinked Networks.

Method	v_2	\bar{M}_C
Weight increase	0.0802	1.1×10^5
Length increase	0.102	4.5×10^4
Calculated*	-	3.4×10^4

* Assumed infinite chain length.

Clearly, reasonable agreement (at least in order of magnitude) was obtained, in view of the precision and accuracy inherent in the measurements and calculations. Probably, the "weight increase" technique above is more accurate than the "length increase" method. However, the crosslink

levels are very low, making accurate assessments via the Flory-Rehner equation difficult.

Ordinarily, the swelling method yields values for M_c smaller than those estimated from composition because of the presence of physical crosslinks (i.e., chain entanglements). The inverted situation suggests that either the AAA is inefficient (resulting in dangling unreacted groups, or both vinyls being incorporated in the same chain), or that the anhydride bond was partly hydrolyzed before the final measurements. Hydrolysis is the more probable cause. While the AAA may have been partly hydrolyzed as received, careful handling procedures are obviously needed (for example, use of a dry-box).

2. PEA-AAA and PEA-TEGDM Networks. In Tables 2-4, values of \bar{M}_c via both swelling and modulus measurements are compared to the theoretical values, $M_c(th)$, calculated on the basis of actual amounts of crosslinker added, assuming infinite primary chain length. Experimental values of \bar{M}_c are shown to agree with theory in Table 1, except for the far right hand column. With no added crosslinks, a value of \bar{M}_c equal to the molecular weight itself is expected, but since infinite chains were assumed in the $M_c(th)$ calculations, a value of ∞ is reported for the case of no crosslinks. Finite values are noted experimentally, with much smaller values obtained via the modulus experiment. This last is because physical entanglements count effectively as crosslinks. None of the materials in Table 1 would dissolve after hydrolysis, although increased swelling values were noted.

Table 2. Characterization of Crosslinked PEA Networks.

1-DOTH	0						
AAA	1.2 ml	0.56	0.56	0.28	0	0	0
TEGDM	0	0	1.4	0.70	2.9	1.4	0
$\bar{M}_c(L) \times 10^4$	0.9	1.3	0.9	1.6	0.8	1.5	135
$\bar{M}_c(wg) \times 10^4$	1.3	1.9	1.0	1.8	0.8	1.7	110
$\bar{M}_c(th) \times 10^4$	1.0	2.0	1.0	2.0	1.0	2.0	∞
$\bar{M}_c(E) \times 10^4$	0.9	1.2	0.9	1.3	0.7	1.2	1.7

EA: 100 ml

Benzoin: 0.4 g

Table 3. PEA Networks with 0.68% 1-Dodecanethiol.

1-DOTH	0.68 ml						
AAA	1.2 ml	0.56	0.56	0.28	0	0	2.4
TEGDM	0	0	1.4	0.7	2.9	1.4	0
$\bar{M}_c(L) \times 10^4$	3.1	6.7	2.2	8.5	2.2	-	1.2
$\bar{M}_c(wg) \times 10^4$	2.9	5.2	2.7	7.6	2.4	-	1.4
$\bar{M}_c(th) \times 10^4$	1.9	3.9	2.0	4.0	2.0	4.1	1.0
$\bar{M}_c(E) \times 10^4$	0.8	1.2	0.9	1.4	0.8	1.2	0.6
After Hydrolysis (NH_4OH)							
$\bar{M}_c(L) \times 10^4$	4.1	9.0	4.0	10.0	2.4	-	-
$\bar{M}_c(wg) \times 10^4$	5.7	8.7	3.5	8.4	2.7	-	-
$\bar{M}_c(E) \times 10^4$	1.2	2.1	1.0	2.1	0.8	1.0	1.3

EA: 100 ml

Benzoin: 0.4 g

Table 4. PEA Networks Capable of Complete Hydrolysis.

1-DOTH	1.36 ml					2.7
AAA	1.2 ml	0.56	0.56	0.28	2.4	2.4
TEGDM	0	0	1.4	0.7	0	0
$\bar{M}_c(L) \times 10^5$	1.8	3.9	0.44	5.3	1.1	0.8
$\bar{M}_c(wg) \times 10^5$	1.8	4.0	0.4	4.7	0.8	0.6
$\bar{M}_c(E) \times 10^4$	1.4	2.0	1.2	3.0	0.75	0.78
After Hydrolysis (NH_4OH)						
$\bar{M}_c(L)$	SOL	SOL	0.54	6.2	SOL	SOL
$\bar{M}_c(wg)$	SOL	SOL	0.5	5.89	SOL	SOL
$\bar{M}_c(E) \times 10^5$	3.5	5.2	0.36	2.6	1.6	1.6

EA: 100 ml

Benzoin: 0.4 g

In an attempt to counteract the accidental gelation reactions, various quantities of 1-dodecanethiol were introduced to promote chain transfer reactions. As shown in Tables 3 and 4, at a level of 1.36% 1-Doth or greater, the polymers are soluble after hydrolysis. The values of $\bar{M}_c(E)$ on the bottom row of Table 4 represent the limiting level of physical crosslinks only.

To summarize the effects of AAA on $\bar{M}_c(E)$, values are plotted in Figure 2 before and after hydrolysis for two different 1-Doth levels. (Note that a decreasing \bar{M}_c value indicates an increased crosslinking level).

b. Creep and Stress Relaxation

Creep response was investigated using Gehman (50,51) and Clash-Berg (52) type creep testers; also tensile creep studies were performed.

For stress relaxation, a special unit was used. The relaxation modulus $E(t)$ was calculated at time t from the equation

$$\frac{w \times 981}{A} = \frac{E(t)}{3} \left(\alpha - \frac{1}{\alpha^2} \right) \quad (11)$$

where w equals the weight applied, A is the cross-sectional area of the sample, and α is the elongation, equal to the final length over the initial length. For high elongations, the engineering strain $(2\alpha^2 + \frac{1}{\alpha})$ was employed for modulus calculations. Tests were confined to PEA-TEGDM Systems.

Results of the Gehman-type creep test are shown in Figure 3, for PEA containing 1.2% AAA, before hydrolysis. The reported T_g of this material, -22°C ., agrees well with the result, and a well defined rubber plateau is approached at -5°C . Addition of 0.68% of 1-Doth increases the rate of creep somewhat, as shown in Figure 4. After hydrolysis, the rate of creep was increased still more, as shown in Figure 6. Even though viscoelasticity increases from Figure 3 through Figure 4, to Figure 5, the actual glass transition temperature probably remains nearly the same, only the molecular weight distributions in relation to the crosslink levels were changed.

Stress relaxation studies on a series of networks is shown in Figure 6 and 7.

The effect of hydrolysis time is shown in Figure 8. The level of 1-Doth, 1.36%, permits solubility after hydrolysis, as noted in Tables 3 and 4. The TEGDM employed however, kept the networks intact. Note that only a small effect is noted on the behavior between 24 hours and

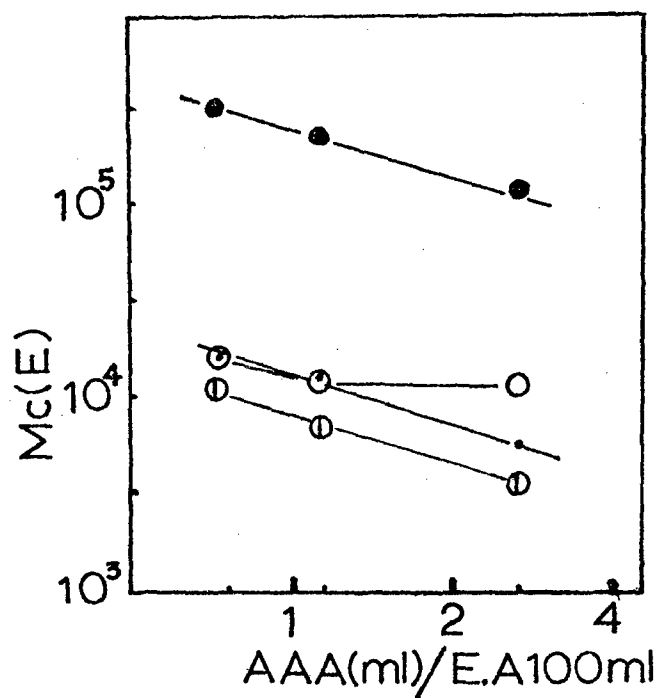


Figure 2. Values of $\bar{M}_c(E)$ as a function of AAA and 1-Doth levels, before and after hydrolysis.
 -●-0.68% 1-Doth before hydrolysis
 -○-0.68% 1-Doth after hydrolysis
 -•-1.3% 1-Doth before hydrolysis
 -●-1.3% 1-Doth after hydrolysis.

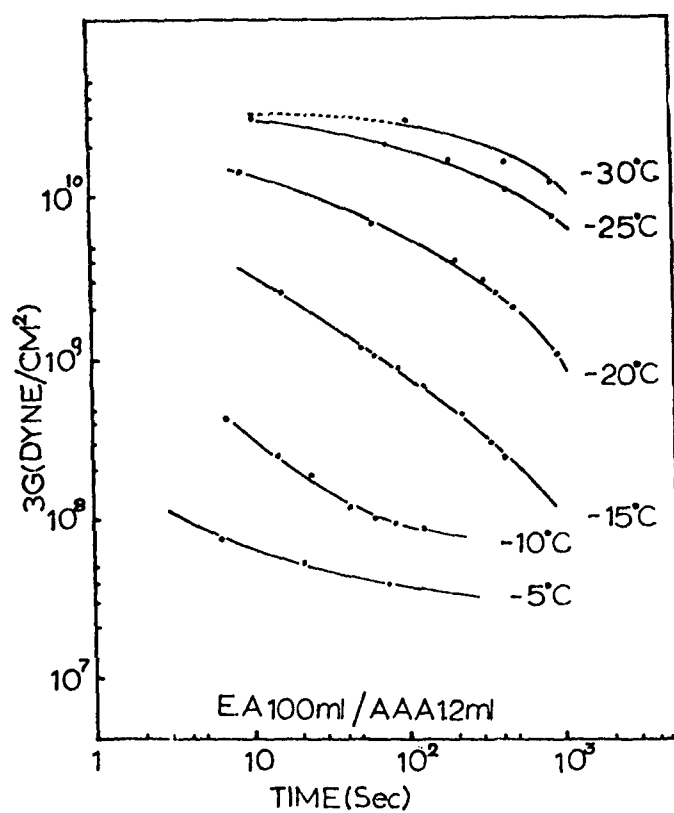


Figure 3. Values of $\log 3G$ vs. time in the glass transition temperature range of PEA.

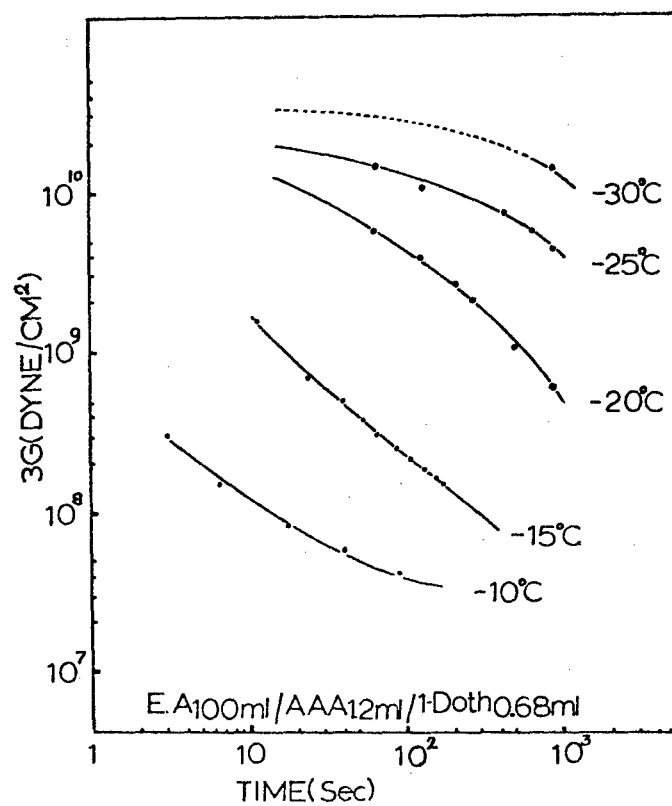


Figure 4. Values of $\log 3G$ vs. time for a series of temperatures for a material containing 0.68% 1-Doth.

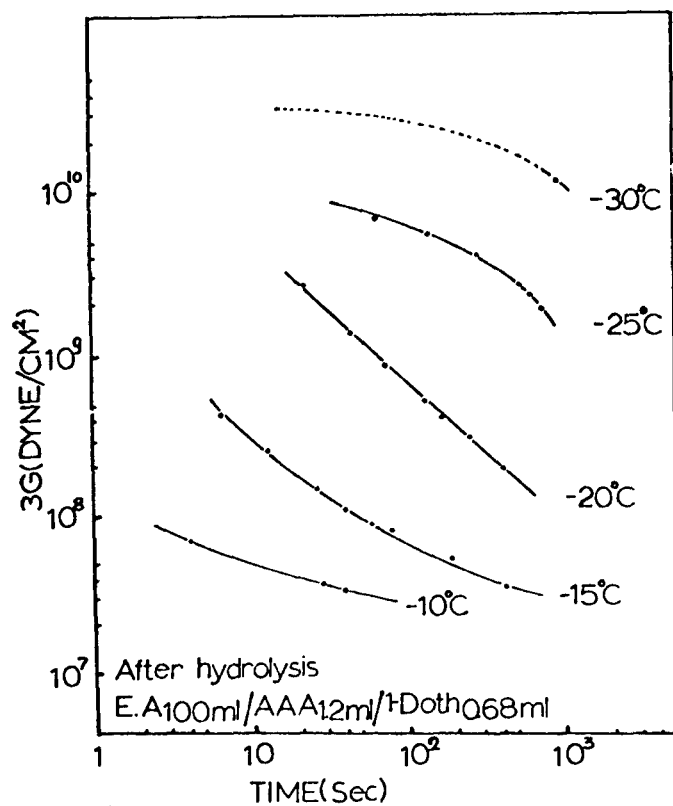


Figure 5. Log 3G vs. temperature for PEA, after hydrolysis, for a PEA containing 1.7 ml of AAA and 0.68% 1-Doth.

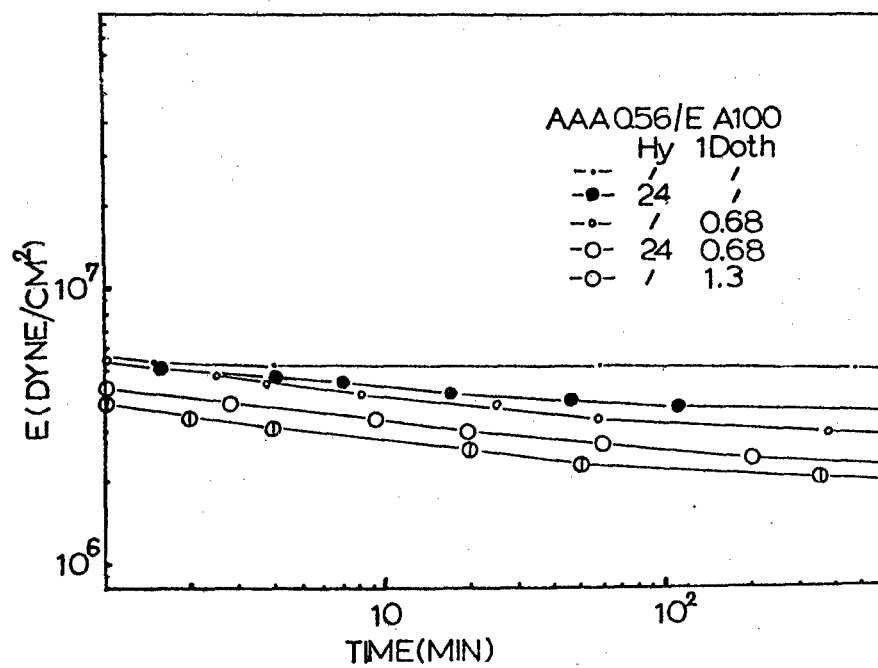


Figure 6. Stress relaxation of PEA networks before and after hydrolysis.

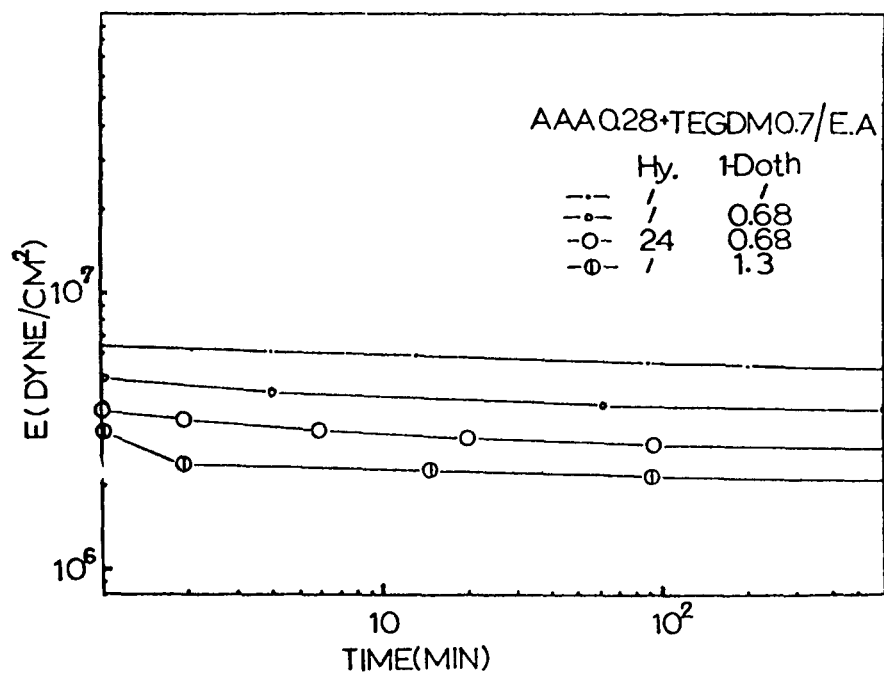


Figure 7. Stress relaxation of PEA networks containing both permanent and temporary crosslink sites.

48 hours of hydrolysis time.

The tensile creep modulus of several networks is shown in Figure 9. At a level of 1.36% 1-Doth, the network structures of the materials without TEGDM is seen to be completely destroyed. Creep was rapid enough to cause sample failure after only a few minutes.

Finally, Figure 10 summarizes the creep modulus behavior of hydrolyzed samples having various levels of 1-Doth. At 0.68% 1-Doth, a network is retained, and the modulus does reach a plateau. At 1.36% 1-Doth, the polymer is just soluble, and failure occurred after about one hour. At 2.7% 1-Doth, creep is much more rapid, due undoubtedly to the lower molecular weight remaining, and the sample failed after only a few minutes.

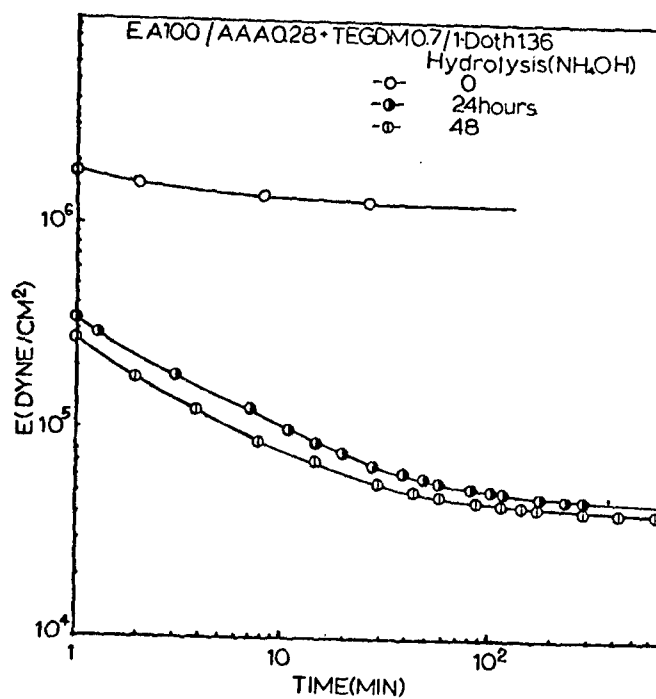


Figure 8. Stress relaxation of PEA networks as a function of hydrolysis time.

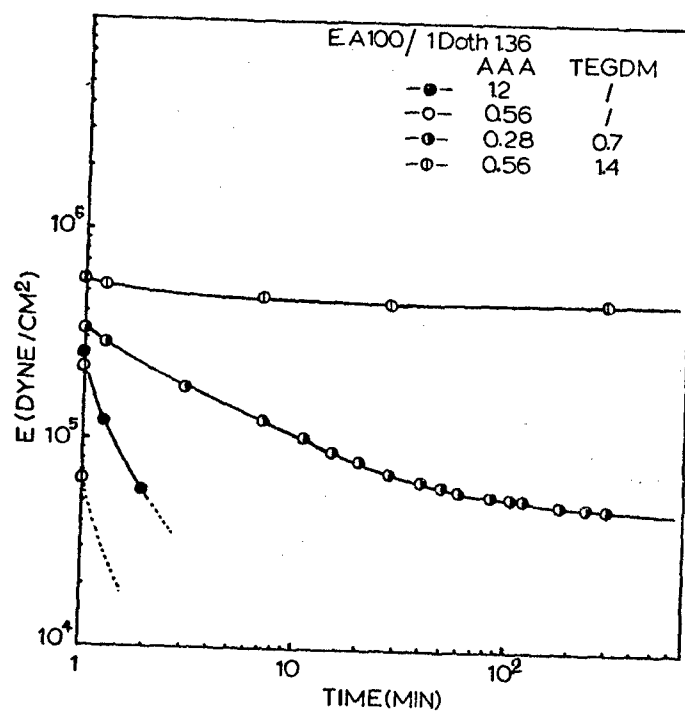


Figure 9. Tensile creep modulus of several PEA samples, after hydrolysis for 24 hours at 25°C.

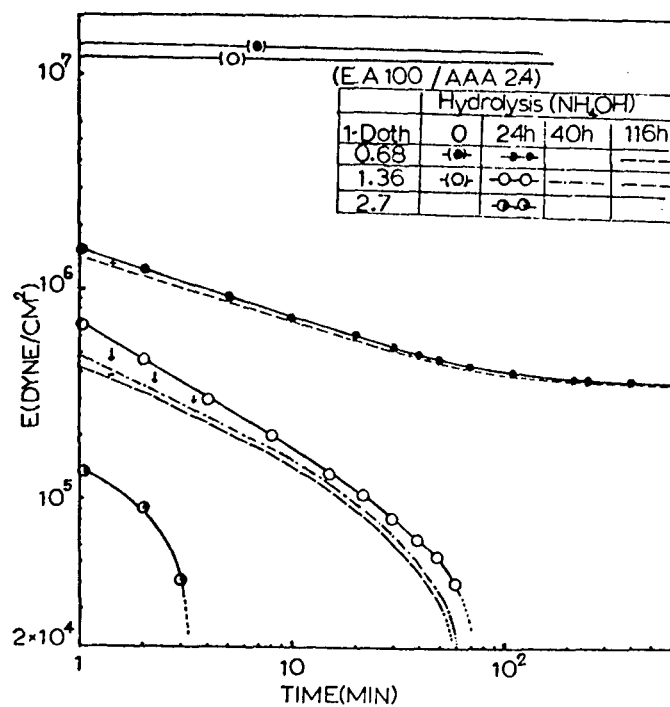


Figure 10. Creep modulus of samples having little or no network properties after hydrolysis for 24 hours at 25°C in 28% NH₄OH.

SECTION VI

SYNTHESIS OF EPOXY NETWORKS

A number of epoxy systems have been intensively studied over the last few years (5-23,36-40), most based on bisphenol A derivatives. Variations have included the nature of the epoxy resin or curing agent (10,11), the length between functional groups, which will help define M_C (11), temperature (5), and the introduction of reaction diluents, which may dilute the network and also alter the state of cure (7). Both amines and polyamides have been used; in the latter case (39,40), the M_C can be varied by changing the amide equivalent content.

For this study, one system considered for selection was the epoxy-amine-diluent system used by Whiting and Kline (7); (Epon 828-diethylene-triamine-styrene oxide.) The system has been characterized thoroughly in terms of % reaction of the epoxy groups, and concentrations of both -OH and -CH₂-O- groups followed as a function of amine and diluent (styrene oxide) contents. A wide variety of degrees of cure are obtainable, and also variations in M_C as a function of stoichiometry. Moreover, values of yield strength, ultimate tensile strengths and fracture energy have been obtained and related to process parameters. A similar system (Epon-828/methylene dianiline (MDA)) was also studied extensively by Bell et. al. (6,36-38), who critically analyzed the stoichiometric aspects of curing and also determined the effects of M_C in other amine-cured resins (by changing the molecular weight of the amine curing agent) on tensile and impact strength.

Bell (37) also showed that the presence or absence of an exotherm had no effect on the curing reaction, that nearly complete curing could be achieved in this system, and that predicted values of M_C agreed well with values estimated by experiment. Later, Selby and Miller (17) studied the Epon-828/MDA system extensively, with emphasis on the effect of stoichiometry on fracture toughness. Since this combination of studies provided excellent background in fracture behavior as well as other properties, the Epon 828-MDA System was selected as a standard of reference for this study.

Another advantage of this system is that no clear evidence for a two-phase structure has so far been adduced for gross heterogeneity of the type reported for other systems (2,8,22,23). Thus Selby and Miller (17) found evidence for craters and hillocks in the micrometer size range, but no relationship between these features and crack propagation behavior. Also, small angle X-ray studies (54) have revealed no evidence for a two-phase structure in the 50 Å to 100 Å size range, and, in these laboratories no evidence (based on modulus-temperature studies) for a two-phase structure has been observed for bisphenol-A-type resins fully cured with

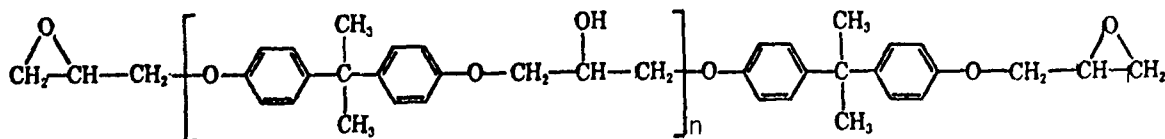
polyamides (39,40,55), though studies of this kind have been used to postulate a two-phase morphology (2,8). It may be noted that nodular structures (size, $\sim 100 \text{ \AA}$) have been observed in "homogeneous" amorphous polymers (56); the question is controversial, and as yet unresolved (57). In any case, any significant degree of two-phase morphology should be readily observable.

For initial study, several series of epoxies were prepared based on the Epon 828-MDA reference resin. Systems include blends to achieve equal equivalent weights but different distributions of molecular weight (and \bar{M}_c), and also homopolymers of varying molecular weight to provide additional standards for comparison. Characteristics of those and related resins are described in sections A-a and A-b, and procedures and results in Section B.

A. Structure and Stoichiometry

a. Structure of Epoxies

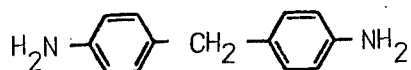
The epoxy prepolymers used in this study all have the following general structure:



where n varies from 0 to 24 (58-60).

As supplied commercially, a distribution of composition usually exists (61,62). It is possible to obtain only two prepolymers which have relatively narrow distributions of molecular weight and hence equivalent weight: Epon 825 (Shell Chemical Company) and Epi-Rez 509 (Celanese Coatings Company). As will be described later, this fact (along with requirements of curing) restricts the control over heterogeneity in molecular weight M (and hence in \bar{M}_c) which can be achieved in blends.

The curing agents are available in several forms and purities, the essential component being methylene dianiline (MDA), also called p,p' -diaminophenyl methane (DDM):



The nominal characteristics (as supplied by the manufacturers) of the epoxy prepolymers are given in Table 5.

Table 5. Characteristics of Epoxy Prepolymers.

Prepolymer	Equivalent wt, g/eq	Composition, wt%		
		n=0	n=1	n=2-8
Epon 825	176	100	-	-
Epon 828	190	75	25	-
Epirez 520-C ^a	475	-	-	-
Epon 1001 ^a	500	11	16	72
Epirez 522-C ^a	600	-	-	-
Epon 1002 ^a	650	-	-	-
Epon 1004 ^a	938	-	-	-

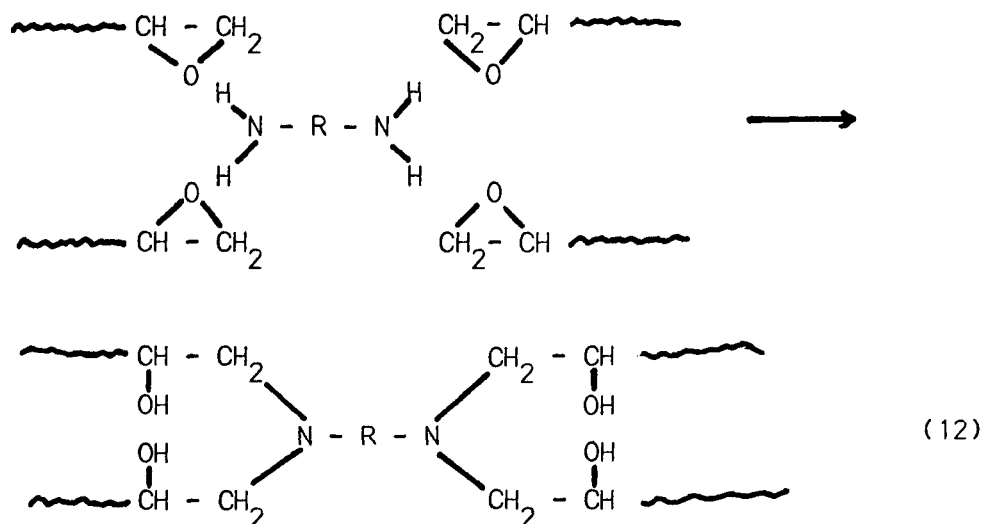
^a Solid at room temperature.

Confirmation of the distributions will require the use of gel permeation chromatography; this characterization has not yet been accomplished on the materials used in this study.

b. Stoichiometry and \bar{M}_c

For estimation of \bar{M}_c , the calculations of Bell (37) may be employed. Bell developed equations for \bar{M}_c based on the stoichiometry of the curing reaction and the amount of primary amine and epoxy groups remaining in the polymer at a given time. Since calculated values were shown to agree well with values estimated from measurements of swelling and the polymer solvent-interaction term χ (equation 9).

With curing conditions used in Bell's and this study, several idealized structures may be expected, depending on the stoichiometry (Figure 11a). In principle, the epoxy prepolymer is difunctional and the amine tetrafunctional so that under conditions of equivalence of functional groups, the following reaction will occur:



At other stoichiometries, structures can be readily visualized by reference to Bell's paper.

Thus, with an amine/epoxy ratio of 2:1 (Figure 11a) enough primary amine groups are present to theoretically react with all epoxy groups and yield linear chains. In fact, as shown by Bell (37), however, some primary amine groups may remain after secondary groups have reacted, thus yielding some crosslinks. In this case, the effective M_c is given by

$$\bar{M}_c = \frac{aM_A + bM_B - X\{(aM_A + bM_B)/[3/2(2a - Y) + (X/2)]\}}{3/2(2a - Y) - (3X/2)} \quad (13)$$

where: a and b are the number of moles of amine and epoxy, respectively; M_A and M_B are the molecular weights of the amine and epoxy, respectively; and X and Y are the numbers of unreacted primary and secondary amine groups, respectively. Since the concentration of unreacted epoxy groups, E , is equal to $2b - 4a + 2X + Y$, analysis of X and E gives Y (37). After analysis, Bell was then able to estimate M_c . From his tabulated data, a value of about 1500 may be estimated.

If, on the other hand, the structure were in fact linear, and conversion complete, \bar{M}_c would in effect become the number average molecular weight

\bar{M}_n as given by

$$\bar{M}_n = \frac{aM_A + bM_B}{a - b} \quad (14)$$

Using this equation, one would have a value for \bar{M}_n of ∞ . In reality, conversion of precisely all the functional groups is not complete; even a minuscule decrease from 100 percent conversion will yield finite molecular weights. Hence the significance of calculated values for \bar{M}_c or \bar{M}_n is questionable unless very accurate analytical data in the concentration of residual functional groups is available.

For the case of equal stoichiometry, when $b=2a$ (Figure 11a), \bar{M}_c is given by

$$\bar{M}_c = (aM_A + bM_B)/3(b-a) \quad (15)$$

when the amine is slightly in excess, equation 15 may be used as well.

When epoxy is up to about 20 percent in excess, \bar{M}_c is given by

$$\bar{M}_c = [aM_A - (b - 4a)M_B]/[3a - 3/2(2b - 4a)] \quad (16)$$

which allows for the presence of not more than one dangling end per branch point. The idealized structure will consist of an amine molecule with epoxy branches.

B. Experimental Details, Results, and Discussion

As mentioned above, several series of unblended and blended epoxies were prepared. General procedures described by Bell (37) and Manson and Chiu (39,40) were followed for systems using liquid epoxies, depending on the system; variations were necessary in the case of solid epoxies. Resins were prepared in two thicknesses: 0.25 in. (6.35 mm) for fracture studies, and 0.020 in. (0.51 mm) for measurement of dynamic mechanical and other properties. Materials, procedures, and general results are discussed below.

a. Materials

The epoxy resins used were all diglycidyl ethers of Bisphenol-A oligomers: Epon series 825, 828, 1001, and 1004 (Shell Chemical Company); and Epirez series 520-C and 522-C (Celanese Coatings Company). Of these prepolymers, Epon 1001 and 1004, and Epirez 520-C and 522-C were solids at room temperature. The curing agent used in most syntheses was methylene dianiline (MDA), obtained in the form of Tonox (Shell Chemical Company) and 99%-pure MDA (Aldrich Chemical Company). In a few cases, the following polyamides were used as curing agents: Versamids 115 and

140 (General Mills Chemicals, Inc.). In the latter case, phenylglycidyl ether (Shell Chemical Company) was used as a reactive diluent. All resins of a given type were taken from a given batch; equivalent weights were used as supplied by the manufacturers.

b. Preparation and Curing

The various procedures for preparation and curing are summarized below. Compositions are given in following sections:

1. The general procedure for systems using liquid epoxy prepolymers with MDA as the curing agent was similar to that used by Bell (37). Following prior heating to 100°C, the resin and curing agent were evacuated for 5-15 min to remove bubbles, mixed, cast, and cured as follows: 45 min in a circulating oven at 60°C; 30 min at 80°C, and 2.5 hr at 150°C; slow cooling to room temperature. The mold assemblies comprised clamped 5-in by 5-in glass plates separated by 0.02-in (0.51 mm) or 0.25-in (6.35 mm) ethylene-propylene copolymer or Teflon spacers were heated to 100°C prior to the casting step. Both Mold Release 225 (Ram Chemical Company) and Epoxy ParFilm (Price Driscoll Co.) were used successfully as mold release agents; sheets of Mylar were also effective. With care, clear, yellowish to brown specimens were obtained from which bubble-free sections could be cut.

The cure cycle used was reported by Bell to give essentially complete curing (37) - a conclusion supported by data presented in section VII. Somewhat higher temperatures were used by Selby and Miller (17), but the effect of curing temperature as a variable was not examined in this study.

2. Higher molecular weight epoxies such as Epon 1001 are solids at room temperature, and are usually used in conjunction with a solvent. In order to avoid at this time the question of a possible role of solvent in network formation, it was decided to conduct curing in bulk. It was difficult to achieve defect-free specimens in these cases, for at the higher temperatures needed to give the fluidity necessary for handling curing proceeded at an undesirably fast rate. However, thin specimens (0.5 mm thick) were successfully made as follows.

The resin was melted at 125°C and evacuated. The curing agent was mixed in and samples cast between glass plates without further evacuation. The curing cycle was modified to 100°C for 1.5 hr., and 150°C for 2.5 hr; dynamic modulus studies indicated complete curing. A similar method was used for Epon 1004. By this technique, it was possible to get bubble-free sections for dynamic modulus studies.

3. For Versamid-cured systems the procedure developed by Manson and Chiu (39,40) was followed. First 6 percent by weight (based on the total mix) of phenyl glycidyl ether was mixed with the epoxy prior to addition of the polyamide in order to reduce viscosity and thus facilitate mixing and removal of bubbles. The epoxy resin was heated to 40°C, and evacuated in a vacuum oven to remove absorbed air and moisture. After the curing agent is heated to 40°C and added to the resin, the total mixture then evacuated for about 5 min. Sheets of samples were formed by use of the mold assemblies described in section b-1.

c. Series A (varied stoichiometry)

This series (with MDA as curing agent) was prepared to provide a standard for comparison with other specimens prepared in this study and with the literature. Table 6 gives the compositions, on the basis of equivalent weights (based in turn on specifications supplied by the manufacturer). Theoretical values of M_c , as calculated by equations 13 to 16, are given in Table 6, along with compositions.

Table 6. Compositions of Series A Epoxy Resins.

<u>Designation</u>	<u>Amine/epoxy Ratio^a</u>	<u>M_c (theoretical)^b</u>
A-7	0.7 : 1	1523
A-8	0.8 : 1	526
A-9	0.9 : 1	383
A-10	1.0 : 1	326
A-10A	1.0 : 1	326
A-11	1.1 : 1	370
A-14	1.4 : 1	592
A-16	1.6 : 1	924
A-18	1.8 : 1	1922
A-20	2.0 : 1	∞ (Linear)

^a All are based on the use of Shell TONOX curing agent, except for the A-10A case, for which 99% MDA was used.

^b For reasons discussed by Bell (37) actual \bar{M}_c values for specimens A-16 to A-20 may be in error. However, estimation of absolute values will require analysis of the residual amine content. In any case, the error will not affect any trends observed in properties as a function of stoichiometry.

Thus this series provides resins covering a wide range in composition, ranging in amine excess from -30 percent to +100 percent.

d. Series B (Blends at equal \overline{M}_C)

For this series, various resins were blended to achieve an epoxy equivalent weight of 190 g/eq (equivalent to that of Epon 828, and to a value for \overline{M}_C of 326). Stoichiometric amounts of MDA were used in all cases. Details are given in Table 7, which also includes data on the blending resins themselves.

Table 7. Compositions of Series B (Blends) Epoxy Resins.

Designation	wt % of						Eq wt	wt %		
	Epon 1004	Epirez 522-C	Epon 1001	Epirez 520-C	Epon 828	Epon 825		n=0	n=1	n=2-8
B-1		-	11.4	-	-	88.6	190	89.9	1.8	8.3
B-2		-	10.3	-	9.6	80.1	190	88.4	4.1	7.5
B-3		10.0	-	-	-	90.0	190	-	-	-
B-4		-	-	11.8	-	88.2	190	-	-	-
B-5		-	-	-	100	-	190	75	25	-
B-6		-	5.7	-	50.0	44.3	190	82.4	13.4	4.2
B-7		-	2.3	-	80.0	17.7	170	-	-	-
B-8		-	-	-	-	100	168	100	-	-
B-9		-	-	100	-	-	475	-	-	-
B-10		-	100	-	-	-	500	11	16	73
B-11		100 ^a	-	-	-	-	600	-	-	>73
B-12	100	-	-	-	-	-	938	-	-	>73

^a Not yet cast.

e. Series C (equal \overline{M}_C but different stoichiometry)

In order to determine whether or not behavior at a given \overline{M}_C depends on whether or not stoichiometry is 1:1, series C was made. This series complements series A but provides direct comparison of resins at equal \overline{M}_C . Table 8 gives the compositions; data for control B-5 are also included.

Table 8. Compositions of Series C Resins.

Designation	\bar{M}_c	Epoxy	Amine/Epoxy Fraction
B-5	326	Epon 828	1.000
C-8	326	Epon 825	1.045
C-9	326	Epon 825	0.956
B-10	740	Epon 1001	1.000
C-11	740	Epon 825	1.531
C-12	740	Epon 828	0.742

f. Series D (Versamid Resins)

Several resins were prepared from Epon 828 using polyamide curing agent, Versamids 115 and 140. It seemed undesirable to examine effects of distribution in \bar{M}_c using Versamid-based resins, which are softer, tougher, and typical of adhesives and coatings rather than rigid, high- T_g resins. However, in view of considerable experience at Lehigh with such resins (39,40,55), and because such resins were expected to be easier to handle than the brittle MDA-cured ones, several specimens were cured. Because of their relative flexibility, they provide a means of examining the effects of network flexibility on viscoelastic and fracture behavior. It was also thought that a two-phase morphology might be possible.

Compositions are given in Table 9.

Table 9. Compositions of Series D (Versamid-cured) Epoxy Resins.

Designation	Relative Amine/Epoxy Proportions				
	Epon 825	Epon 828	Epon 1001	V-115 ^a	V-140 ^a
D-1	-	-	1.0	1.0	-
D-2	-	1.0	-	-	1.0
D-3	1.0	-	-	-	1.0

^a Amine equivalent weights are: V-115 and V-140, 238 and 385 g/eq, respectively.

g. Series E (Unblended Resins, equal Stoichiometry)

To provide a baseline for examining the effects of \bar{M}_C at constant stoichiometry, resins based on the following prepolymers were synthesized using stoichiometric amounts of MDA as curing agent: Epons 825, 828, 834, 1001, 1002, and 1004.

C. Discussion

Using the techniques described, it was possible to prepare specimens suitable for testing, albeit with considerable difficulty in the case of the solid epoxies. Reproducibility of casts appears to be reasonable (see section VII).

With respect to the blends, it is clear that there are limits on the number of blends that can be prepared from resins which themselves have a distribution. In this case, the limit of variation of individual M_C values within a blend has been a factor of about 3.

It should be noted also that while the broadest distributions achieved are relatively broad on a weight basis, they are much less broad on a number basis. This must be borne in mind in interpreting effects on behavior.

SECTION VII

GENERAL CHARACTERIZATION OF EPOXY NETWORKS

A. Introduction

A principal aim in the epoxy portion of the program is to study effects of network structure on ultimate properties such as strength, toughness, and fatigue resistance, as well as on behavior at small-deformation such as creep or stress relaxation. Adequate correlation requires thorough characterization of the polymers concerned - an ideal procedure all-too-often unrealized in practice.

Some studies in the literature have been concerned with several aspects of behavior, for example, tensile strength as a function of \bar{M}_C (7,36) in epoxies rather well characterized in terms of dynamic mechanical behavior. Other studies, for example of fracture toughness and fatigue not included such characterization, and sometimes the epoxies themselves are not specified (63-66). It was therefore decided to establish a standard series of well-characterized polymers against which specimens having varying distributions of M_C and other network characteristics could be compared.

Parameters of particular interest are the crosslink density as expressed by M_C , which also reflects the degree of cure, and the viscoelastic behavior, which reflects the segmental mobility and energy dissipation characteristics. In particular, viscoelastic response is often sensitive to differences in network structure. Microscopic examination is also important, to verify the presence or absence of a two-phase morphology.

This section describes progress to date with the characterization of the resins discussed in section VI. Materials and characterization are discussed in more detail below.

a. Crosslink Density

The degree of cure and crosslink can be analyzed in several ways, the two most common involving determination of swelling (and sol-gel ratio) and modulus in the rubbery state. While, as will be seen, absolute values may not be obtained in densely crosslinked systems, values still give an excellent indication of relative network characteristics.

Thus Whiting and Kline (7) showed that the swelling of epoxy-amine-diluent systems was very sensitive to the nature of the network; the measurements were used to indicate relative values of \bar{M}_C . Values of \bar{M}_C

can also be estimated from swelling using the Flory-Rehner equation (equation 9). Use of this or modified empirical equations (2) has had some success with epoxy resins (7,37); in any case, the values can be correlated with values derived from mechanical tests. In principle, distribution functions can be estimated for M_c from measurements of swelling as a function of pressure; in practice, this is difficult (2).

Values of M_c can also be determined from moduli measured by dynamic mechanical spectroscopy using a Rheovibron or similar unit. Although the kinetic theory of rubber (equation 17a) is not valid for highly crosslinked systems, an approximation (2) may be useful (equation 17b):

$$\begin{aligned} \text{a) } G &= nRT = \frac{\rho RT}{M_c} \\ \text{b) } \log G &\approx 7.0 + 293 \rho / M_c \end{aligned} \quad (17)$$

where G is the shear modulus, ρ the density, n the number of moles of network chains per unit volume, and \bar{M}_c the average molecular weight between crosslinks. In our experience (39,40) equation 16 held well for several epoxy resins (cured with polyamides), yielding values of M_c in excellent agreement with prediction; equation 17 may be better when the rubbery modulus is greater than, say, 10^8 dyn/cm². Values of \bar{M}_c have also been estimated from the elevation of the glass transition temperature, T_g , by crosslinking (2,6):

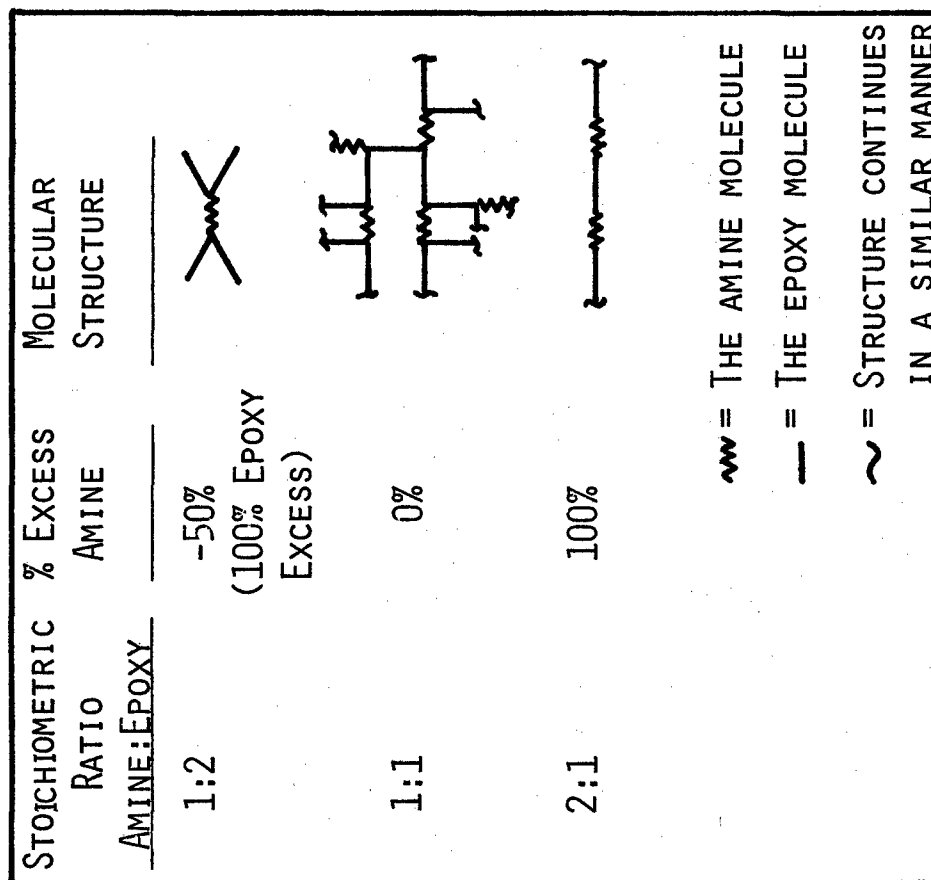
$$\bar{M}_c = \frac{3.9 \times 10^4}{T_g - T_{g0}} \quad (18)$$

where T_{g0} is the transition temperature of uncrosslinked polymer (made by incompletely curing an epoxy-amine mixture).

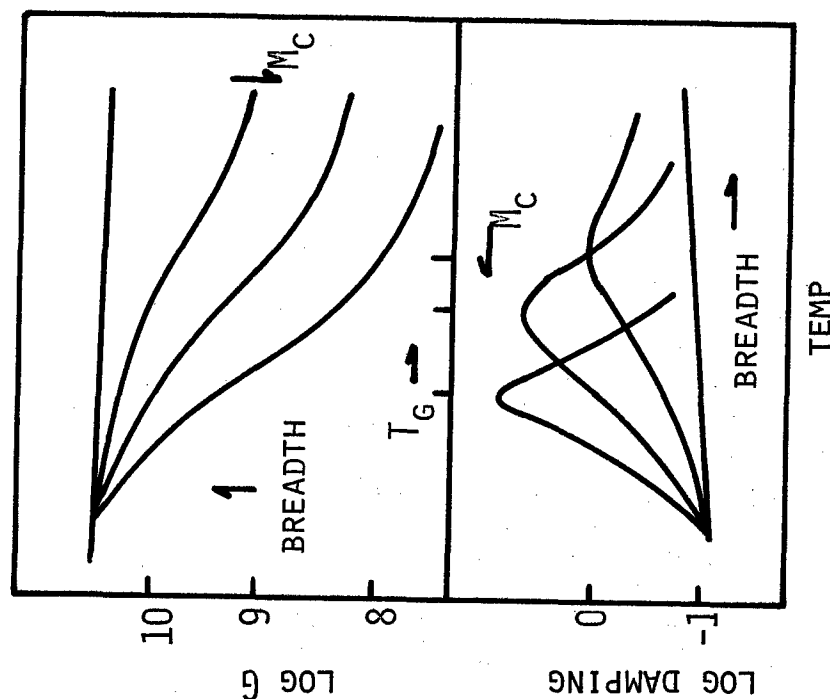
b. Effects of Crosslinking and Network Structure

Crosslinking profoundly affects the viscoelastic behavior of polymers: the T_g , the damping (as measured by $\tan \delta$ or E'' - see section b), and the slope of the glass transition (2,6,7). In addition, crosslinking affects the characteristics of the next loss peak appearing as one lowers the temperature from T_g - a peak often called the " β " peak, as distinct from the " α " peak corresponding to the T_g (18). Some changes are shown in Figure 11.

As M_c decreases (and crosslink density increases) T_g shifts to higher temperatures, and at very low values (densely crosslinked systems such as phenolic resins) may disappear altogether. Also the damping peak is broadened and heightened as crosslink density increases, the maximum



(A)



(B)

FIGURE 11. SCHEMATA SHOWING (A) EFFECTS OF CROSSLINKING STOICHIOMETRY ON MOLECULAR STRUCTURE, AND (B) EFFECTS OF CROSSLINKING ON MODULUS-TEMPERATURE BEHAVIOR.

occurring when stoichiometry is optimum. Effects of stoichiometry and diluents are readily observed (1,6,7). The distribution of crosslinks is believed to be in large part responsible for the noticeable broadening of the glass transition as M_c decreases (1, chapter 4); this effect is also seen with crystallinity. Presumably a spread in crosslink distribution (or crystallinity) will result in a spread in relaxation times and hence slope of the transition.

Stress relaxation and creep are also sensitive to network characteristics (2,23), though most scientific work on characterized specimens appears to have been concerned with rubbers. In general, creep of highly crosslinked systems in the glassy state is very slow, probably lower at high loads, long times, and temperatures just below T_g than for less crosslinked systems (2). The stress relaxation technique (which is essentially equivalent to the inverse of a creep test) can often reveal long-time effects, when coordinated long range molecular motions or disentanglements first become important. Each type of test has been used successfully to predict the modulus of epoxies at long times (67); correlations using time-temperature superposition principles (25) in the form of master curves is feasible.

B. Experimental Details, Results, and Discussion

In this section, characterization to date by swelling and dynamic mechanical spectroscopy will be presented and discussed, as well as preliminary examination of morphology by electron microscopy. Analysis of the resins to determine unreacted functional groups has not yet been made; for the present purpose, the extent of cure can be inferred from the mechanical studies. Differential scanning calorimetry is also being used to characterize the state of cure, but results are not yet ready for discussion.

a. Swelling

Preliminary swelling tests have been made on Series A and Series B resins. Two techniques have been used: swelling of powder in chloroform vapor to get a swelling ratio (7) and swelling in liquid acetone (37).

In the first technique, finely ground powder (about 0.1 g) was placed in a desiccator over about 100 ml of chloroform. Weights were measured after 24 hr., and the swelling ratio calculated as the ratio of the final to initial weight.

In the second technique, small specimens (0.5-in by 0.5-in x 0.020-in) were cut from plates and soaked in 150 ml of acetone for 15 days with agitation. Swollen specimens were weighed after drying of acetone from the surface. The sol fraction was determined by evaporating the residual acetone to dryness or by weighing the dried samples after the

swelling test was complete. The swelling ratio, q , is given by

$$q = \frac{\text{Final Volume}}{(1 - \text{wt fraction sol}) \times \text{original volume}} \quad (19)$$

For calculation of \bar{M}_C using the Flory-Rehner equation, values of χ were interpolated from values given by Bell (39).

1. Series A Epoxy Resins (Varied Stoichiometry)

Although data are not yet complete, (correction for solubility not applied, due to scatter in the data) it may be seen from Figure that both methods indicate a minimum at or near the stoichiometric ratio. Also results so far tend to agree with those reported by Bell (37) - see Figure 12, which shows \bar{M}_C (calculated using the Flory-Rehner equation) as a function of stoichiometry. However, \bar{M}_C values are lower than predicted by stoichiometry (section VI-c).

Tests are being repeated to check reproducibility, especially of specimens taken from various portions of a cast plate, and to correct for the sol fraction.

During the course of swelling test numerous cracks were observed on all specimens. On closer observation the number and sizes of cracks seemed dependent on stoichiometry, their being more and larger cracks the further away from equal stoichiometry. On solvent evaporation the cracks close up, but reappear on soaking after 2 to 3 hr. Figure 13 shows large cracks in specimen A-16 (about 30 μm in width) with smaller ones (about 7 μm) branching out. It is possible that such cracking, which resembles stress-cracking, may be sensitive to details of the network.

2. Series B Epoxy Resins (Broad Distribution)

Data are summarized in Table 10.

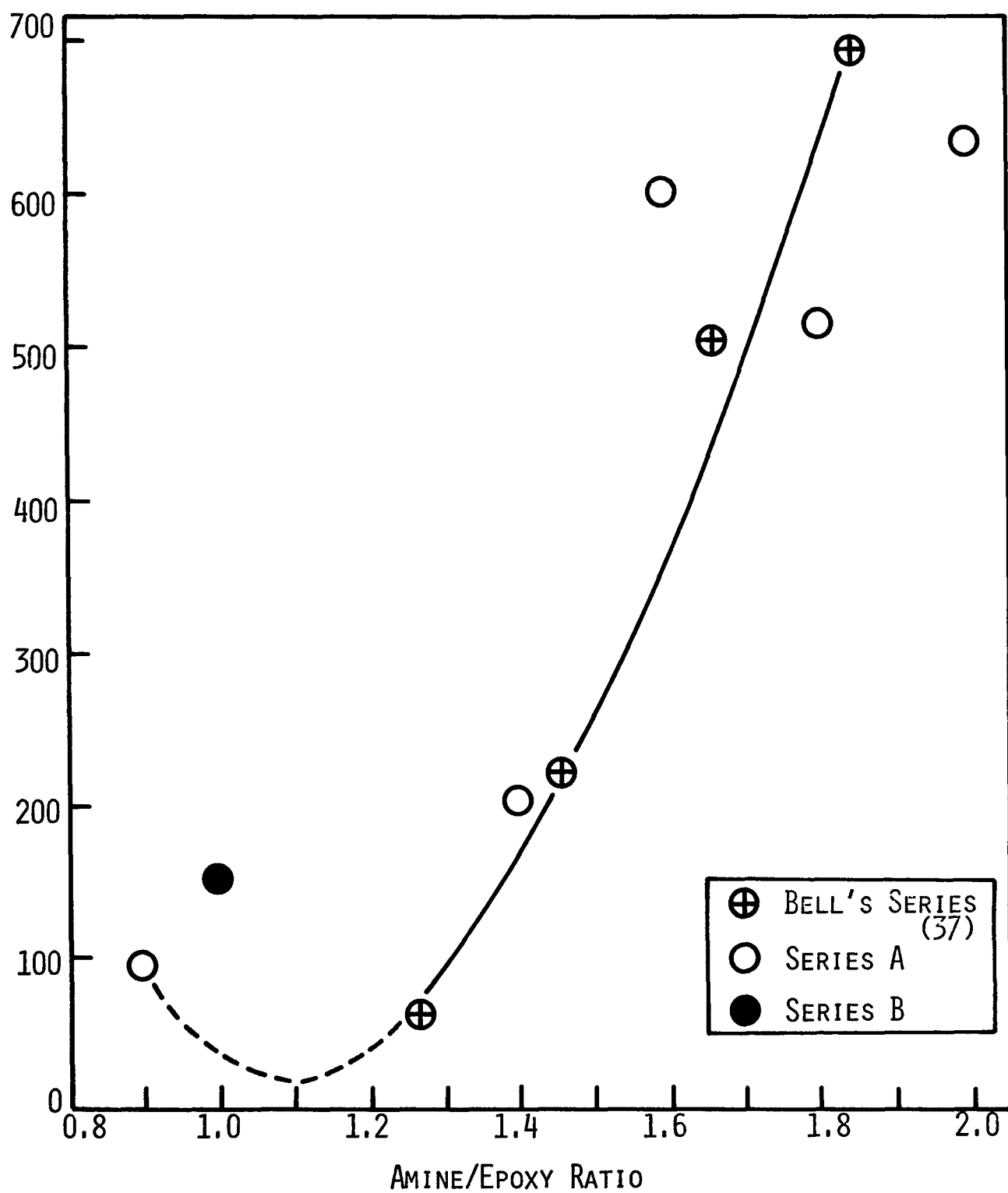


FIGURE 12. COMPARISON OF M_c DATA FROM SWELLING TESTS: SERIES B (POINT INCLUDES ALL SPECIMENS).

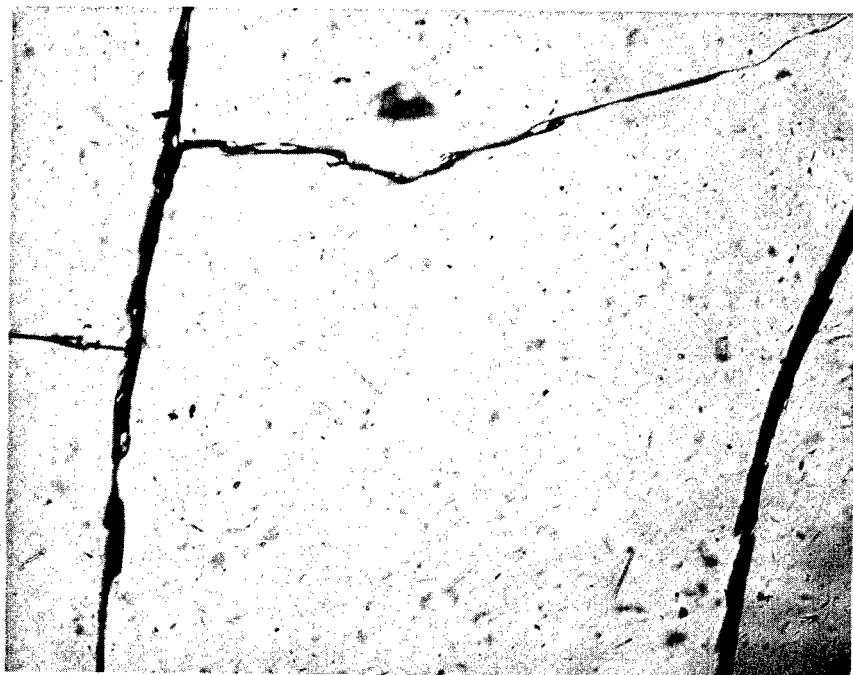


FIGURE 13. SOLVENT-INDUCED CRACKING DURING SWELLING OF A SERIES A EPOXY RESIN (A-16), AS OBSERVED BY OPTICAL MICROSCOPY (66.5X).

Table 10. Swelling Behavior of Series B Epoxy Resins^a.

Sample No.	Approx wt % of Molecules ^a having			Swell Ratio, q			% Sol		
	n=0	n=1	n=2-8	Spec a	Spec b	av.	Spec a	Spec b	av.
B-1	89.86	1.82	8.32	0.255	0.253	0.254	0.46	0.37	0.42
B-2	88.41	4.06	7.53	0.256	0.255	0.256	0.49	0.59	0.54
B-6	82.44	13.41	4.15	-	-	-	-	-	-
B-5 ^b	75.00	25.00	0.00	0.262	0.261	0.262	0.67	0.55	0.61
B-4	similar to 1			0.258	0.257	0.258	0.36	0.35	0.36
B-7	lower ^c than B-1	~1	higher than B-1	0.255	0.247	0.251	0.40	0.30	0.35

^a All specimens blended to give $\bar{M}_c = 326$.

^b Nominal composition for Epon 828 (control specimen).

^c Quantitative analysis not available.

It is interesting to note that use of the Flory-Rehner equation yields a value for M_c of close to 160 for all specimens. This value is about half that given by stoichiometry, 326; the value also does not agree with the value given in Figure 12. Clearly, swelling results can be used only for relative comparisons, and then only within a given series. It should be noted that after correction for the sol fraction, the data for series A at 1:1 stoichiometry will agree rather well with those for Series B.

At first glance, the values of swelling do appear to be very nearly equal. However, there does appear to be a slight trend towards higher sol fraction and swelling ratio when the proportion of material with $n=1$ is high, and the proportion with $n=2-8$ is low. It seems likely that the effect of the former is dominant. Thus the longer chains may well permit a higher degree of swelling than is possible with short chain ones. An effect of distribution in M_c is therefore possible, though not clearly proven.

b. Dynamic Mechanical Spectroscopy

Measurements of complex Young's moduli (1) were made using a Rheovibron viscoelastometer, model DDV-II, (Toyo Measuring Instrument Company). The instrument applies a sinusoidal tensile strain to one end of a sample, and measures the stress sensed at the other end. Transducers permit the reading of the absolute dynamic modulus $|E^*|$ (the ratio of maximum stress to maximum strain) and the phase angle δ between the

strain and the stress. The storage modulus, E' , the loss modulus, E'' , and the dissipation factor, $\tan \delta$, are given as follows:

$$\begin{aligned} E' &= |E^*| \cos \delta \\ E'' &= |E^*| \sin \delta \\ \tan \delta &= E''/E' \end{aligned} \quad (20)$$

E'' and $\tan \delta$ are measures of the energy dissipated irreversibly, and E' a measure of the energy stored reversibly.

The experimental procedure was as follows. Thin strips (1x2 mm) were cut out carefully from 0.020-in sheets and polished well along the edges using fine sand paper. It was found that heating to above T_g prior to cutting helped minimize shattering of the more brittle specimens. Measurements were made at 110 Hz and a heating rate of 1°C/min over a temperature range from -80°C to about 40°C above the T_g . The T_g and β -transition temperature were taken from the major and lower maxima, respectively, on the loss modulus (E'') vs. temperature curves. The slope change of E' ($d \log E'/dt$) at T_g was obtained in the region of $T_g \pm 4^\circ\text{C}$. Typical original data are reproduced on Figure 14 in order to show the kind of scatter encountered. Several points may be noted. First, the duplicate run (on the same specimen) gave excellent reproducibility in the transition region, thus indicating essentially complete curing. An exception was specimen A-10A, cured with 99% MDA instead of TONOX. This specimen gave incomplete curing, as shown in Table 11; T_g and slope (n) increased and decreased, respectively, (indicating further curing) on repeated runs. Second, however, reproducibility of absolute values of E , E' , and $\tan \delta$ in the glassy range is less good, with a 40% variation between the highest and lowest value (at 0°C). This behavior seems to be characteristic of the Rheovibron instrument: good reproducibility of transition temperatures, but variation in absolute moduli, especially in the glassy state.

Fluctuations in reading were often encountered at low temperatures due to ice formation on the surface of the specimen; this problem was also mentioned by Arridge & Speake (18). However, this problem has been resolved satisfactorily by sweeping dry nitrogen through the specimen chamber. Also correction of the instrumental correction factor (K) to allow for slight size variations from specimen to specimen seems to improve reproducibility of absolute values. Good reproducibility also requires frequent recalibration of temperature readings. By following these precautions, runs by different operators give transition temperatures which agree within 2 to 3 degrees.

To evade the problems of cutting specimens and of using thin specimens whose behavior may not reflect that of thick ones an acoustic resonance-type unit (Nametre spectrometer, Model XV) has been purchased.

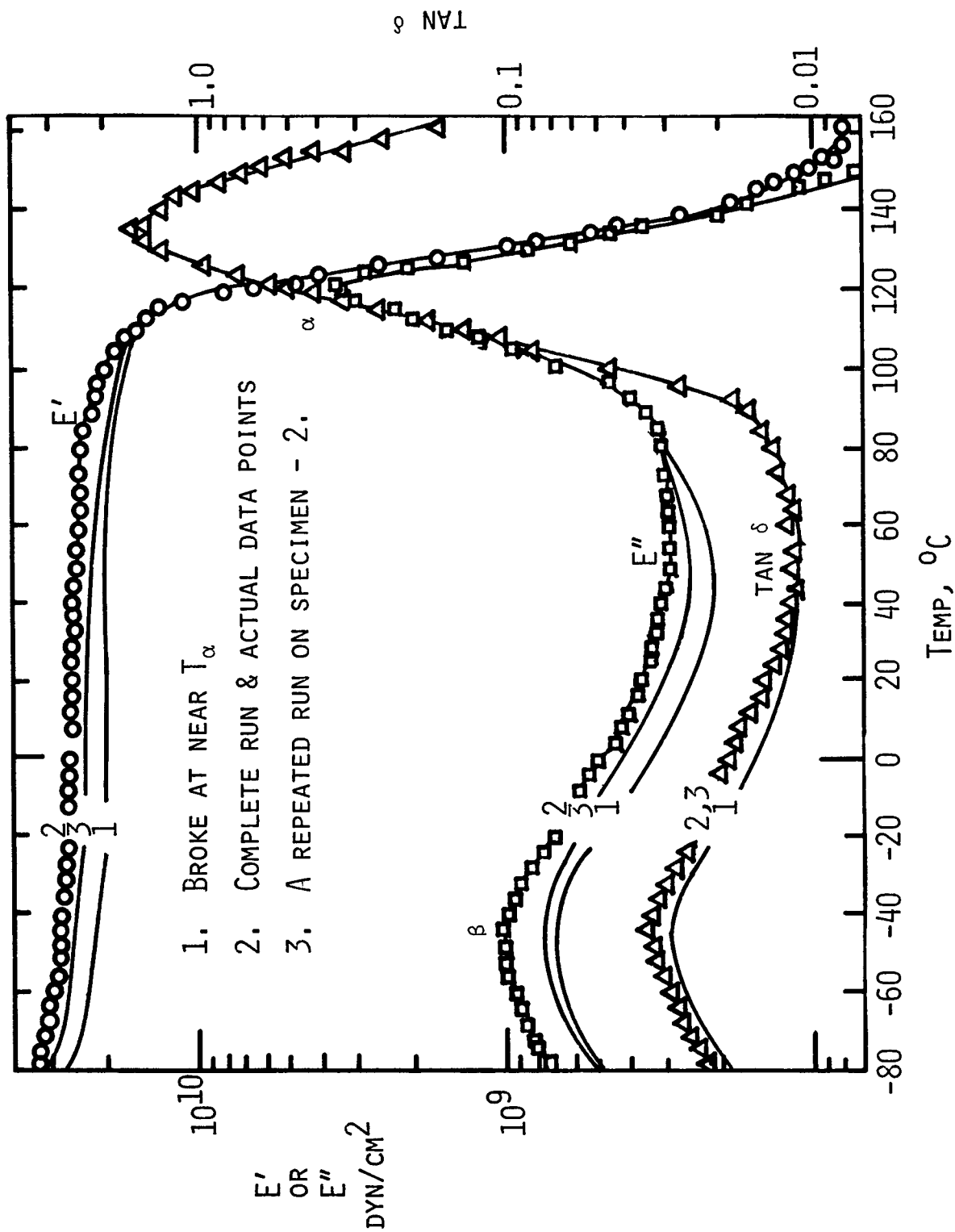


FIGURE 14. DYNAMIC MECHANICAL DATA FOR A-20 EPOXY RESIN, $F=110$ Hz.

The transitions of interest should be visible at frequencies between about 100 and 2000 Hz for temperatures between -150°C and 250°C (Kline used a resonance device in all his epoxy studies). A specially designed transducer has been ordered for use with 0.25-in specimens.

1. Series A Epoxy Specimens (Variable Stoichiometry)

Three transitions are often evident in the dynamic spectra of epoxies, as one descends in temperature; one at high temperature, (α peak), one at a lower temperature, and one at a still lower temperature. The α -peak is associated with the glass transition, while the lowest-temperature peak is attributed to motions of the glycidyl group (18). The middle peak is claimed to be an artefact associated with incomplete curing (18); after careful recalibration of the Rheovibran used in this study, small peaks seen earlier disappeared. Thus, attention may be focussed on the upper and lower peaks. Since in these studies, we now see only two peaks, the lower-temperature one will be called " β ", in conformity with conventional practice. (In some literature, this peak may be called " γ "; nomenclature is not standardized.) It may also be noted that with one exception no evidence for incomplete curing or a two-phase morphology is seen in the dynamic spectra, as has been noted in other studies (1,2,8); re-running of a specimen gives essentially the same curve as before.

Data are presented in Tables 11 to 13, and displayed in Figures 15 to 17. It may be seen that increased crosslinking raises the temperatures at which the α and β transitions occur, as reported in other studies (6,7,18). Curiously, values of T_g are inexplicably high - higher than those noted by Bell (39) [even after allowance for the higher frequency used in this study] and higher than predicted, based on the curing temperature (5). At present, no explanation in terms of temperature error or adiabatic heating is tenable.

Increased crosslinking also increases the value of the rubbery modulus, E_r' (which was estimated using the theory of rubber elasticity, equation 10, and decreases the slope of the α -transition, in conformity with prediction (1). It is interesting that the slope is a function of stoichiometry only when the amine is in excess; the amine appears to sharpen the transition, perhaps by enhancing mobility of the chain segments. The maximum value of $\tan \delta$ at the α -transition is also decreased, as reported by Murayama and Bell (6), but is increased at the β -transition, as reported by Arridge and Speake (18).

Arridge and Speake (18) have also noted that the relative decrease in E' as one passed (upwards) through the β transition is related to the degree of cure - the greater the decrease, the greater the crosslink density. While values of E' are quantitatively uncertain, the value of the percent decrease in modulus between $(-70 \text{ to } -80)^{\circ}\text{C}$ and $(+20 \text{ to } +30)^{\circ}\text{C}$ was found to increase, from 21 for sample A-18 (amine in excess) to 69 for sample A-10A (equal stoichiometry).

Table 11. Dynamic Mechanical Data of Series A Epoxy Resins (Variable Stoichiometry).

Specimen	Amine/ Epoxy Ratio	T_{α}^a °C	T_{β}^a °C	$d \log E'/dT$ at $T_{\alpha}(n)$ dyn/cm ² -deg	$\tan \delta_{\max}$		$E'_r \times 10^{-8}^b$ dyn/cm ²
					Value	Temp. (°C)	
A-7	0.7	132	-47	0.050	1.10	148	1.54
A-8	0.8	162	-47	0.050	0.91	177	2.59
A-9	0.9	197	-42	0.038	0.72	213	4.55
A-10	1.0	198	-45	0.056	0.70	206	4.00
A-10A	1.0 ^c	192-198	-42	0.043-0.050	0.76-0.68	202-206	4.13-4.25
A-11	1.1	190	-40	0.056	0.82	201	3.82
A-14	1.4	164	-45	0.067	1.08	176	2.40
A-16	1.6	141	-47	0.077	1.25	153	1.38
A-18	1.8	136	-45	0.083	1.30	149	1.25
A-20	2.0	119	-45	0.083	1.60	133	0.78

^a From maxima in E'' vs. temperature curve.

^b Storage modulus in rubbery state (at $\geq T_g + 40$).

^c Epon 828/99% MDA. This specimen was shown to have incomplete curing; first runs on new specimens gave $T_{\alpha}=192$, $n=0.050$ and repeated runs on the same specimen gave $T_{\alpha}=198$, $n=0.043$, i.e., further curing on scanning.

Table 12. The β Transition of Series A Epoxy Resins (Variable Stoichiometry).

Specimen	Amine/ Epoxy Ratio	$\tan \delta_{\max}$		E''_{\max}	
		Temp °C	Value	Temp °C	Value 10^{-9} dyn/cm ²
A-7	0.7	-40	0.025	-47	0.68
A-8	0.8	-40	0.032	-47	1.3
A-9	0.9	-32	0.044	-42	1.2
A-10	1.0	-35	0.036	-45	1.0
A-10A	1.0	-30	0.041	-42	1.5
A-11	1.1	-30	0.038	-40	1.0
A-14	1.4	-36	0.041	-45	1.0
A-16	1.6	-40	0.033	-47	0.94
A-18	1.8	-40	0.032	-45	0.84
A-20	2.0	-40	0.032	-45	0.88

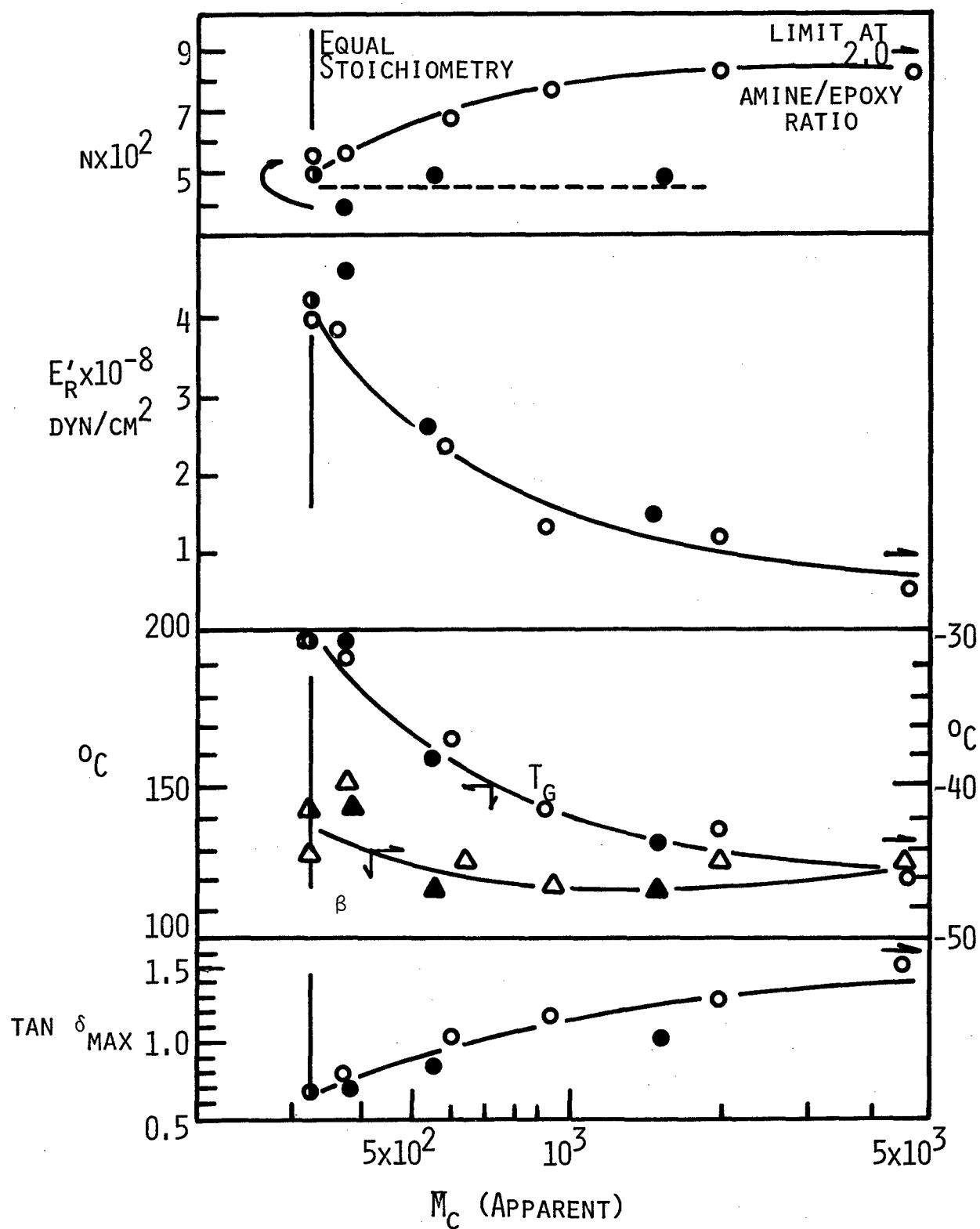


FIGURE 15. DYNAMIC MECHANICAL PROPERTIES OF SERIES A EPOXY RESINS AS FUNCTIONS OF \bar{M}_c . \circ , AMINE IN EXCESS; \bullet , EPOXY IN EXCESS; \bullet , SPECIMEN A-10A.

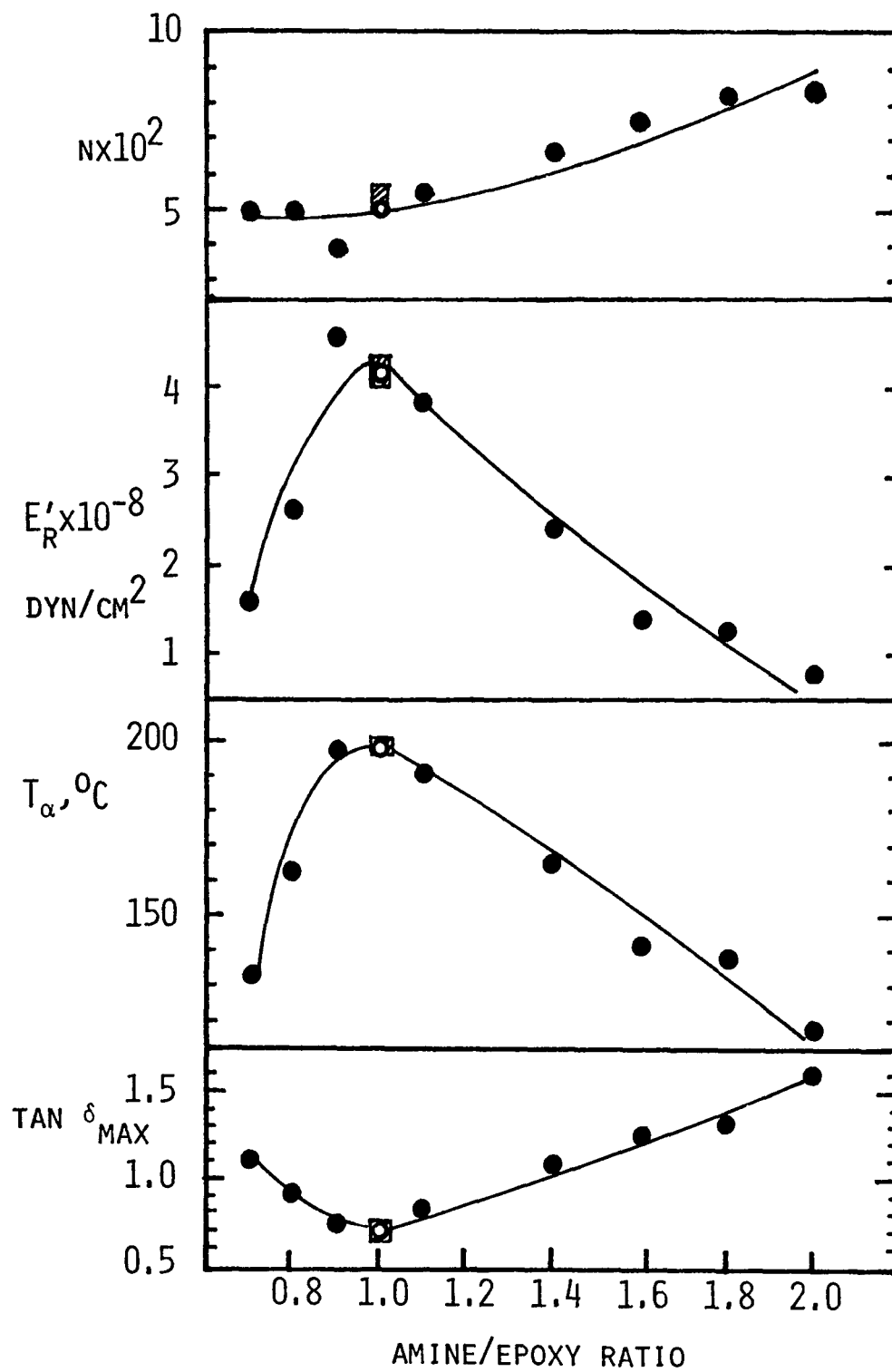


FIGURE 16. DYNAMIC MECHANICAL PROPERTIES OF SERIES A EPOXY RESINS AS FUNCTIONS OF STOICHIOMETRY: \circ , A-10A; \square , SERIES B.

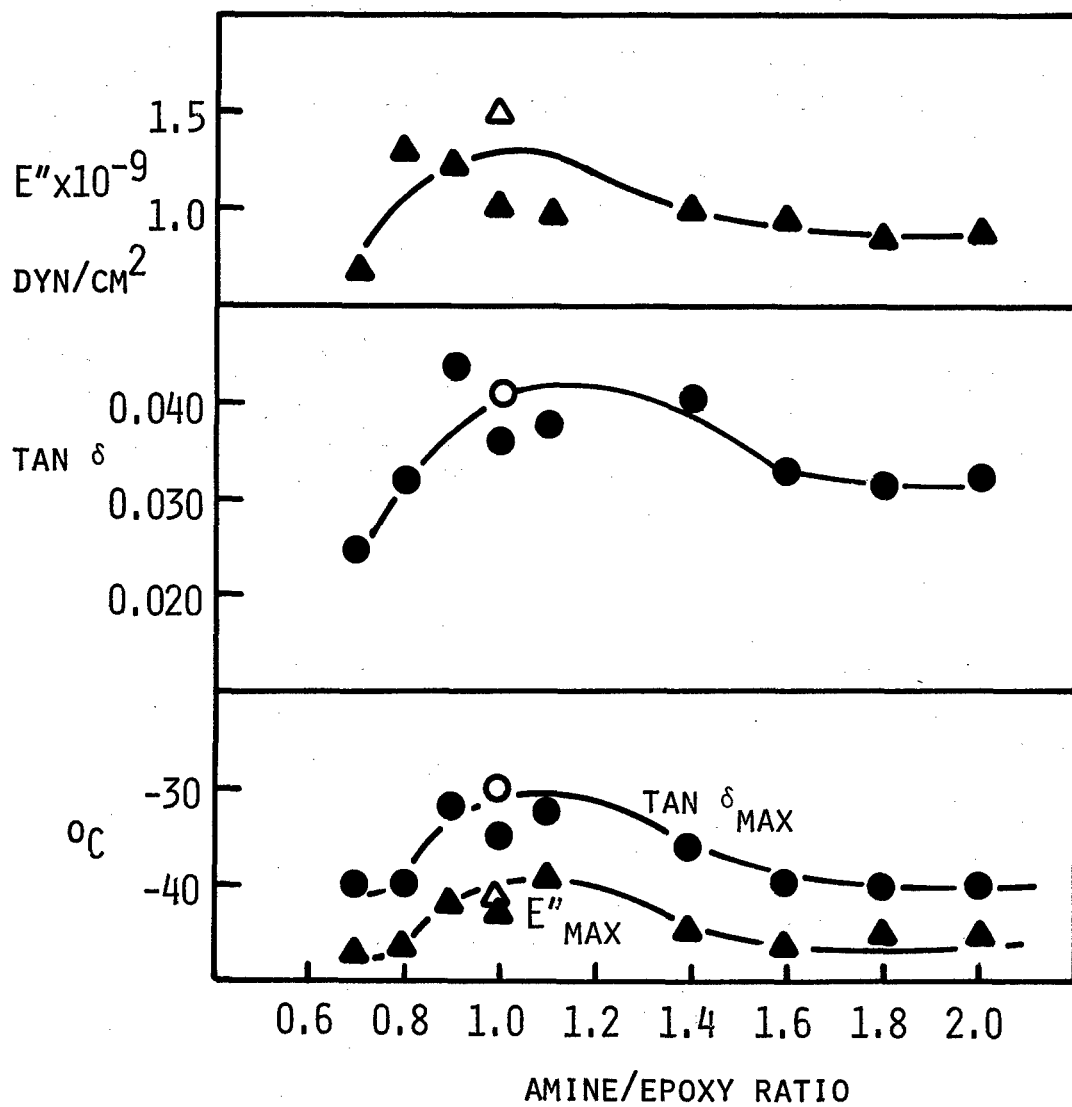


FIGURE 17. β TRANSITION OF SERIES A EPOXY RESIN :
OPEN A-10A.

Values of M_c estimated from E'_c and the shift in T_g [using a value of 80°C for T_{go} , following Bell (39)], are given in Table 13. Agreement seems reasonable, especially in view of the difficulties in applying the theory of rubber elasticity to highly crosslinked systems.

Table 13. Average Molecular Weight Between Crosslinks, \bar{M}_c , for Series A Epoxy Resins.

Specimen	Amine/ Epoxy Ratio ^a	From Stoichiometry	From Vibron Data		From Stress Relax'n At 150°C
			E'_r	T_g Shift	
A-7	0.7	1523	727	696	1361
A-8	0.8	526	458	464	-
A-9	0.9	383	282	317	86
A-10	1.0	326	316	325	-
A-10A	1.0	326	302	325-445	-
A-11	1.1	370	328	348	-
A-14	1.4	592	496	494	728
A-16	1.6	924	815	600	1561
A-18	1.8	1922	886	650	1613
A-20	2.0	∞ (Linear)	1392	907	2414

^a Amine/Epoxy Ratio on equivalent weight basis.

2. Series B Epoxy Resins (Broad Distribution)

Preliminary data for this series are given in Table 14; see also Figure 15. It may be seen that the blends comprising this series behave very much like the reference resins of Series A. In earlier measurements, slopes of the α -transition had appeared to be higher than for the reference B-5 resin. However, on recalibration of the Rheovibron unit, the values now fall close to those for B-5.

Blending of 25 percent of an epoxy having $n=1$ with an epoxy having $n=0$ (the case of Epon 828) does change the viscoelastic behavior significantly (Table 15). Since at the same time \bar{M}_C is increased by 7 percent, it is not yet feasible to separate possible effects of distribution in M_C from effects of a change in the average value.

Table 14. Dynamic Mechanical Data of Series B^a.

Sample No.	$\tan \delta^c$ at β	T_{β}^c $^{\circ}\text{C}$	T_g^c $^{\circ}\text{C}$	E_r' $\times 10^{-8}$ dyn / cm ²	Slope (n) $\frac{d(\log E)}{dT}$
B-1	.048	-40	198	4.0	.050
B-2	.043	-38	198	4.0	.056
B-6	.028	-35	198	4.0	.055
B-5 ^b	.036	-45	198	4.0	.056
B-4	.038	-44	198	4.0	.050
B-3	.038	-41	198	4.0	.054

^a All specimens blended to give $\bar{M}_C = 326$; for compositions see Table 7.

^b Nominal composition for Epon 828 (control specimen).

^c $\tan \delta(\max)$, seen near T_g , ranges between 0.70 and 0.71 in all cases.

Attempts are being made to broaden the distribution of M_C still more at a given average value, if necessary by using a solvent to facilitate mixing. In any case, statistical comparison with the master plots of viscoelastic data now available will be possible.

Satisfactory theories for dense networks do not appear to exist, though it is supposed that the distribution of M_C is not Gaussian (25). Reliance must therefore be placed on experiment.

3. Series E Epoxy Resins (Unblended Resins)

Data obtained so far are presented in Table 15. Clearly all the viscoelastic parameters change significantly as a function of molecular weight of the epoxy resin, and hence \bar{M}_c . Indeed comparison with the data in Figure 15 shows excellent agreement. Thus, regardless of how a given value of \bar{M}_c is obtained - whether by changing stoichiometry for a given resin, or by changing the molecular weight of the epoxy at a given stoichiometry - the viscoelastic behavior seems to be determined by \bar{M}_c . We are not aware that this reciprocity has been noted previously.

It will be interesting now to blend, for example, E-6 and E-1 to give a mixture with \bar{M}_c equivalent to that of E-3 or E-4.

Table 15. Viscoelastic Parameters for Series E Epoxy Resins (Homopolymers).

Sample	Epoxy Resin ^a	\bar{M}_c	$T_{g'}^o$ °C	$\frac{\text{Tan } \delta(\text{max})}{\text{Value}}$	$\frac{\text{Temp}}{^\circ\text{C}}$	Slope, $\frac{d \log E'}{dT}$	$E'_r \times 10^{-7}$ dyn / cm ²	Temp of β Peak, °C
E-1	825	308	203	.62	220	.039	45	-35
E-2	828	326	198	.71	210	.056	42	-45
E-3	834	413	-	-	-	-	-	-
E-4	1001	740	145	1.15	155	.077	10	-53
E-5	1002	940	-	-	-	-	-	-
E-6	1004	1324	125	1.52	137	.095	6.8	-55

^a Epon Series, all bisphenol-A-based (Shell Chemical Co.).

c. Morphology

Techniques have been developed for high resolution electron (EM) and transmission electron microscopy (TEM) and scanning electron microscopy (SEM). In the former case, specimens were cut with a microtome equipped with a glass knife. In the latter case, specimens were either fractured in liquid nitrogen, or used as a free surface; acetone extraction (15) and ion etching (17) and use of carbon-platinum replicas,

were used in order to reveal any morphological features. Specimens were carbon-coated prior to examination by the SEM. Magnifications used range up to 80,000X.

While studies are still in progress, several micrographs have been obtained. For example, the fracture surfaces of a thin film of D-1 (Epon-1001/Versamid 115 system) which had been previously extracted with acetone resembled that of many other polymers. Similarly a sample of B-5 (MDA-cured) was ion-etched, but revealed only a one-phase structure when examined with a range of magnification from 20,000X to 80,000X.

Using replication (Figure 18), a micrograph was obtained for specimen D-2 which generally resembled those reported by Morgan and O'Neal (15). While it is possible that the features do reflect the true network structure, further work will be required for confirmation. On the other hand, when specimen D-2 was examined in the SEM, after acetone etching, no features at all could be distinguished at magnifications up to 40,000X. Similarly, using TEM, no structure was seen in the replica of specimen D-2 (polyamide-cured), at a magnification of 130,000X.

In any case, EM, TEM, and SEM may well prove useful in elucidating effects of composition on network structure, especially after extraction of soluble material by acetone (which seemed to also reflect the distribution in M_c - see section B-a.). It will be necessary to determine what is artefact and what is not a classical problem in electron microscopy.

d. Stress Relaxation

Preliminary stress relaxation tests using a Tobolsky-type relaxometer (33) have been made with two specimens (A-9 and A-20) at 150°C. Results are summarized in Table 16. No relaxation occurred with specimen A-9 ($T_g > 150^\circ\text{C}$) after 1000 min, while a 25 percent decrease occurred with specimen A-20 ($T_g < 150^\circ\text{C}$). For greater convenience, a high-temperature chamber has been fitted to the Instron tester. Once tested, future experiments will be made with this unit.

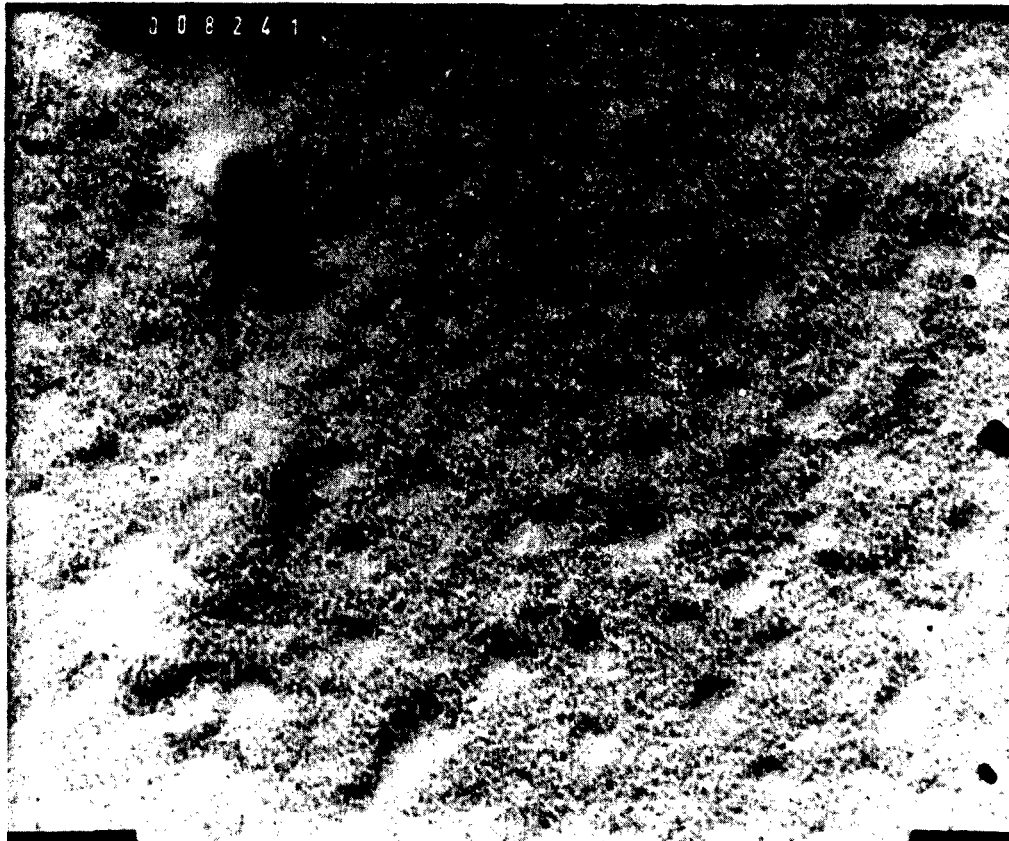


FIGURE 18. ELECTRON MICROGRAPH OF POLYAMIDE-CURED EPOXY RESIN, SAMPLE D-2, ETCHED IN ACETONE 7 DAYS, 130,000X ($1000 \text{ \AA} = 0.77 \text{ cm}$).

Table 16. Stress Relaxation of Series A Epoxy Resins at 150°C.

Specimen	$E(t)^a$	Comments
A-7	7.75×10^7	slight discoloration, no relaxation to 400 min.
A-9	1.22×10^9	slight discoloration, no relaxation to 400 min.
A-14	1.45×10^8	heavy discoloration, 3% decrease in E_r at 400 min.
A-16	6.76×10^7	heavy discoloration, 3% decrease in E_r at 400 min.
A-18	6.54×10^7	heavy discoloration, 5% decrease in E_r at 400 min.
A-20	4.37×10^7	heavy discoloration, 15% decrease in E_r at 400 min; 25% decrease

^a All resins except A-9 are apparently rubbery at 150°C, so that $E(t) \equiv E_r(t)$.

e. Discussion

A series of reliable standard resins has now been characterized for comparison with blends of various kinds as well as specimens with other network variations such as diluents. While swelling results tend to be erratic, dynamic mechanical data are more reproducible and consistent than might have been expected.

Variations in crosslink density affect many properties, including swelling, α and β transitions (both position and other characteristics), and E_r^1 . E_r^1 , T_g , and the slope of the α -transition are especially sensitive to changes in M_c close to stoichiometry.

Effects of broadening the distribution of M_c are not seen in values of T_g or E_r^1 . Indeed, if \bar{M}_c is, as is generally supposed, a number-average parameter, then an exceptionally broad distribution would be required to have much effect. On the other hand, the swell ratio seems to be sensitive to the details of the \bar{M}_c distribution. Earlier measurements of the slope of the α transition seemed to indicate an effect of distribution; later work has not confirmed such an effect.

stress relaxation may also be sensitive in the transition region.

Properties related to fracture, which involve plastic deformation and hence a strong dependence on weight-average molecular weight, may also be expected to be sensitive. In any case, still broader distributions need to be prepared, even if they cannot be made without changing \bar{M}_c . With the reference curves now in hand, comparison will be facilitated. Also, distributions may play a greater role at non-stoichiometric compositions.

SECTION VIII
FRACTURE TOUGHNESS, STRENGTH AND FATIGUE
CRACK PROPAGATION (FCP) OF EPOXY NETWORKS

A. Introduction

Work is in progress with measurements of fracture toughness, fatigue crack propagation, and stress-strain behavior. The first two topics are emphasized, because it was necessary to demonstrate feasibility of testing. The study of stress-strain response is important but not ready for reporting.

a. Fracture Toughness

Fracture toughness may be measured using either of two approaches, based on concepts of either a critical energy balance or a critical stress intensity factor (28,68).

The former concept is due originally to Griffith (69), who showed that crack instability in an ideally brittle solid should occur at a stress, σ , when the following relationship holds:

$$\sigma = \sqrt{\frac{2ES}{\pi a}} = \sqrt{\frac{EG_c}{\pi a}} \quad (21)$$

where E is Young's modulus, S the surface energy of the solid, a the crack length, and $G_c (=2S)$ the critical strain energy release rate. Put simply, the release of strain energy must exceed the amount of energy required to break bonds and form new surface.

In fact, values determined for S invariably greatly exceed those calculated on the basis of bond fracture energies (28). Thus, even a brittle epoxy exhibits a value for S the order of 10^4 erg/cm² - two orders of magnitude greater than calculated; more ductile resins show even greater discrepancies. Thus S should be considered as an "effective" fracture energy that includes a dominant contribution from plastic deformation, evidence for which is seen by electron microscopy.

The second concept is due to Irwin (70), who suggested that crack instability could be expressed in terms of the stress intensity factor K - a measure of the degree of stress amplification at the crack tip. Since K can be calculated from the applied stress, crack length, and geometry,

it is an especially convenient parameter for correlation purposes.

Catastrophic crack propagation will occur when either σ or K reach critical levels (σ_c or K_c), corresponding in turn to critical values of S or G . The two concepts are essentially equivalent,

$$G_c E = \frac{K_{Ic}^2}{(1-\nu^2)} \quad (22)$$

for the case of interest here, plane strain, where ν is Poisson's ratio. K_{Ic} is a useful material constant, though it depends on temperature and on the mode of crack opening. (For simplicity, we shall use " K_c " below.)

b. Fatigue Crack Propagation

Fatigue failure may occur by two mechanisms: (1) a thermal mode in which failure occurs by melting due to hysteretic heating, and (2) a mechanical mode comprising the initiation and propagation of a crack. The rate of temperature rise, $\Delta \dot{T}$, characteristic of thermal failure is a function of stress amplitude, σ , frequency, f , and the loss modulus, G'' (25):

$$\Delta \dot{T} = C f G'' \sigma^2 \quad (23)$$

where C is a constant, and G'' is itself a function of f and T . While temperatures can, indeed, rise in the fatigue of, for example, epoxy resins in composites due to such hysteretic heating of a whole specimen (71), this study is concerned with low-frequencies and loads well below those which will cause large temperature rises (68). Of course, there may be hysteretic effects locally, but the volume of polymer affected is small, and any effect will be seen as an effect on the mechanical propagation rate.

Failure of a resin takes place in two stages: initiation of a crack, and propagation of the crack to catastrophic rupture. While in some cases, the initiation step may be the critical one, frequently in plastics the propagation step is the most important (28,68). Thus, most polymers contain flaws introduced during processing. Such flaws will begin to grow after a certain number of cycles - the number being lower the higher the stress applied. However, the important point in determining fatigue life is the number of cycles required to grow these flaws to a size which meets the requirements of catastrophic fracture (see equation 21). In fact, frequently most of the fatigue life is in the stage of crack propagation. Hence measurements of fatigue crack propagation are of special interest in the characterization of toughness in an engineering plastic; in addition, approximate values of a quasi-fracture toughness may be obtained as well (see below).

The crack propagation regime can be examined exclusively by precracking (notching) the test specimen so that the artificial flaw is essentially ready to propagate. This approach has received increased attention recently (68) and was adopted in this investigation.

A useful parameter to characterize the fatigue crack propagation (FCP) response in notched specimens is the stress intensity factor (70). Derived from principles of fracture mechanics (70), the stress intensity factor describes the stress conditions at the tip of the advancing crack and is defined by

$$K = Y\sigma\sqrt{a} \quad (24)$$

where K is the stress intensity factor, Y a correction for specimen geometry, σ the stress, and a the crack length.

Fatigue crack propagation data are generated by cycling notched samples within a constant load range and recording crack growth over the corresponding number of fatigue cycles. Under fatigue conditions K will also vary over a range defined by ΔK (calculated from equation 24) will also increase, enabling the measurement of the rate of crack growth per cycle, da/dN , over a range of ΔK . It has been shown (68), that the relationship between da/dN and ΔK could often be represented by a simple equation of the form:

$$\frac{da}{dN} = A\Delta K^m \quad (25)$$

where A and m are constants for a given polymer. Other relationships exist, but offer no special advantage in discerning trends in the effects of chemical structure and composition (68).

In addition, using equation 25, an approximate value of K_C may be estimated from the value of ΔK_{max} , the last value of ΔK noted prior to catastrophic failure, and the load range. It has been shown that good agreement can be obtained with values of K_C measured independently from static fracture tests (72).

Using this relationship between da/dN and ΔK , it is possible to analyse the FCP response of a polymer as a function of external variables such as frequency and temperature (73,74) and structural variables such as molecular weight composition, and plasticization (72,74,75). Using equation 25, many correlations between fatigue and structural parameters have been made successfully. The following factors have been shown to enhance FCP resistance: crystallinity, high molecular weight, linearity vs: crosslinking, and presence of a rubbery inclusion. Several specific points in these studies are worth noting in more detail.

First, while studies of controlled crosslinking have not been made, until now, earlier work in these laboratories showed that crosslinking tends to increase the slope of the da/dN curve and, at least at high values of ΔK to decrease ΔK_{max} significantly; each of these effects is a measure of decreased toughness. Further, studies with a densely crosslinked epoxy resin showed that stable FCP behavior could be obtained only for a few cycles, and then only by increasing the temperature. (A new possible solution to working with such brittle thermoset resin is described later; see section B-a, below).

Second, there is an unexpectedly large effect of molecular weight in linear polymers such as poly(methyl methacrylate) and poly(vinyl chloride) (72,74,76); in fact, it was shown that da/dN varies with the term $e(\exp)1/M$. Values of K_C also depend strongly on M , rising sharply as M exceeds the critical value required for chain entanglements to become effective, and levelling off more or less asymptotically at higher values of M - say, the order of 10^5 . However, even though M is in the nearly asymptotic range, the FCP rate at a given ΔK still depends strongly on M . Hence a strong specific effect of fatigue per se exists - an effect attributed to a disentanglement of chains due to cyclic loading. The higher the average molecular weight, the greater the resistance to fatigue; a high-molecular-weight tail in a broad distribution also gives, for the same average M , enhanced fatigue resistance (75).

Third, the β transition appears to play a role not only in strength phenomena such as yielding but also in FCP and its sensitivity to frequency. Thus FCP is highest at the temperature and frequency corresponding to the β transition (74), and the greater the sensitivity of FCP rate (at a given ΔK) to frequency - the rate being reduced by an increase in frequency.

Fourth, it has been abundantly clear that crazing in advance of the crack tip is a nearly universal phenomena in fatigue as well as in static crack growth. Under some conditions (72) the craze grows incrementally with each cycle, and the crack then strikes through, yielding one striation per cycle on the fracture surface. Under other conditions, the craze may grow for many cycles before the crack strikes through, yielding one striation for many cycles (so-called "discontinuous growth bands"). While precise explanations of the role of structure in craze formation do not yet exist, it seems likely that stable crazes, and hence a degree of crack growth resistance, require the presence of even a small proportion of high molecular weight material (78). Little is known yet about crazing in epoxies in general (15), and nothing about crazing and fatigue. It does seem likely that crazing will tend to be suppressed by tightly crosslinked networks. In any case, fracture surface morphology ("fractography") can help in elucidating the micro-mechanisms of failure (77).

Finally, relatively little has been published on fatigue in monolithic epoxy resins. Schrager (79) has noted increases in the shear modulus and dissipation factor in an epoxy resin; a similar effect has been noted by Outwater and Murphy (64). It was suggested that cycling may have enhanced the degree of cure. Outwater and Murphy also found that da/dN was a linear function of ΔK . Sutton (63) described FCP in a "representative commercial epoxy-resin" cured with tetraethylene pentamine, and also found that equation 25 and a variant which takes account of mean stress held very well. The response was quite sensitive to mean stress; with da/dN at constant ΔK increasing by two orders of magnitude for a 5-fold change in load ratio (K_{min}/K_{max} from 0.1 to 0.5). Tomkins and Biggs (80) suggested that FCP in a brittle epoxy resin is dominated by crack branching - a phenomenon possibly related to crazing.

In any case, epoxy resins tend to behave like brittle solids in fatigue, exhibiting low values of ΔK_{max} , high values of the slope of the $da/dN - \Delta K$ curve (~ 10) at room temperature, and a strong sensitivity to mean stress.

B. Experimental Details, Results and Discussion

a. Experimental Details

Fatigue test specimens used were cast sheets (see section VI-B) 1/4-in (0.635 cm) x 3-in (7.62 cm) x 3-in (7.62 cm) in dimensions. Such specimens are commonly referred to as "compact tension" specimens. A 1/4-in (0.635 cm) notch was first cut into the edge using a saw; a vee was then cut using a fine jeweller's saw. Specimens were mounted using pin grips.

To start the crack, a sharp razor blade was drawn across the tip of the vee, and cycling was then begun at a low load. The load was gradually increased until the crack was observed to begin growing. This procedure was satisfactory for all specimens except those having 1:1 stoichiometry, though great care was necessary since only a slight increase in load sufficed to induce catastrophic rupture.

For the 1:1-stoichiometry specimens, the above procedure proved to be ineffective, and stable cracks could not be grown. However, it was found that stable crack growth could be induced by rubbing the razor blade to the vee while the specimen was being cycled. In this way, a crack could be initiated with considerable delicacy. Discovery of this procedure constitutes a significant advance in dealing with specimens such as brittle epoxies. The technique also works with other polymers which are prone to fail before a stable crack can be induced, and may well open up the possibility of studying refractory materials which are otherwise most difficult to handle.

For compact tension specimens, ΔK is given by (74)

$$\Delta K = \frac{Y\Delta P\sqrt{a}}{BW} \quad (26)$$

where ΔP is the load range, B the specimen thickness, W the specimen width, a the crack length, and

$$Y = 29.6 - 185.5(a/w) + 655.7(a/w)^2 - 1017(a/w)^3 + 638.9(a/w)^4. \quad (27)$$

All fatigue tests were performed on an MTS electrohydraulic closed loop testing machine operated at a test frequency range of 10 Hz and with the ratio $P_{\min}/P_{\max}=0.1$. Crack growth rates were monitored with the aid of a travelling microscope in increments of approximately 0.25mm. All fatigue tests were run in laboratory air.

While fractographic examination is planned, pictures have not yet been taken. However, by optical microscopy, the fracture surfaces resemble closely those found for polystyrene (81).

b. Fracture Toughness

Data are given in Table 17 for Series A, Series B, and Series D resins; see also Figures 19 to 22. It is clear that, as expected, K_{IC} is a smooth and nearly linear function of the amine ratio. In terms of fracture energy, we have a range from 1.0×10^4 erg/cm² to 4.4×10^5 erg/cm². Thus the anticipated brittleness is confirmed. Presumably the effect of excess amine is to enhance ductility, and hence local plastic deformation and G_C , more than it decreases E . On the other hand, an excess of epoxy resin has the effect of decreasing K_{IC} , perhaps by giving branched structures. In comparison, tensile strength is independent of stoichiometry in this system (36).

These results are in contrast to those reported by Selby and Miller (17) and Bell (36). As shown in Figure 23, the former found a peak in fracture toughness by several "static" techniques; the latter found a peak in impact strength. Since Selby and Miller obtained considerable variation in the intensity of the peak, and only a slight one in one case, depending on the method of determination, it may be that the disagreement reflects differences in the test methods. Also, testing under impact loading may not necessarily be correlatable with testing in fatigue.

It is interesting to note that, although a statistical comparison has not yet been made, there appears to be a tendency for Series B (broad distribution) resins to be somewhat tougher than controls. In Series D (polyamide-cured), the narrow-distribution resin exhibits a significantly lower value of K_{IC} than the broader distribution one. Since

Table 17. Fracture Toughness and Fatigue Characteristics of Epoxy Resins.

Specimen	Amine/ Epoxy Ratio	ΔK_I^a	K_{IC}^b , MPa \sqrt{m}	Slope of da/dN Curve
A-7	0.7	0.50	0.58	9.3
A-8	0.8	-	-	-
A-9	0.9	0.49	0.63	19.3
A-10 ^c	1.0	-	-	-
A-10A	1.0	0.53	0.73	11.1
A-11	1.1	0.58	0.78	7.7
A-14	1.4	0.75	0.93	17.6
A-16	1.6	0.72	0.93	18.3
A-18	1.8	0.79	0.98	19.0
A-20	2.0	0.83	1.07	9.9
D-2	1.0	0.68	1.00	7.9
D-3	1.0	0.68	1.22	7.9
B-1	1.0	0.53	0.72	13.6
B-2	1.0	0.57	0.80	11.6
B-3	1.0	0.57	0.76	15.8
B-4	1.0	0.57	0.78	10.8
B-5 ^c	1.0	0.53	0.72	13.6

^a At da/dN = 3×10^{-4} mm/cyc.

^b Calculated from relationship $K_{IC} = \Delta K_{max}/0.9$.

^c A-10 and B-5 are equivalent; A-10A is similar, but cured with 99% MDA instead of TONOX.

Epon 825 has a slightly lower \bar{M}_c than Epon 828, however, resolution of this question will require more study.

Finally, in terms of fracture toughness, an equal-stoichiometry epoxy behaves rather like a polystyrene or poly(methyl methacrylate) (68), except for a much higher T_g .

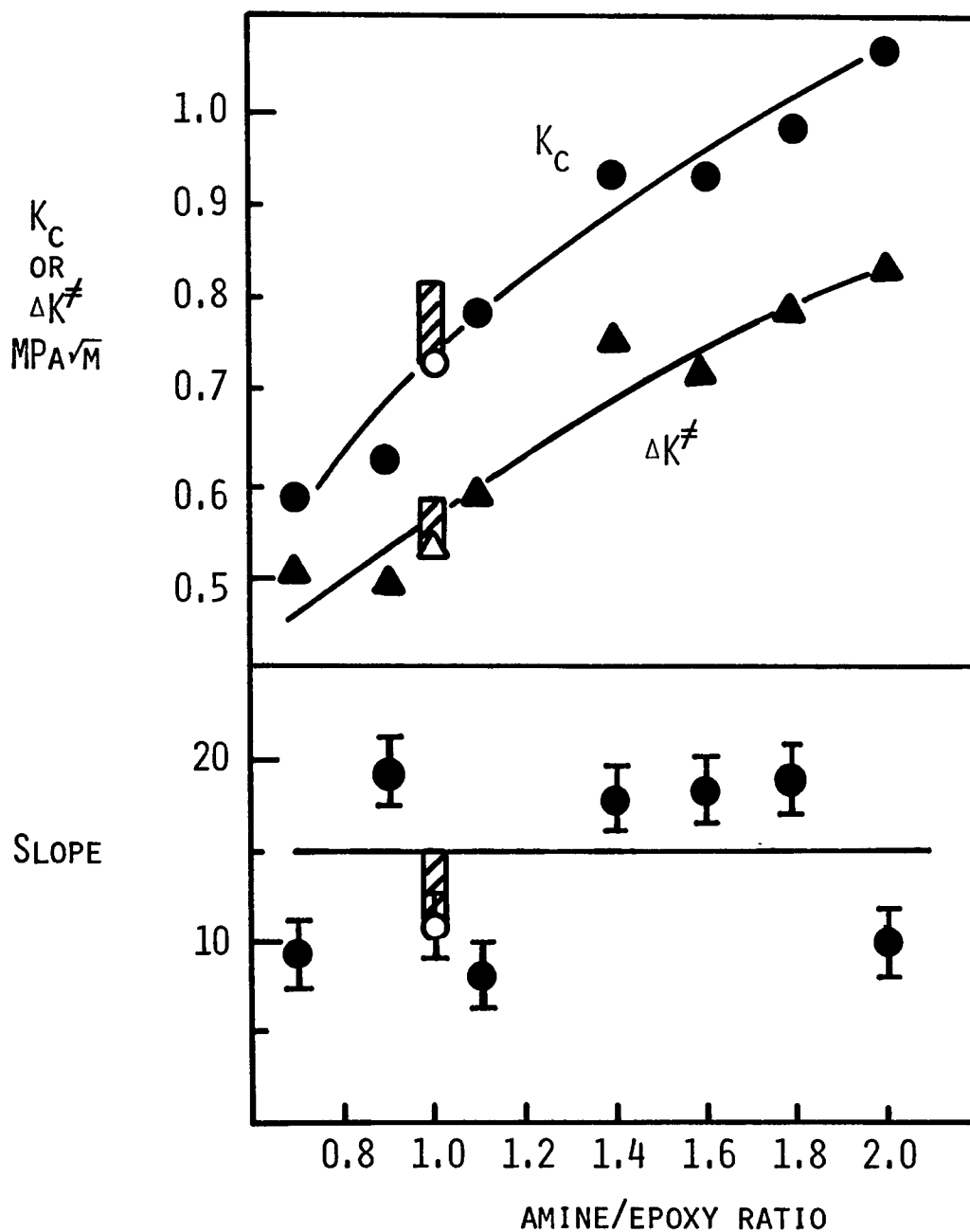


FIGURE 19. FRACTURE TOUGHNESS, K_C , AND FCP PARAMETERS ΔK^Σ (ΔK AT 3×10^{-4} MM/CYC), AND SLOPE OF THE da/dN CURVE AS A FUNCTION OF THE STRESS INTENSITY FACTOR RANGE, ΔK , AS FUNCTION OF STOICHIOMETRY: CIRCLES AND TRIANGLES FOR SERIES A, OPEN CORRESPONDING TO A-10A; SHADED AREA FOR SERIES B.

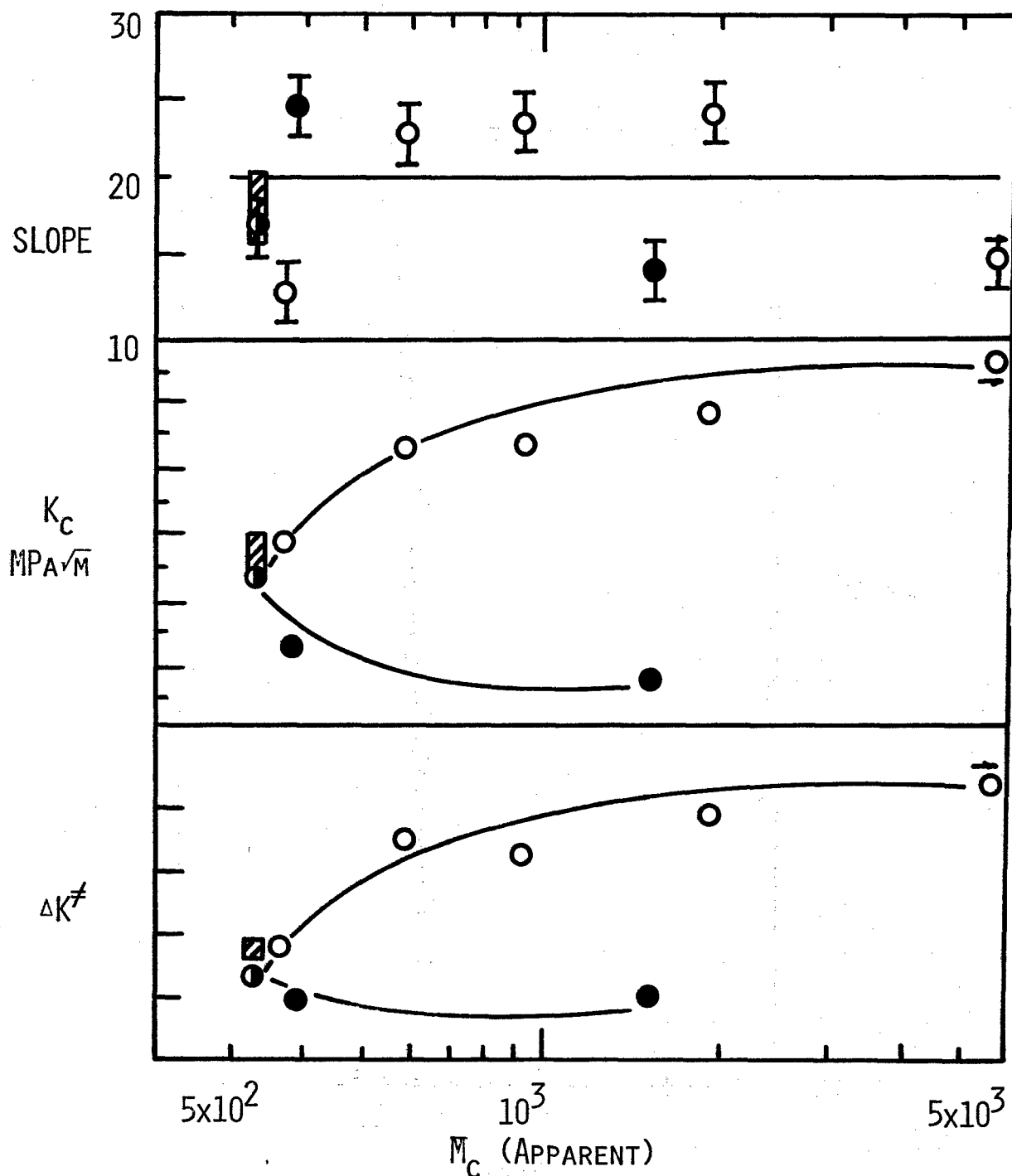


FIGURE 20. FRACTURE TOUGHNESS, K_C , AND FCP PARAMETERS $\Delta K^\#$ (ΔK AT 3×10^{-4} MM/CYC), AND SLOPE OF THE da/dN CURVE AS A FUNCTION OF THE STRESS INTENSITY FACTOR RANGE, ΔK , AS FUNCTION OF M_C : OPEN CIRCLE AMINE EXCESS IN SERIES A, CLOSED CIRCLE EPOXY EXCESS, SHADED AREA FOR SERIES B.

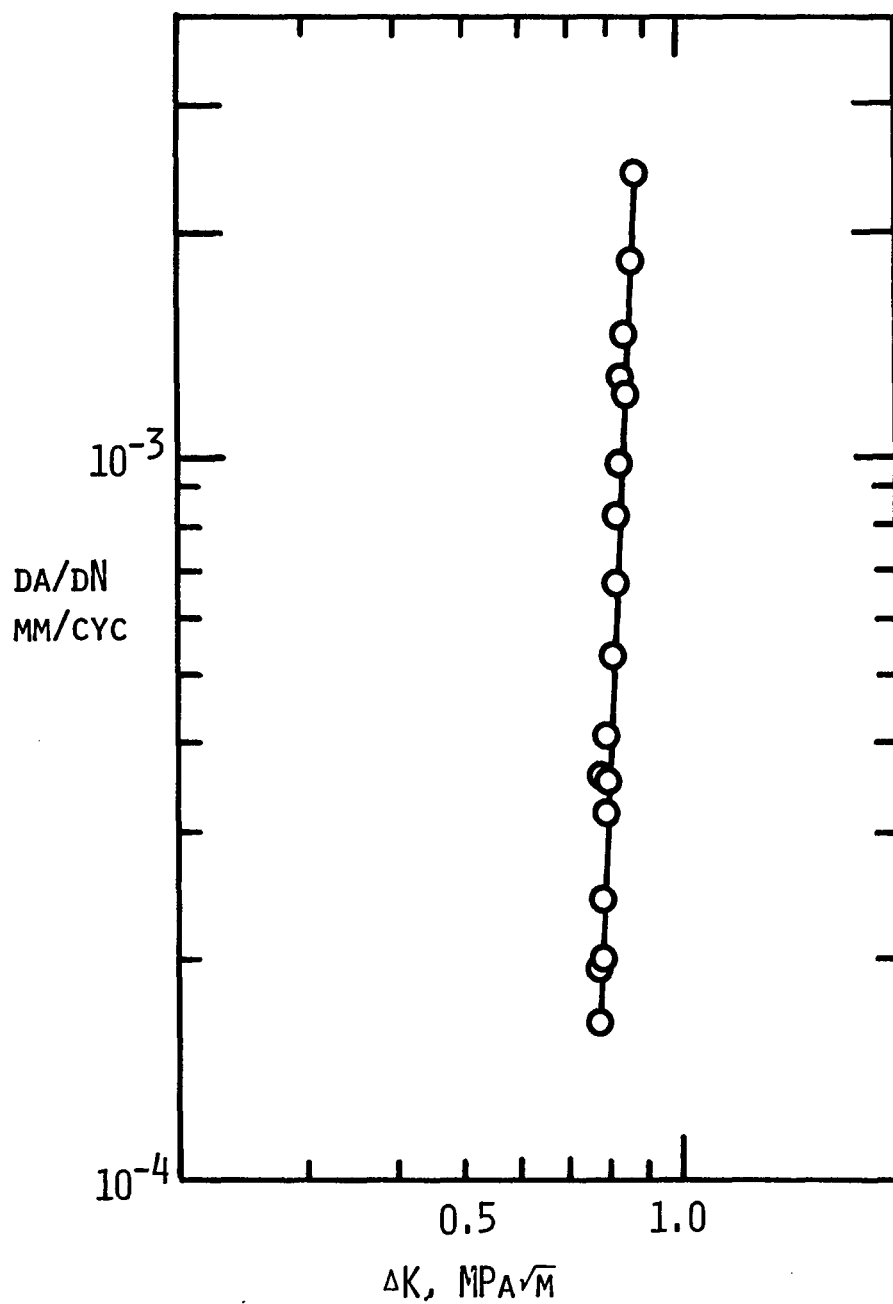


FIGURE 21. TYPICAL FCP BEHAVIOR AS A FUNCTION OF ΔK . SPECIMEN, A-18; $F=10$ Hz.

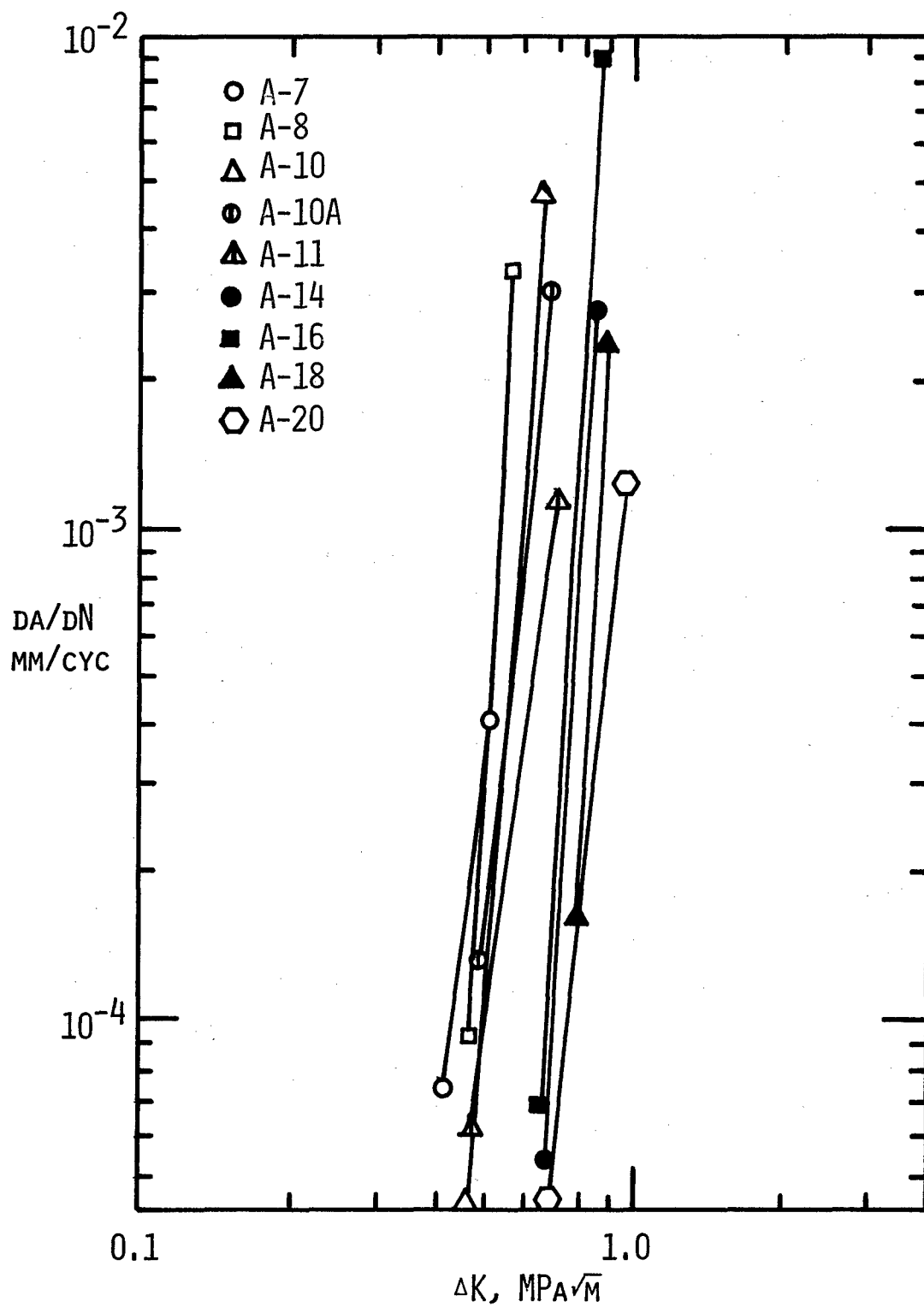


FIGURE 22. FCP BEHAVIOR OF SERIES A EPOXY RESINS; F=10 Hz.

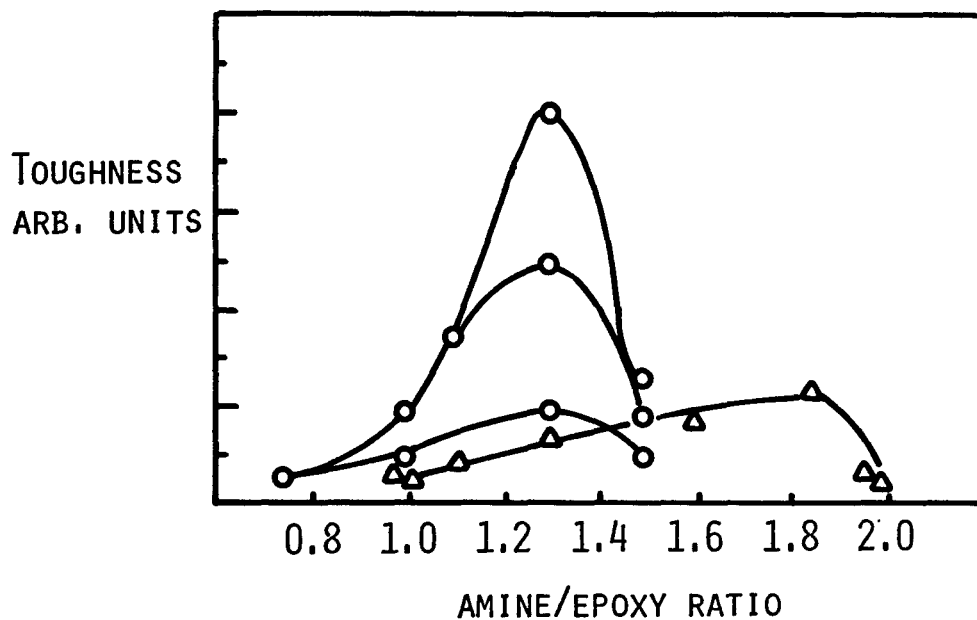


FIGURE 23. FRACTURE TOUGHNESS AND IMPACT STRENGTH (IN ARBITRARY UNITS) OF EPON 828/MDA EPOXY RESINS AS A FUNCTION OF AMINE/EPOXY RATIO: O, DATA OF SELBY AND MILLER (17) FROM 3 DIFFERENT MEASUREMENTS OF TOUGHNESS; Δ, DATA OF BELL (36) FOR IMPACT STRENGTH.

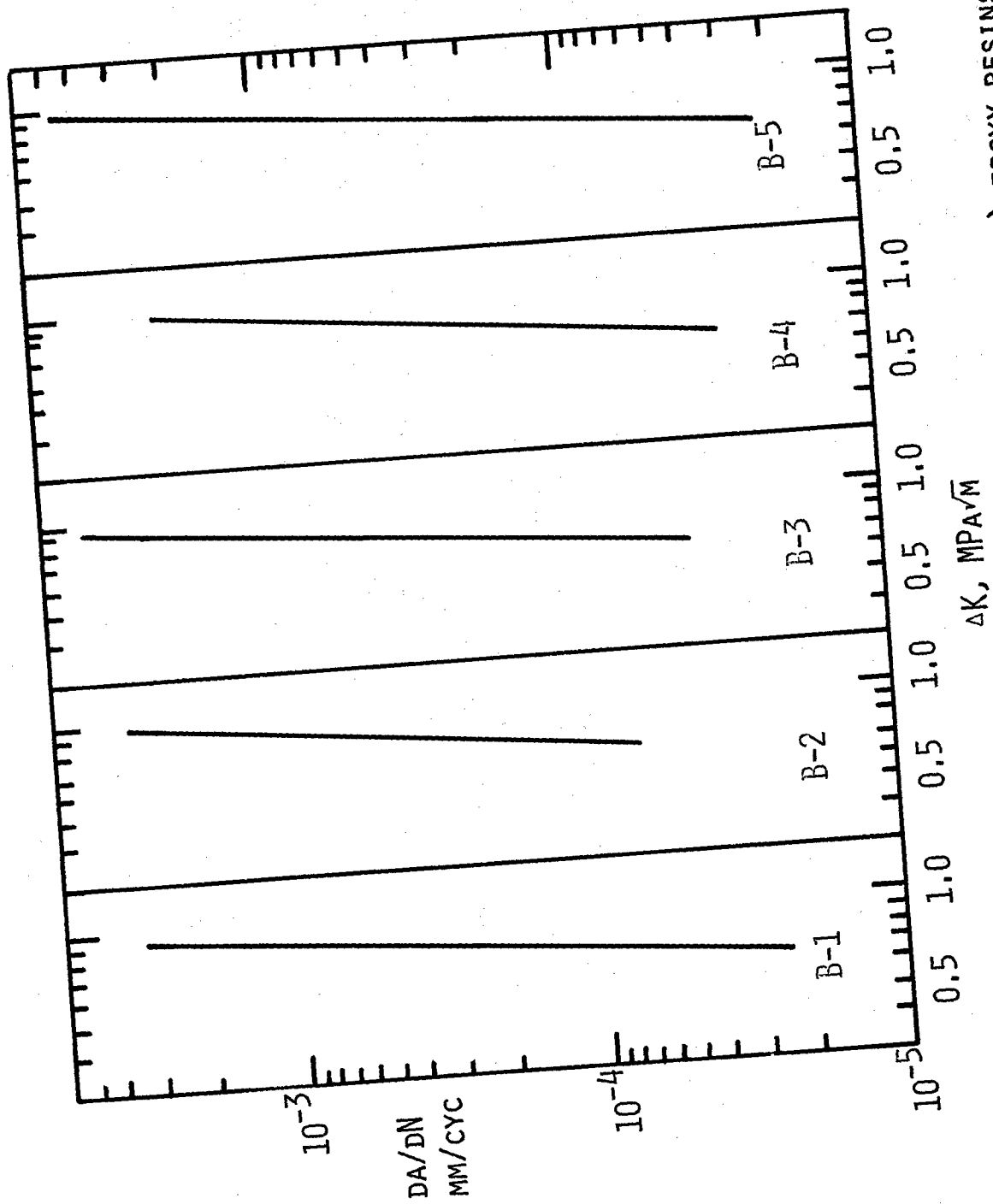


FIGURE 24. FCP BEHAVIOR OF SERIES B (BROAD DISTRIBUTION) EPOXY RESINS:
RATE OF CRACK GROWTH PER CYCLE AS A FUNCTION OF ΔK ; $F=10$ Hz.

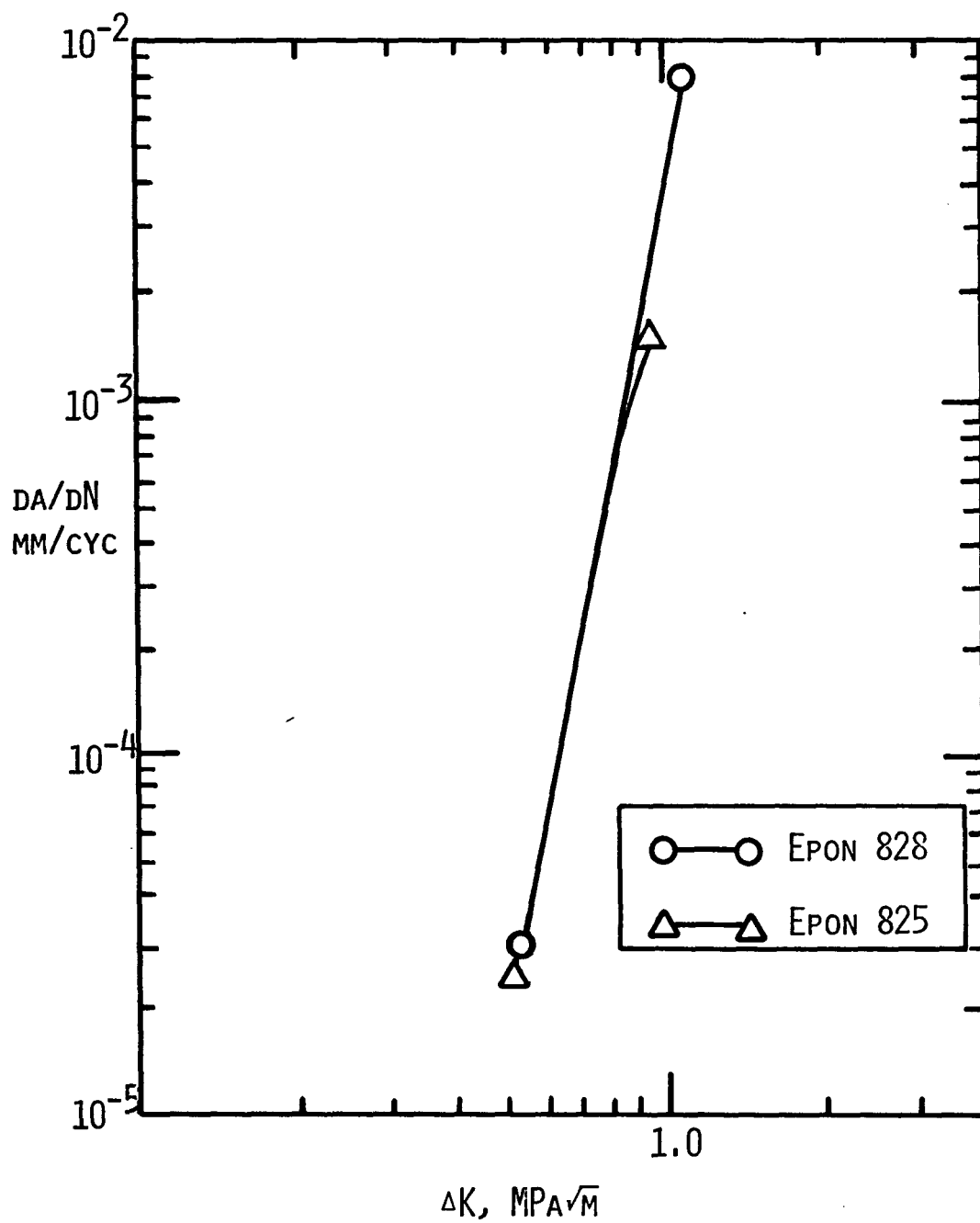


FIGURE 25. FCP BEHAVIOR OF SERIES D (POLYAMIDE-CURED) EPOXY RESINS: ONLY THE FIRST AND LAST POINTS SHOWN; F=10 Hz.

c. Fatigue Crack Propagation (FCP)

Several FCP parameters are presented in Table 17 and Figure 20. The behavior itself is illustrated in Figures 21 to 25, inclusive.

First, the data show that, just as K_{IC} did, values of ΔK^{\ddagger} (a measure of the energy to drive a crack at a given velocity) increase as the amine content increases, at least with Series A. Data for Series B fall, within experimental error, on the same curve. In contrast, the Series D resins are identical in their behavior, except for their K_{IC} values. This finding is in contrast with the results of Selby and Miller (17) and Bell (36), who found maxima in static K_{IC} and impact strength, respectively, as a function of amine/epoxy ratio.

In any case, the results are quite self-consistent, and should serve as a standard of reference for future work. Indeed, ΔK^{\ddagger} correlates well with K_{IC} - a relationship suggested earlier by Manson and Hertzberg (68). Thus, in contrast to metals, it was shown that the higher the static fracture toughness, K_{IC} , the greater the value of ΔK required to drive a fatigue of interest here exhibit a similar phenomenon.

It would be interesting to examine the effects of temperature, frequency, and compositional and curing parameters. Perhaps a distribution in M_c at non-stoichiometric ratios or in the presence of a network diluent may show enhanced effects. The technique used can probably also be adapted to other brittle epoxies.

Also the fracture surface morphology should be helpful in interpretory behavior, especially with respect to the micromechanisms of failure, for example, the effect of network structure on crazing relative to shear response.

The relatively small effects of distribution at equal stoichiometry may reflect the fact that an absolute increase in M_c , not just in the breadth of the distribution, is required to change deformation behavior greatly. Thus, 25 percent of a fraction with $n=1$ has a major effect on the properties of the resin based on a diglycidyl ether of bisphenol-A ($n=0$), but also changes M_c somewhat.

SECTION IX

CONCLUSIONS AND RECOMMENDATIONS

A. Model Networks

a. Conclusions

Based on research to date, the following conclusions may be made:

1. Controllable decrosslinking of model networks may be achieved by hydrolyzing deliberately introduced anhydride linkages in copolymers of styrene and ethyl acrylate with acrylic acid anhydride, the latter being used as a site for growth of crosslinks of polystyrene or poly (ethyl acrylate). A rapid and convenient technique for hydrolysis was discovered, based on the use of ethylene diamine as a cleaving agent for the styrene-based polymers, and ammonium hydroxide for the ethyl acrylate based systems. After hydrolysis, values of \bar{M}_c revert to values in good agreement with values found for the uncrosslinked polymers. Reasonable agreement may be obtained between results based on swelling techniques and the measurement of rubbery modulus, as long as allowance is made for the contribution of physical entanglements.

2. In conjunction with hydrolyzable crosslinks, permanent crosslinks may be introduced by copolymerization of diethyleneglycol dimethacrylate along with acrylic acid anhydride and ethyl acrylate. Use of a chain transfer agent, 1-Dith, prevents parasitic crosslinking reactions.

3. Creep and stress relaxation behavior of the ethyl acrylate systems reflects the network characteristics as determined by the crosslink density prior to hydrolysis, and by the ratio of hydrolyzable to permanent crosslinks.

4. Thus the systems mentioned should be useful in preparing networks with variable network structures.

5. Preparation of Bamford-type networks for control of the distribution of \bar{M}_c appears to be not as easy as expected. In particular, synthesis of the mixed anhydride of trichloroacetic acid and acrylic acid has posed considerable difficulty, and optimum reaction conditions have not yet been found. However, a crude product, expected to contain the desired anhydride, has been obtained by the use of pyridine with acryloyl chloride and trichloroacetic acid. Problems appear to lie in the heterogeneity of the reaction system, and in removal of the pyridinium hydrochloride by-product.

b. Recommendations for Further Work

The following recommendations for continued research are made:

1. Since the mixed anhydride would be an ideal comonomer for styrene to give controllable networks, synthetic studies should be continued in an attempt to purify the present crude product, and to find an optimum solvent and HCl-acceptor.

2. Specifically, other solvents such as styrene or carbon tetrachloride should be tried, as well as different temperatures, and the use of aqueous trisodium phosphate as an HCl-acceptor.

3. Other methods such as the possibility of an anhydride interchange reaction should be explored.

4. In any case, the Bamford synthesis itself should be developed, even without the incorporation of hydrolyzable crosslinks, for it still offers the possibility of making networks with controlled variations in crosslink characteristics.

5. Also, the polystyrene system with hydrolyzable crosslinks should be pursued, and the viscoelastic behavior examined as a function of hydrolysis, partial hydrolysis giving dangling chain ends.

B. Epoxy Networks

a. Conclusions

Based on research so far, the following conclusions may be made:

1. Satisfactory experimental techniques have been developed for the synthesis of bisphenol-A-epoxy/MDA and bisphenol-A-epoxy/polyamide resins with the following variations in crosslinking: variable \bar{M}_c (by changing stoichiometry or molecular weight of the epoxy); and variable distribution of \bar{M}_c (by blending epoxies of different molecular weights). Attainment of essentially complete curing has been demonstrated.

2. Standard techniques have been used to determine the following: stress-strain behavior; viscoelastic response (using the Rheovibron elasto-viscometer); stress relaxation; swelling; response to differential scanning calorimetry; and morphology (using high-resolution electron microscopy by replica and transmission techniques, and scanning electron microscopy). Also, a standard fatigue fracture technique was successfully modified to conveniently determine the quasi-static fracture toughness and fatigue crack propagation rates as a function of stress intensity factor range and any other fatigue variables of interest.

3. Thus a precise baseline of viscoelastic and fracture response has been established for use in comparing the effects of any desired

variation in composition or network structure.

4. The viscoelastic response is a well-behaved function of \bar{M}_c . Various viscoelastic parameters depend in a quite regular fashion on \bar{M}_c whether a given value of \bar{M}_c is achieved by changing stoichiometry or by changing the molecular weight of the epoxy--the latter correlation being apparently new. As the degree of crosslinking is increased the following parameters are increased in conformity with expectation: T_g (or T_α), T_g , the rubbery modulus, and the breadth of the α and β transitions. However, the absolute values of T_g are higher than reported by others using similar curing conditions. The following parameters are decreased by increasing crosslinking: the magnitude of $\tan \delta$ at its maximum value near T_g ; and the slope of the modulus-temperature curve at T_g . In the case of the transition slope, the relationship depends on whether or not the amine or epoxy is in excess. With the broad- \bar{M}_c -distribution specimens studied so far, the distribution breadth appears to have little effect on the viscoelastic parameters, perhaps because of insufficient breadth.

5. The swelling ratio and the soluble fraction are decreased by increased crosslinking, as expected, though results are more variable than the viscoelastic results. Swelling and solubility appear to be higher, the broader the distribution of \bar{M}_c .

6. Stress relaxation is, as expected, inhibited by crosslinking with no relaxation at 150°C for equal-stoichiometry resins but some for amine-rich specimens, after 4000 sec.

7. In contrast to results reported by others, fracture toughness, K_{Ic} , is a smooth, linear function of the amine/epoxy ratio from less-than-to greater-than-stoichiometric amine contents. All specimens are quite brittle, with values of K_{Ic} ranging from about 1.1 (excess of amine) to 0.6 (excess of epoxy) MPa \sqrt{m} . The stress intensity factor range, ΔK , required to drive a crack at constant velocity under cyclic loading behaves in a generally similar fashion, while the slope of the curves of crack growth rate per cycle vs ΔK also appears to be independent of the stoichiometry range of excess amine. (FCP behavior does not appear to have been described before as a function of composition.) Broad- \bar{M}_c -distribution specimens, at a constant average \bar{M}_c show a tendency to have slightly higher values of K_{Ic} and ΔK .

8. Preliminary high-resolution electron microscopy reveals a variety of surface features in the resins after etching and replication, while scanning and transmission electron microscopy has not yet confirmed the existence of such features. The question of whether or not a two-phase morphology exists is not yet resolved. Inspection of fracture surfaces by optical microscopy revealed considerable variation in the extent of plastic deformation, depending on the stoichiometry and ΔK level; definite conclusions about the relationships will require further work.

b. Recommendations for Further Work

The following recommendations for continued research are made:

1. The following work should be completed on a suitable range of specimens made to date: determination of stress-strain behavior at high and low strain rates; determination of stress relaxation master curves to predict behavior at long times; measurements of fracture toughness and fatigue crack propagation characteristics; and determination of the morphology in bulk and on fracture surfaces.

2. Preparation of specimens including the following variations in crosslinking and network parameters should be completed: temperature of cure, presence of network diluents such as solvents, and greater variations in the distribution of molecular weight (and hence M_c) in the epoxy components. Narrow-distribution resins should be obtained, if possible.

3. Characterization of these specimens should be performed as follows: viscoelastic, stress-strain, stress relaxation and fracture behavior; and state of cure by chemical or instrumental analysis, or swelling. Prepolymers should be characterized by gel chromatography.

4. If time and budget permits, exploratory measurements of viscoelastic response and fracture behavior should be made on specimens of an appropriate epoxy having an even higher T_g than those examined to date.

5. Correlations of all behavior should be made, and the effects of network structure interpreted in terms of the best available network theories.

LIST OF SPECIAL CHEMICAL STRUCTURES AND ABBREVIATIONS

<u>Material</u>	<u>Structure</u>	<u>Symbol</u>
Mixed anhydride of acrylic acid and trichloroacetic acid	$\text{Cl}_3\text{C}-\overset{\overset{\text{O}}{\parallel}}{\text{C}}-\text{O}-\overset{\overset{\text{O}}{\parallel}}{\text{C}}-\text{CH}=\text{CH}_2$	TCAAAMA
Acrylic acid anhydride	$\text{CH}_2=\text{CH}-\overset{\overset{\text{O}}{\parallel}}{\text{C}}-\text{O}-\overset{\overset{\text{O}}{\parallel}}{\text{C}}-\text{CH}=\text{CH}_2$	AAA
Tetraethylene-glycol dimethacrylate	$\text{CH}_2=\overset{\overset{\text{CH}_3}{\mid}}{\text{C}}-\overset{\overset{\text{O}}{\parallel}}{\text{C}}-\text{O}-\text{CH}_2\text{CH}_2\text{CH}_2\text{CH}_2\text{O}-\overset{\overset{\text{O}}{\parallel}}{\text{C}}-\overset{\overset{\text{CH}_3}{\mid}}{\text{C}}=\text{CH}_2$	TEGDM

<u>Material</u>	<u>Structure</u>	<u>Symbol</u>
Methylene dianiline (p, p'-diaminodiphenylmethane)		MDA
Epoxy prepolymer*	(See section VI-A)	**Epon 825, etc.
Polyamide (Versamid)	--	V-115, V-140

**Registered trade-mark.

SECTION X

REFERENCES

1. L. E. Nielsen, "Mechanical Properties of Polymers and Composites", Vol. 1, Marcel Dekker, Inc., New York, 1974.
2. L. E. Nielsen, "Crosslinking-Effect on Physical Properties of Polymers", Monsanto/Washington University/ONR/ARPA Association, Report HPC-68-57, May, 1968; J. Macromol. Sci.-Rev. Macromol. Chem., C3 (1), 69 (1969).
3. "Aerospace Structural Adhesives", report of the National Materials Advisory Board, Publication NMAB 300, National Academy of Sciences/National Academy of Engineering, DOD contract no. MDA-903-74-C-0167, July 1974.
4. C. H. Bamford and G. C. Eastmond, "Synthesis, Morphology and Properties of AB Crosslinked Copolymers", in "Recent Advances in Polymer Blends, Blocks and Grafts", Ed. by L. H. Sperling, Plenum, 1974.
5. J. K. Gillham, J. A. Benci, and A. Noshay, "Isothermal Transitions of a Thermosetting System", J. Appl. Polym. Sci., 18, 951 (1974).
6. T. Murayama and J. P. Bell, "Relation Between the Network Structure and Dynamic Mechanical Properties of a Typical Amine-cured Epoxy Polymer", J. Polym. Sci.-A2, 8, 437 (1970).
7. D. A. Whiting and D. E. Kline, "Effect of Stoichiometric Concentration of Hardener and Percentage Styrene Oxide on the Crosslinking and Mechanical Properties of an Epoxy Resin Cured with DEAPA", J. Appl. Polym. Sci. 18, 1043-52 (1974).
8. A. S. Kenyon and L. E. Nielsen, "Characterization of Network Structure of Epoxy Resins by Dynamic Mechanical and Liquid Swelling Tests", J. Macromol. Sci.-Chem., A3(2), 275 (1969).
9. D. H. Solomon and J. J. Hopwood, "Molecular Weight Distribution in Alkyd Resins, III. Presence of Microgel in Alkyd Resins", J. Appl. Polym. Sci., 10, 1893 (1966).
10. O. Delatycki, J. C. Shaw, and J. G. Williams, "Viscoelastic Properties of Epoxy - Diamine Network", J. Polym. Sci.-A2, 7, 753-762 (1969).
11. J. P. Bell and W. T. McCarvill, "Surface Interaction Between Aluminum and Epoxy Resin", J. Appl. Polym. Sci. 18, 2243-47 (1974).

12. F. R. Dammont and T. K. Kwei, "Dynamic Mechanical Properties of Aromatic, Aliphatic, and Partially Fluorinated Epoxy Resins", *Polymer Prepr.*, 8, 920 (1967).
13. J. L. Kardos, "Interface Modification in Reinforced Plastics", lecture, U. of Utah Conference Series on Adhesion, June, 1974.
14. T. Hirai and D. E. Kline, "Dynamic Mechanical Properties of Non-stoichiometric, Amine-Cured Epoxy Resin", *J. Appl. Poly. Sci.*, 16, 3145-3157 (1972).
15. R. J. Morgan and J. E. O'Neal, "Structural Parameters Affecting the Mechanical Properties of Epoxies", *Polymer Prepr.*, 16(2), 610 (1975).
16. N. Hata, "Viscoelastic Properties of Epoxy Resins. I. Effect of Prepolymer Structure on Viscoelastic Properties", *J. Appl. Polym. Sci.*, 15, 2371 (1971).
17. K. Selby and L. E. Miller, "Fracture Toughness and Mechanical Behavior of an Epoxy", *J. Mater. Sci.*, 10, 12-24 (1975).
18. R. G. C. Arridge and J. H. Speake, "Mechanical Relaxation Studies of the Cure of Epoxy Resins: I. Measurement of Cure", *Polymer*, 13 (9), 443 (1972).
19. T. Hirai and D. E. Kline, "Effect of Heat Treatment on Dynamic Mechanical Properties of Nonstoichiometric, Amine-cured Epoxy Resins", *J. Appl. Polym. Sci.* 17, 31 (1973).
20. J. N. Sultan and F. J. McGarry, "Effect of Rubber Particle Size on Deformation Mechanisms in Glassy Epoxy", *Polym. Eng. Sci.*, 13, 1 (1973).
21. K. Shibayama, T. Tanaka, and D. H. Solomon, "The Effect of Glyceride Composition on the Mechanical Properties of Alkyd Resin Films", *J. Macromol. Sci.*, A-1, 1531 (1967).
22. R. E. Cuthrell, "Epoxy Polymers II. Macrostructure", *J. Appl. Polym. Sci.*, 12, 1263 (1968).
23. R. E. Cuthrell, "Macrostructure and Environment-Influenced Surface Layer in Epoxy Polymers", *J. Appl. Polym. Sci.*, 11, 949 (1967).
24. P. J. Flory, "Principles of Polymer Chemistry", Cornell University Press, 1953.
25. J. D. Ferry, "Viscoelastic Properties of Polymers", 2nd edition, Wiley, 1970.

26. T. L. Smith, "Relations Between Ultimate Tensile Properties of Elastomers and their Structures", Proc. Roy. Soc. (London), 282, 102 (1964).
27. F. Bueche and J. C. Halpin, "Fracture of Amorphous Polymeric Solids: Reinforcement", J. Appl. Phys., 35, 3142 (1964).
28. E. H. Andrews, "Fracture in Polymers", American Elsevier, 1968.
29. A. T. DiBenedetto and A. D. Wambach, "The Fracture Toughness of Epoxy-Glass Bead Composites", Int. J. Polym. Mater., 1, 159 (1972).
30. L. H. Sperling, T. C. P. Lee and A. V. Tobolsky, "Thermodynamic Stability of Elastomeric Networks at High Temperatures", J. Appl. Polym. Sci., 10, 1831 (1966).
31. L. H. Sperling and A. V. Tobolsky, "Thermoelastic Properties of Poly(dimethyl siloxane) and Poly(ethyl acrylate) as a Function of Temperature", J. Macromol. Chem., 1, 799 (1966).
32. L. H. Sperling, E. J. Zaganianis and A. V. Tobolsky, "Elastomeric and Mechanical Properties of Poly-m-carboranylene siloxanes", J. Macromol. Sci.-Chem., A1, 1111 (1967).
33. L. H. Sperling and A. V. Tobolsky, "Network Relaxation Properties of Crosslinked Poly(ethyl acrylate) and Polydimethylsiloxane", J. Polym. Sci., Part A-2: 6, 259 (1968).
34. A. Guinier and G. Fournet, "Small Angle Scattering of X-rays", Wiley, 1955.
35. W. R. Krigbaum and R. G. Goodwin, "Direct Measurement of Molecular Dimensions in Bulk Polymers", J. Chem. Phys. 43, 4523 (1965).
36. J. P. Bell, "Mechanical Properties of a Glassy Epoxide Polymer: Effect of Molecular Weight Between Crosslinks", J. Appl. Polym. Sci., 14, 1301 (1970).
37. J. P. Bell, "Structure of a Typical Amine-Cured Epoxy Resin", J. Polym. Sci.-A2, 8, 417-437 (1970).
38. C. J. Lin and J. P. Bell, "The Effect of Polymer Network Structure Upon the Bond Strength of Epoxy-Aluminum Joints", J. Appl. Polym. Sci. 16, 1721 (1972).

39. J. A. Manson and E. H. Chiu, "Permeation of Liquid Water in a Filled Epoxy Resin", J. Polym. Sci.-Symp. No. 41, 95-108 (1973).
40. J. A. Manson and E. H. Chiu, "Effect of Water on the Behavior of Glass-bead-filled Epoxy Resin", Polym. Prepr., 14, 469 (1973).
41. R. W. Lenz, "Organic Chemistry of Synthetic High Polymers", Interscience, 1967. (Reviews work by M. Szwarc, et. al.).
42. R. B. Wagner and H. D. Zook, "Synthetic Organic Chemistry", Wiley, New York, 1961, pp. 558-564.
43. J. B. Polza and T. M. Spotswood, "Acetic Propionic Anhydride", J. Am. Chem. Soc., 71, 2938 (1949).
44. C. F. H. Allen, et al., "Acid Anhydrides", Organic Syntheses, 26, pp. 1-3, (1946).
45. Quotation from Polysciences, Inc., Warrington, Pa.
46. Private Communication, W. E. Broxterman, Dow Chemical Company, July 2, 1975.
47. "Polymer Handbook", ed. by J. Brandrup and E. H. Immergut, Interscience, New York, 1966.
48. V. Huelck, D. A. Thomas and L. H. Sperling, "Interpenetrating Polymer Networks of Poly(ethyl acrylate) and Poly(styrene-*eo*-methyl methacrylate). I. Morphology via Electron Microscope", Macromol., 5, 340 (1972).
49. P. J. Flory and J. Rehner, "Statistical Mechanics of Crosslinked Polymer Networks. I, Rubberlike Elasticity", J. Chem. Phys., 11, 512 (1943).
50. ASTM Standards, American Society for Testing Materials, Philadelphia, Pa. 1958, ASTM D 1053-58T.
51. ASTM D-1043, American Society for Testing Materials, Philadelphia, Pa., 1974.
52. R. F. Clash, Jr. and R. M. Berg, "Vinyl Elastomers. Low Temperature Flexibility Behavior", Ind. Eng. Chem., 34, 1218 (1942); ASTM D 1043-51.
53. A. V. Tobolsky, "Properties and Structure of Polymers", Wiley, 1960, Chapter 4.
54. R. N. Haward, ed., "The Physics of Glassy Polymers", Applied Science Publishers, London, 1973, p. 130.

55. J. W. Vanderhoff, J. A. Manson, G. W. Poehlein, and H. D. Leidheiser, "Exploratory Development of Improved Water Base Coatings", Final Report, AFML Contract F3365-73-C5179, January, 1975.
56. K. Neki and P. H. Geil, "Morphology-Property Studies of Amorphous Polycarbonate", J. Macromol. Sci.-Phys., B-8, 295 (1974).
57. Symposium "The Physical Structure of Amorphous State", Amer. Chem. Soc. Meeting, Atlantic City, September, 1974, G. Allen and S. E. B. Petrie, Chairman; see Polym. Prepr., 15 (2), 1-336 (1974).
58. Anon., Technical Literature, The Dow Chemical Company, n. d.
59. H. Lee and K. Neville, "Handbook of Epoxy Resins", McGraw-Hill, 1967.
60. "Epoxy Resins, Chemistry and Technology", Ed. by C. A. May and Y. Tanaka, Marcel Dekker, Inc., New York, 1973.
61. H. Batzer and S. A. Zahir, "Studies in the Molecular Weight Distribution of Epoxide Resins. I. Gel Permeation Chromatography of Epoxide Resins", J. Appl. Polym. Sci., 19, 585-620 (1975); "II. Chain Branching in Epoxide Resins", *ibid*, 19, 601-607 (1975).
62. W. A. Dark, E. C. Conrad, and L. W. Crossman, Jr., "Liquid Chromatographic Analysis of Epoxy Resins", J. Chromat., 91, 247-260 (1974).
63. S. A. Sutton, "Fatigue Crack Propagation in an Epoxy Polymer", Eng. Frac. Mech., 6, 587 (1974).
64. J. O. Outwater and M. C. Murphy, "On the Fatigue of Epoxy Resin", 26th Annual Tech. Conf., 1971, Reinforced Plastics/Composite Div., The Society of the Plastics Industry, Inc. Section 10A, p. 1.
65. L. J. Broutman and S. K. Gagger, "Fatigue Behavior of Epoxy and Polyester Resins", 27th Annual Tech. Conf., 1972, Reinforced Plastics/Composite Div., The Society of the Plastics Industry, Inc., Section 9B, p. 1.
66. R. Griffiths and D. G. Holloway, "Fracture Energy of Epoxy Resin Materials", J. Mater. Sci., 5, 302 (1970).
67. P. S. Theocaris, "Viscoelastic Properties of Epoxy Resins Derived from Creep and Relaxation Tests at Different Temperatures", Rheol. Acta, 2, 92, (1962).
68. J. A. Manson and R. W. Hertzberg, "Fatigue Failure in Polymers", Crit. Rev. Macromol. Sci., 1, 433 (1973).

69. A. A. Griffith, "The Phenomena of Rupture and Flow in Solids", Phil. Trans. Roy. Soc. (London), 221, 163 (1921).
70. G. R. Irwin, "Fracture", in Handbuch der Physik, VI, 551 (1958).
71. J. W. Dally and L. J. Broutman, "Frequency Effects in the Fatigue of Glass Reinforced Plastics", J. Compos. Mater., 1, 424 (1967).
72. S. L. Kim, M. Skibo, J. A. Manson and R. W. Hertzberg, "Effect of Molecular Weight on Fatigue Crack Propagation in PMMA", Polymer Prepr., 16 (2), 559 (1975).
73. G. C. Martin and W. W. Gerberich, "Temperature Effects on Fatigue Crack Growth in Polycarbonate", J. Mater. Sci., 11, 231 (1976).
74. R. W. Hertzberg, J. A. Manson, and M. Skibo, "Frequency Sensitivity of Fatigue Processes in Polymeric Solids", Polym. Eng. Sci., 15, 252 (1975).
75. S. L. Kim, M. Skibo, R. W. Hertzberg and J. A. Manson, "Effects of Molecular Weight and Plasticization on Fatigue Crack Propagation in Polymers", Polym. Prepr., 17 (1), 144 (1976).
76. J. A. Manson, M. Skibo, and R. W. Hertzberg, "Effects of Molecular Weight and Plasticizer on FCP in PVC", to be presented, Second Conference on Poly(Vinyl Chloride), Lyon, France, July, 1976.
77. M. Skibo, R. W. Hertzberg, J. A. Manson, and S. L. Kim, "On the Discontinuous Nature of Fatigue Crack Propagation in Polymers", accepted, J. Mater. Sci., 1976.
78. S. Wellinghoff and E. Baer, "The Mechanism of Crazing in Polystyrene", J. Macromol. Sci.-Phys., B-11(3), 367 (1975).
79. M. Schrager, "Fatigue as Monitored by the Torsion Pendulum", J. Polym. Sci., Part A-2, 8, 1999-2014 (1970).
80. B. Tomkins and W. D. Biggs, "Low Endurance Fatigue in Metals and Polymers, part 3", J. Mater. Sci., 4, 544 (1969).
81. M. Skibo, R. W. Hertzberg and J. A. Manson, "Fatigue Fracture Processes in Polystyrene", J. Mater. Sci., 11, 479 (1976).